AD NUMBER
AD091769
CLASSIFICATION CHANGES
TO: unclassified
FROM: confidential
LIMITATION CHANGES
TO: Approved for public release, distribution unlimited
FROM: Distribution authorized to U.S. Gov't. agencies and their contractors; Foreign Government Information; NOV 1955. Other requests shall be referred to the British Embassy, 3100 Massachusetts Avenue, NW, Washington, DC 20008.
AUTHORITY
DSTL, AVIA 6/18020, 10 Dec 2008; DSTL, AVIA 6/18020, 10 Dec 2008

AD 91769

NOTICE: THIS DOCUMENT CONTAINS INFORMATION AFFECTING THE NATIONAL DEFENSE OF THE UNITED STATES WITHIN THE MEANING OF THE ESPIONAGE LAWS, TITLE 18, U.S.C., SECTIONS 793 and 794. THE TRANSMISSION OR THE REVELATION OF ITS CONTENTS IN ANY MANNER TO AN UNAUTHORIZED PERSON IS PROHIBITED BY LAW.

CONFIDENTIAL - DISCREET

ROYAL AIRCRAFT ESTABLISHMENT
FARNBOROUGH, HANTS

REPORT No: AERO.2561

THE CALCULATIONS OF THE DERIVATIVES INVOLVED IN THE DAMPING OF THE LONGITUDINAL SHORT PERIOD OSCILLATIONS OF AN AIRCRAFT AND CORRELATION WITH EXPERIMENT

by

H.H.B.M.THOMAS, B.Sc., A.F.R.Ae.S. and B.F.R.SPENCER, B.Sc.

NOVEMBER, 1955

CONFIDENTIAL - DISCREET

U.D.C. No. 533.6.013.412 : 533.6.013.423

Report No. Aero 2561

November, 1955

ROYAL AIRCRAFT ESTABLISHMENT, FARNBOROUGH

The calculations of the derivatives involved in the damping of the longitudinal short period oscillations of an aircraft and correlation with experiment

by

H. H. B. M. Thomas, B.Sc., A.F.R.Ae.S.

and

B. F. R. Spencer, B.Sc.

SUMMARY

Apart from an attempt to calculate the contribution of a tailplane to the damping in pitch of an aircraft over the speed range this note is a review of the existing information on the subject, from both experimental and theoretical sources.

A comparison of theory and experiment seems to indicate that theory gives a fairly reliable estimate of trends. There are a number of points requiring further investigation, and these are brought out in the discussion and conclusions at the end of the paper.

The main conclusion to be drawn from the available information is that tailless aircraft, having leading edge sweep of less than 55° or thereabouts, and of moderate or large aspect ratio, are almost certain to suffer some loss of damping in the transonic speed range, the severity of this loss depending on the sweep, the aspect ratio, the moment of inertia in pitch, and the relative density μ.

It seems likely that the addition of a tailplane in a suitable position would remove most, if not all, of this loss, but this requires further investigation particularly as regards incidence effects.

LIST OF CONTENTS

LIST OF APPENDICES

LIST OF ILLUSTRATIONS

LIST OF ILLUSTRATIONS (Contd)

LIST OF ILLUSTRATIONS (Contd)

1 Introduction

Until aircraft flew transonically the damping of the short period (high frequency) oscillatory mode of an aircraft was normally so good that the derivatives governing it had been studied but little. Recent flight experience revealed a serious loss of damping in pitch of the short period oscillation at transonic speeds, and resulted in an increased interest in the stability derivatives involved.

In general, the forces and moments acting on an aircraft depend on the time history of the motion in addition to the instantaneous values of the variables, and the importance of this, particularly for flight at transonic speeds, has become widely recognised. Accordingly, the derivatives discussed in this paper are oscillatory derivatives (pertaining strictly to simple harmonic motion) (as discussed by Neumark and Thorpe, T17). For subsonic and supersonic speeds sufficiently removed from that for Mach number unity the dependence of the derivatives on the "reduced" frequency $\left(\omega = \frac{n\bar{c}}{V}\right)$ is such that for the frequency range of interest in aircraft stability the derivatives themselves may be regarded as constant, but theory and experiment indicate that at transonic speeds the frequency has a pronounced effect on the value of some derivatives.

The last few years have seen the development of theories for calculating the appropriate derivatives to various degrees of approximation at subsonic, sonic, and supersonic speeds. At the same time such derivatives have been measured using different experimental techniques for a number of wings, and for complete aircraft. The stage has been reached now when a review of the present state of knowledge, and its implications for aircraft design, is desirable. This is the object of the present note.

In addition, an advance on the theoretical side is made by an approximate calculation of the damping contribution of a tailplane operating behind a wing in oscillatory flow. The results are compared with the currently used simple steady downwash delay approximations. No experimental data is available for comparison.

Acknowledgements are due to Mrs. S. Swift who did most of the lengthy computation and Miss F. M. Ward who also helped with the computation and prepared some of the illustrations.

The authors also wish to acknowledge the assistance given by Miss M. Jones of A.V. Roe Ltd. with the calculations relating to the Avro 707.

2 Derivatives involved in the damping of the short period longitudinal oscillation

The equations of motion of an aircraft assuming the forward speed remains constant (or neglecting the phugoid motion), and in the usual moving wind-body axes system, are (see, for example, Ref. T17),

$$\left.\begin{aligned} \frac{d\hat{w}}{d\tau} &= z_\theta\ \theta + \left(1 + \frac{z_q}{\mu}\right)\hat{q} + z_w\ \hat{w} + \frac{z_{\dot{w}}}{\mu}\frac{d\hat{w}}{d\tau} \\ \frac{d\hat{q}}{d\tau} &= \frac{\mu m_\theta}{i_B}\theta + \frac{m_q}{i_B}\hat{q} + \frac{\mu m_w}{i_B}\hat{w} + \frac{m_{\dot{w}}}{i_B}\frac{d\hat{w}}{d\tau} \end{aligned}\right\} \quad (1)$$

The determinantal equation, in its general form, readily follows

$$\Delta(\lambda) = A_1\lambda^3 + B_1\lambda^2 + C_1\lambda + D_1 = 0 \quad \text{(characteristic equation)} \qquad (2)$$

where:

$$A_1 = 1 - \frac{z_{\dot{w}}}{\mu},$$

$$B_1 = -z_w - \left(1 - \frac{z_{\dot{w}}}{\mu}\right)\frac{m_q}{i_B} - \left(1 + \frac{z_q}{\mu}\right)\frac{m_{\dot{w}}}{i_B},$$

$$C_1 = \frac{z_w m_q - z_q m_w}{i_B} - \left(1 - \frac{z_{\dot{w}}}{\mu}\right)\frac{m_\theta}{i_B} - \left(1 + \frac{z_q}{\mu}\right)\frac{m_w}{i_B},$$

$$D_1 = \frac{\mu}{i_B}\left(z_w m_\theta - z_\theta m_w\right).$$

It will be seen later that the derivatives z_θ and m_θ are at most only of the order ω^2, and the available experimental data do not enable a numerical assessment of these derivatives to be made. If on this basis we are prepared to neglect these the only derivatives involved in the damping of the short period oscillation are those contained in the expression for B_1, and of these we may ignore the effects of $z_{\dot{w}}$ and z_q as these are divided by μ, usually large. It should be stressed that given a full knowledge of the derivatives it is neither necessary nor perhaps desirable to make these approximations.

Accepting, for the moment, this approximate approach we find that the damping depends on three derivatives z_w, m_q, and $m_{\dot{w}}$. Furthermore, the latter two occur in combination as the sum of the two derivatives which can be shown to be equal to the pitching derivative $m_{\dot{\theta}}$, in the fixed axes system.

The discussion that follows is therefore mainly concerned with these two derivatives z_w, and $m_{\dot{\theta}}$, but unavoidably other derivatives enter into the relationships giving the dependence of z_w and $m_{\dot{\theta}}$ on axis position. The transfer from one axis to another is a very common adjustment to be applied to test results for their application to aircraft design, of which we shall say more later.

In the absence of detailed information on the effect of frequency we shall be assuming that we may neglect those quantities which theory indicates as being of order ω^2 or less.

3 Wing derivatives (inviscid theory, infinitely thin aerofoil)

We deal first with the isolated wing. Here we have available theories which assume generally that the wing is infinitely thin, the flow is inviscid, and that shock waves are absent. Further simplifying assumptions introduced into the more fully developed subsonic and supersonic theory make necessary a brief account of theory according to speed regimes.

3.1 Wing in subsonic oscillatory flow

In the extension of his subsonic lifting surface theory from steady flow to oscillatory flow of low frequency, Multhopp (see ref. T6 by Garner) shows that using the transformation

$$I(x,y,z,t) = R\ell\, \bar{I}(x,y,z)\, e^{i\omega(t+\lambda x)} \qquad (3)$$

with an appropriate choice of λ reduces the continuity equation to,

$$(1-M^2)\frac{\partial^2 \bar{I}}{\partial x^2} + \frac{\partial^2 \bar{I}}{\partial y^2} + \frac{\partial^2 \bar{I}}{\partial z^2} + \frac{\omega^2 M^2}{V^2(1-M^2)}\bar{I} = 0 . \qquad (4)$$

He then proceeds to neglect the last term, and thereby reduces the problem to the solution of the generalised Laplace equation,

$$(1-M^2)\frac{\partial^2 \bar{I}}{\partial x^2} + \frac{\partial^2 \bar{I}}{\partial y^2} + \frac{\partial^2 \bar{I}}{\partial z^2} = 0 . \qquad (5)$$

It is important to note that his assumptions go further than a mere assumption of low frequency, since it is implied that,

$$\frac{\omega M}{V\sqrt{1-M^2}} \ll 1.$$

This restricts the range of Mach number over which the theory may be applied with reliance.

The next stage in the calculation is the setting-up of the downwash equation in the form given in ref. T6. This in turn is split into two parts, see equations for w_1 and w_2 in ref. T6. The influence functions involved in the two equations being given it is possible to reduce, as was done in the steady flow problem, the problem to the calculation of the local lift and pitching moment at a number of chordwise sections from a set of linear equations satisfying the downwash condition at two points of each section. Details of the analysis and computation are given in ref. T6.

3.2 Wing in oscillatory flow at transonic speeds

We have mentioned the possibility of error in the Multhopp approach as the Mach number is increased. To overcome this difficulty, and in particular to enable him to deal with the sonic problem, Mangler, ref. T12, returns to the unmodified continuity equation,

$$\left(\frac{\partial^2}{\partial x^2} + \frac{\partial^2}{\partial y^2} + \frac{\partial^2}{\partial z^2}\right)\bar{I} = M^2\left(\frac{in}{V} + \frac{\partial}{\partial x}\right)^2 \bar{I} , \qquad (6)$$

where I (the enthalpy) $= \bar{I}(x,y,z)\, e^{int}$.

Using a distribution of doublets over the wing of strength

$$\ell(x,y,t) = \bar{\ell}(x,y)\, e^{int} \qquad (7)$$

we then obtain for $\bar{I}$,

$$\bar{I}(x,y,z) = -\frac{zV^2(1-M^2)}{2\pi}\iint_S \bar{\ell}(x',y')\left\{1 + e\,\frac{inrM}{V(1-M^2)}\right\} e^{-ihr}\,\frac{dx'dy'}{r^3} \qquad (8)$$

where

$$h = \frac{\varepsilon nM}{\sqrt{(1-M^2)}} \{M(x'-x) + \varepsilon r\} \qquad (8)$$

$$r = \sqrt{(x-x')^2 + (1-M^2)\{(y-y')^2 + z^2\}}$$

and $\varepsilon = +1$, $M < 1$ and -1 for $M > 1$.

Introduction of $\bar{l}$ into the last of the Euler equations leads to the downwash equation,

$$\frac{\bar{w}}{V}(X,y,0) = \lim_{z\to 0}\left\{\frac{\partial}{\partial z}\frac{z(1-M^2)}{8\pi}\int_{-\infty}^{X}\left[\iint_S \bar{l}(x',y')\, e^{-iH}\left\{1 + i\varepsilon\frac{nrM}{\sqrt{(1-M^2)}}\right\}\frac{dx'dy'}{r^3}\right]dx\right\}, \qquad (9)$$

where $H = h + \frac{n(X-x)}{u}$ can be written

$$H = \frac{nM}{\sqrt{(1+M)}}\left[\frac{(1+M)}{M}(X-x) + (x-x') + \frac{(1+M)\{(y-y')^2 + z^2\}}{(x-x') + \varepsilon r}\right], \qquad (10)$$

a form which gives no difficulty as $M \to 1$. A further transformation enables the downwash equation to be written after considerable manipulation in the form,

$$\frac{\bar{w}}{V}(X,y,0) = \frac{1}{8\pi}\iint_S L(x'y')\left[e^{-iH}\left(\varepsilon - \frac{x'-x}{r}\right)\right]_{\substack{x=X\\ z=0}}\frac{dx'dy'}{(y-y')^2}$$

$$+ \frac{1}{8\pi}\int_{-\infty}^{X}\int_{-s}^{s} L_t(x_t,y')\left[e^{-iH}\left(\varepsilon - \frac{x'-x}{r}\right)\right]_{\substack{x'=x_t\\ z=0}}\frac{dy'dx}{(y-y')^2} \qquad (11)$$

where $L(x',y')$ is a modified loading.

This form of the downwash equation embodies no restrictive assumptions regarding either frequency or Mach number. In aircraft stability we are interested in small values of the reduced frequency, ω, and hence we need only retain terms of the first order in the downwash. This simplifies somewhat the equation for the downwash, which is then split into its real and imaginary parts. The resulting equations, in forms appropriate to each of the speed regimes, are given in ref. [12].

By means of these equations it is formally feasible to construct solutions for oscillatory flow throughout the Mach number range, provided solutions can be obtained to the problem of steady flow with arbitrary incidence distribution. This would yield a continuous theoretical solution fairing into the Multhopp solution at lower subsonic Mach number, passing through the sonic solution, and fairing into the existing solutions on the supersonic side. These latter are, of course, based on similar assumptions to the Multhopp subsonic solution, namely, the free stream Mach number must be

sufficiently removed from unity, and the reduced frequency small enough that we may neglect terms involving $\frac{\omega^2}{(M^2-1)}$.

To date the above comprehensive theory has only been applied to a particular family of wings - the delta - and even then only at sonic speeds. Recent experience with Multhopp's scheme for the solution of steady flow problems suggests that it is sufficiently accurate to be used in the solution of the integral equations even when M is quite near to unity (see also section 3.4). An extension of the theoretical work on these lines would undoubtedly be valuable, since the sonic solutions show that the derivatives $z_{\dot{w}}$ and $m_{\dot{w}}$, and hence $z_{\dot{\theta}}$ and $m_{\dot{\theta}}$ depend markedly on the reduced frequency, containing as it does a term $\log \omega$.

3.3 Wing in supersonic oscillatory flow

By a similar argument to that of the subsonic case but with obvious modification the problem of an oscillating wing in supersonic flow sufficiently removed from sonic can be reduced to steady flow problems. The usual methods of solving steady flow problems then become applicable, and we have derivatives which are independent of the reduced frequency, see references T28, 31, 32, 33, 36, 37, 39, 40, 41, 45.

3.4 Comparison of Multhopp's subsonic theory with other theories

Apart from the Multhopp scheme of calculation for wings at subsonic speeds there exists an extension of the Falkner lifting surface theory, and also extensions of the Lawrence theory, which is an improved slender wing theory. These are described in refs. T9,19, T10,22. In addition, the "slender" wing theory gives exact results in the limiting case $A \to 0$. We shall now compare results based on these theories with those obtained using Multhopp's method. Garner has already provided a comparison of the results of ref. T9 (Lehrian) with results he obtained by use of Multhopp's approach. These are reproduced here as Fig.6. The agreement for both types of wing considered is very good.

In ref. T10 Lawrence and Gerber describe a method, which like that of ref. 19 (Lehrian) deals with the problem in more general terms, there being no restriction on the frequency of the oscillation, and give results for delta wings of various aspect ratio. These, converted into our derivatives $z_{\dot{w}}$, $z_{\dot{\theta}}$, and $m_{\dot{\theta}}$, are compared with results based on Multhopp's theory in Figs. 1,2,3. Included on the same figures are results in the limiting case $A \to 0$ ("slender wing theory"), see, for example, ref. T49, and the extension of Multhopp's method to this limit. [This is to be discussed more fully in a subsequent paper.] The various results are in close agreement, and it is particularly encouraging to note the smallness of the error in Multhopp's approach even when extended to the limit $A \to 0$.

The lifting surface theory due to Lawrence has been used to obtain stability derivatives (i.e. assuming ω small), and the solutions for the cropped delta wing family have been largely prodigested in a paper by Stone (Ref. T22). Typical results for delta wings are given in Fig.4, whilst in Fig.5 the values of z_q for wing of aspect ratio 1.848 for various axis positions are compared with results based on Multhopp's method. The agreement is good throughout the entire range of axis position. The same is not true of the results for $m_{\dot{\theta}}$ of a cropped delta wing (see Fig.6). However, Multhopp's theory and that based on the Falkner approach are in good agreement for both the cropped delta wing and the arrowhead wing of Fig.6.

4 Tailplane contribution to the damping of the wing-tailplane combination

Before the advent of highly swept winged aircraft capable of transonic speeds it was usual to make quite sweeping simplications in the calculations

of the tailplane contribution to $m_{\dot{\theta}}$. This was usually split into the contributions to m_q and $m_{\dot{w}}$. For the first of these the procedure was simply to introduce an additional incidence $\frac{q\ell}{V}$ at the tail aerodynamic centre.

This leads to the following simple result,

$$\Delta m_q \approx \left(\frac{\partial \epsilon}{\partial \alpha}\right)^2 \frac{S_t}{S} z_{w_t} \ell \qquad (12)$$

where z_{w_t} is the force derivative for the tailplane. Occasionally an efficiency factor was included to allow for the presence of the wing and body.

The second term in $\Delta m_{\dot{\theta}}$ ($\Delta m_{\dot{w}}$) was obtained[m3] by assuming that the downwash at the tailplane corresponds to that generated in steady flow at a time earlier than the instant considered, the interval of time being that needed for the air to pass from the wing to the tailplane, that is, ℓ/V. This assumption leads to another simple relationship,

$$\Delta m_{\dot{w}} \approx \Delta m_q \frac{d\epsilon}{d\alpha} . \qquad (13)$$

Combining the two results,

$$\Delta m_{\dot{\theta}} = \left(\frac{\partial \epsilon}{\partial \alpha}\right)^2 \frac{S_t}{S} z_{w_t} \left(1 + \frac{d\epsilon}{d\alpha}\right) . \qquad (14)$$

Now whereas such simplifying assumptions could well be justified for straight wing aircraft at relatively low Mach numbers, and large tailplane arm, it is questionable whether such is now-a-days the case. Some attempt to improve on the above approximations has been made, but investigations to date lack sufficient generality, e.g. do not apply if wing is swept. To assess the unsteady flow effects in relation to the tailplane contribution requires that we calculate m_{w_t}, m_{q_t}, and $m_{\dot{w}_t}$ for the tail alone, the moment arising from the force on the tail, and superimpose the effects of downwash. In doing which we are required to calculate the downwash arising from each of the three wing pressure distributions associated with the w, q, and $\dot{w}$ derivatives respectively, the above simplified treatment being clearly incomplete in this respect. Calculations on these lines have recently become available for the rectangular and delta wings with tails at supersonic speeds (see section 4.3). Similar calculations for subsonic speeds, and for sonic speed, using the theories discussed in section 3 as a basis are given in Appendices I and II at the end of the paper.

The results for each of the speed regimes are now summarised.

4.1 Subsonic flow

In Appendix II the downwash at a point behind an oscillating wing is calculated assuming that the tailplane lies in the plane of the wing wake, or since we further assume no displacement or deformation of the vortex sheet that the wing and tailplane are coplanar. Restricting our attention to oscillations of small amplitude this implies calculation of the downwash in the plane $z = 0$ of the coordinate system.

With these assumptions the analysis of Appendix II shows that the downwash can be written in the form

$$\frac{\bar{w}}{V} = \vartheta^* \left\{ F_1 + F_2 \, i\omega \frac{\bar{c}}{V} \right\} , \qquad (15)$$

where F_1 is the function of the downwash associated with the loading $\bar{l}_1$, and F_2 is the function associated with all three loadings $\bar{l}_1$, $\bar{l}_2$, $\bar{l}_3$. These load contributions which go to make up the loading of the oscillating wing (see equation (3a) Appendix II) allow of the following physical interpretation,

$\bar{l}_1$ is the loading due to unit uniform incidence,

$\bar{l}_2$ is the loading due to steady pitching oscillation $\left(\frac{q\bar{c}}{V}\right)$ about the origin, or incidence $\frac{x}{\bar{c}}$,

and $\bar{l}_3$ is that arising from a time lag between the loading and its induced downwash (the incidence is a function of ii, jj, and ℓ_1).

Provided that the tailplane is small compared with the wing we may further assume that it is sufficient to take a mean downwash. The results then obtained for the force and moment derivatives are,

$$\Delta z_{\dot{\vartheta}} = \frac{S_t \bar{c}_t}{S\bar{c}} \left[(1+\bar{F}_1) z_{\dot{\vartheta}_t} + \frac{\bar{c}}{\bar{c}_t} \left\{ \frac{\ell}{\bar{c}} + \bar{F}_2 + \frac{x}{\bar{c}} \frac{M^2}{(1-M^2)} \bar{F}_1 \right\} z_{\vartheta_t} \right] \qquad (16)$$

and,

$$\Delta m_{\dot{\vartheta}} = \frac{S_t}{S} \left(\frac{\bar{c}_t}{\bar{c}} \right)^2 \left[\frac{\ell}{\bar{c}_t} (1+\bar{F}_1) z_{\dot{\vartheta}_t} + \frac{\ell\bar{c}}{\bar{c}_t^2} \left\{ \frac{\ell}{\bar{c}} + \bar{F}_2 + \frac{x}{\bar{c}} \frac{M^2}{(1-M^2)} \bar{F}_1 \right\} z_{\vartheta_t} \right.$$
$$\left. + (1+\bar{F}_1) m_{\dot{\vartheta}_t} + \left\{ \frac{\ell}{\bar{c}} + \bar{F}_2 + \frac{x}{\bar{c}} \frac{M^2 \bar{F}_1}{(1-M^2)} \right\} m_{\vartheta_t} \right] , \qquad (17)$$

where z_{ϑ_t}, $z_{\dot{\vartheta}_t}$, $m_{\dot{\vartheta}_t}$ and m_{ϑ_t} are derivatives for the isolated tailplane. The last term in $\Delta m_{\dot{\vartheta}}$ can be omitted if we make the usual choice of definition of ℓ, the tail arm, i.e. the distance from the aircraft C.G. to the aerodynamic centre of the tailplane.

Of the tailplane derivatives involved in the above expressions z_{ϑ_t} is considerably larger than the others, particularly if we make $m_{\vartheta_t} = 0$ by choosing ℓ as above, and so a reasonable approximation would be expected if we ignore all terms except those involving z_{ϑ_t}. This yields,

$$\Delta z_{\dot{\vartheta}} \approx \frac{S_t}{S} \left\{ \frac{\ell}{\bar{c}} + \bar{F}_2 + \frac{x}{\bar{c}} \frac{M^2}{(1-M^2)} \bar{F}_1 \right\} z_{\vartheta_t} \qquad (18)$$

and,

$$\Delta m_{\dot{\vartheta}} \approx \frac{S_t}{S} \frac{\ell}{\bar{c}} \left\{ \frac{\ell}{\bar{c}} + \bar{F}_2 + \frac{x}{\bar{c}} \frac{M^2}{(1-M^2)} \bar{F}_1 \right\} z_{\vartheta_t} . \qquad (19)$$

Ignoring the difference between z_{ϑ_t}, z_{w_t}, and $\frac{1}{2}a_{1_t}$, we can write these relationships as,

$$\Delta z_{\vartheta}^{\cdot} = -\frac{S_t}{S}\left\{\frac{\bar{\ell}}{\bar{c}} + \bar{F}_2 + \frac{\bar{x}}{\bar{c}}\frac{M^2}{(1-M^2)}\bar{F}_1\right\}\frac{a_{1_t}}{2} \qquad (20)$$

and,

$$\Delta m_{\vartheta}^{\cdot} = -\frac{S_t \ell}{S\bar{c}}\left\{\frac{\bar{\ell}}{\bar{c}} + \bar{F}_2 + \frac{\bar{x}}{\bar{c}}\frac{M^2}{(1-M^2)}\bar{F}_1\right\}\frac{a_{1_t}}{2}. \qquad (21)$$

To reduce these to the very simple forms with which we opened this section we refer to Appendix I, from which it follows that $\bar{F}_2$ contains a term which can be written approximately $-\frac{\ell}{(1-M^2)\bar{c}}\cdot\frac{d\varepsilon}{d\alpha}$ provided ℓ is large. Thus assuming ℓ is large, and accordingly retaining only terms involving $\left(\frac{\ell}{\bar{c}}\right)^2$ the above expressions reduce to the extremely simple forms of equation (14).

It is desirable to compare the various approximations for typical aircraft layouts at different Mach numbers.

4.11 Comparison of values of $\Delta z_{\vartheta}^{\cdot}$ and $\Delta m_{\vartheta}^{\cdot}$ as given by the various approximations

The calculation of the functions F_1 and F_2 is fairly straightforward, and follows from Appendices I and II. In computing these the influence functions as given by the N.P.L. Tables, and as given by the first term of the appropriate series of Appendix I were used. Two planforms were chosen, with tailplanes of similar geometry, the first a typical sweptback wing, aspect ratio 3.0, leading edge sweep 45°, and taper ratio 0.4, and the second a cropped delta, aspect ratio 3.0, leading edge sweep 45° and taper ratio 1/7.

To study the variation of F_1 and F_2 over the tailplane area the functions were evaluated at points distributed as shown in Figs. 10 and 11 (behind the first of our wings). The function F_1 is seen to depend markedly on the spanwise location, but for tailplanes at 1.5 to 2 mean chords behind the trailing edge but little on the longitudinal distance. The implication here is that for layouts such as these it is generally necessary to average F_1 in the y-direction. A linear interpolation between the points corresponding to $\nu = 0$, and 1 ($\eta = 0$, 0.3827) should suffice. It is seen from this figure that the asymptotic approximations (see Fig.9) to influence functions give results in remarkably good agreement with exact values.

A similar set of calculations for F_2 yields Fig.11. This shows that F_2 varies more rapidly with both x and y for the same variation of the coordinates. The variation is such that the nett effect for a sweptback tailplane is not large, which suggests that we could approximate $\bar{F}_2$ by a reasonable choice of a point on the centre line only.

From the mean values of F_1 and F_2 so determined we obtain the contributions of the tailplane to $z_{\dot{\vartheta}}$ and $m_{\dot{\vartheta}}$. The calculated values according to the various approximations of section 4.1 are compared in Table I for a typical tailplane arrangement, whose geometry is similar to the main wing, and for which,

$$\frac{S_t}{S} = 0.15, \quad \frac{\bar{c}_t}{\bar{c}} = 0.45, \quad \frac{\ell}{\bar{c}} = 2.019, \quad \frac{\bar{x}}{\bar{c}} = 2.925.$$

Results of similar calculations for a cropped delta wing-tailplane arrangement are given in Table II and Fig.15. Here it is assumed that,

$$\frac{S_t}{S} = 0.0998, \quad \frac{\bar{c}_t}{\bar{c}} = 0.316, \quad \frac{\ell}{\bar{c}} \begin{cases} 1.503 \\ 2.202 \end{cases}, \quad \frac{x}{\bar{c}} = \begin{cases} 2.498 \\ 3.25 \end{cases}.$$

It is seen that the simplest of the approximations (those of equations (12)-(14)) provide reasonable estimates except at extreme C.G. positions, but that even in these cases the approximation of equations (20) and (21) are still acceptable.

The direct comparison with experiment is not possible, as tests of wings alone, and with tailplanes do not appear to have been made to date. It is, however, hoped that it will be possible later to compare the results for the delta wing-tail combination with flight test data for the tailless, and tailed version of the Boulton-Paul aircraft.

4.2 Sonic flow

Also given in Appendix II are calculations, based on the same assumptions as those of section 4.1, for which the stream Mach number is unity. As the wing loading has only been determined for the delta wings complete calculations are only given for this family of wings.

The downwash angle at the tailplane can be written in the form,

$$-\frac{w}{V} = \theta + \dot{\theta}\frac{\bar{c}}{V}\vartheta(x), \qquad (22)$$

where $\vartheta(x)$ is given by equation (II.29) of Appendix II.

From this we get,

$$\Delta z_{\dot{\theta}} = \frac{S_t}{S} z_{\theta_t}\left(\frac{\ell}{\bar{c}} - \bar{\vartheta}(x)\right) \qquad (23)$$

and

$$\Delta m_{\dot{\theta}} = \frac{S_t}{S}\frac{\ell}{\bar{c}}\left(z_{\theta_t} + \frac{\bar{c}_t}{\ell} m_{\theta_t}\right)\left(\frac{\ell}{\bar{c}} - \bar{\vartheta}(x)\right). \qquad (24)$$

If we refer to Appendix II we see that in general it is not possible to reduce these to the simplified form of equation (14), by making $x \to \infty$. By mere choice of definition of ℓ we can eliminate the m_{θ_t} term in the expression for $\Delta m_{\dot{\theta}}$, as in section 4.1.

We shall now try to assess the way in which $\vartheta(x)$ depends on other parameters assuming we may replace the terms in x by their limits, that is, write,

$$\vartheta(x) \approx 2 - \frac{x_o}{\bar{c}} + \cot^2\Lambda_\ell \ln\frac{\gamma\omega}{4}\cot^2\Lambda_\ell - \frac{\ell}{\bar{c}}.$$

With $\Lambda_\ell = 45°$,

$$\vartheta \approx 1.1909 - \frac{x_o}{\bar{c}} + \ln\omega - \frac{\ell}{\bar{c}}.$$

With $\Lambda_\ell = 60°$,

$$\beta \propto 1.3641 - \frac{x_o}{c_o} + \frac{1}{3}\ln\frac{\ell}{c_o} .$$

It follows that in the usual range of sweep for delta wings β is negative, but tends to become positive as sweepback is increased. In limit $\Lambda_\ell \to 90°$, $\beta \to 2 - \frac{x_o}{c_o} - \frac{\ell}{c_o}$. Accordingly, tailplanes tend to become less efficient as means of providing damping as the sweep of the wing is increased, but this is offset, of course, by an increasing contribution from the wing. In the absence of both theory and experiment for a wide range of wing planforms and tails it is not possible to say if this is a general result.

However, it may be instructive to consider the case of the delta family of wings a little more closely. Calculations have been made for delta wings having leading edge sweepback of 45° and 60°, and each fitted with a tailplane of the cropped delta wing type. This particular configuration, as well as the position of the tail relative to the wing (in these calculations $\frac{x_o}{c_o}$ is kept constant at 2.498) was chosen to allow the maximum use of the results relating to Fig.15, but has the disadvantage that this tail position does not bring out so forcibly the tendency for the $m_{\dot\theta}$ at transonic speeds to become more nearly equal on fitting a tail. However, the trend is certainly present in the results of Fig.14, and the above argument for large tail arms shows that this balance of wing and tail contributions is more marked for tailplanes placed further aft than those of Fig.14.

4.3 Supersonic flow

A discussion of the same problem in supersonic flow is given in ref. T44, (Ribner) which is confined to a wing performing heaving oscillations. Ref. T38 (Martin, Diederich and Bobbitt) gives a more complete discussion covering steady pitching and heaving, together with results for the rectangular and triangular wings with tailplanes.

There is, as is to be expected, a general resemblance between the expression obtained for the tailplane contribution to $z_{\dot\theta}$ and $m_{\dot\theta}$ and those for the subsonic flow. Here, however, we cannot so readily relate the general expressions to the well-known approximations given in section 4, but by considering the limiting condition $x \to \infty$ in the various examples dealt with in detail, i.e. the rectangular and triangular wings, it can be seen how the general expressions tend to the simple ones. For example, if we take the triangular wing performing heaving oscillations, and retain the notation of ref. T38, we have, as $x \to \infty$,

$$E(K_4) \to K(K_4) \to \int_0^1 \frac{d\lambda}{\sqrt{1-\lambda^2}} = \frac{\pi}{2} \qquad (25)$$

since $K_4 \to 0$.

Also from equation (44b) of ref. T38,

$$\frac{\partial}{\partial z}\left(\frac{\Pi_a}{\alpha V}\right) \to -\frac{1}{E'(Bm)} , \qquad (26)$$

and from equation (45b),

$$\frac{\partial}{\partial z}\theta_q \rightarrow -\frac{2}{\pi}K_q \quad (27)$$

and finally from equation (46b),

$$\frac{\partial \theta_2}{\partial z} \rightarrow -\frac{\alpha x}{B^2 E(Bm)} \rightarrow -\frac{\alpha x}{B^2}\frac{\partial}{\partial z}\left(\frac{\Omega_\alpha}{\alpha V}\right). \quad (28)$$

From these relationships it follows that for large values of x we may approximate to the function σ_2 of equations (74) and (78) by writing,

$$\sigma_2 \approx -\frac{\alpha c}{V}\frac{\partial}{\partial z}\left(\frac{\Omega_\alpha}{\alpha V}\right), \quad (29)$$

and hence retaining only the terms of order x (or ℓ) in equation (78) we arrive at the approximation of equation (80) of ref.1, that is, the well-known downwash delay approximation of section 4 above. Retaining terms in K_4^2 it is easily shown that for other than extreme positions of the aircraft C.G. the approximation is reasonable over a wide range of tail arm length. This is confirmed by the numerical results given in ref.T8, some of which are reproduced here as Figs. 12 and 13.

5 Wing-body combinations

There exists no solution of the problem of the oscillating wing-body combination in general. If, however, the wing-body combination is slender, we can use the "slender wing theory" approach. Results for various bodies in combination with delta wings are given in refs. T27 (Nonweiler) and T47 (Henderson). Although it may be possible to obtain solutions on the basis of linearised theory for wing-body combinations at supersonic speeds using methods already available for the steady flow problem such a procedure would involve considerable labour. Ref. T47 suggests a means of constructing an approximation to the solution of the problem of the oscillating delta-wing-body combination for all aspect ratios at supersonic speeds, based on the results of the "slender wing theory". Comparison of these approximate results in the case of steady lift suggests that the approximation has some value, but the experimental data for oscillatory derivatives (Figs. 20,21,23) do not seem to be so encouraging. It should be noted that the configurations studied in both refs. T27 and T47 are such that the body ends at the wing trailing edge.

6 Wings of finite thickness

In the preceding sections we have discussed the solutions based on the neglect of thickness of the wing as well as the viscosity of the fluid. Just as in the case of the steady flow derivatives these assumptions can introduce appreciable errors in our results. For this reason it is perhaps opportune to discuss such investigations as have been made before we make some comparisons of theory and experiment.

Essentially, all available work is confined to the two-dimensional case. The earliest attempt to include the effect of thickness and viscosity is due to W.P. Jones[T23], and is based on the use of an equivalent thin aerofoil whose shape is determined in such a manner as to yield the expected steady flow derivatives (as obtained from experiment or generalised data). This device was used to calculate the oscillatory derivatives for a Joukowski aerofoil in an incompressible fluid, but the method is quite general, and can be applied at all flow conditions.

Woods[T20] takes the underlying notion of the Jones' theory a stage further in a method which in effect deals separately with thickness and viscosity. In this theory the rear stagnation point is allowed to oscillate about the trailing edge in phase with the local relative incidence, and with an amplitude determined by equating the steady theoretical lift derivative to its experimental value. Furthermore the position of the "profile centre" (mid-chord point for flat plate) is adjusted to give the experimental aerodynamic centre. In as much as the flow around an aerofoil oscillating in a compressible fluid can be related to a flow in an incompressible fluid we can deal with the problem of the two-dimensional aerofoil at subsonic speeds in this way. Woods' results are in good agreement with Jones' for the Joukowski aerofoil (15% t/c), and indicates that $-m_{\dot{\theta}}$ can be reduced by as much as 20% for aerofoils of half this thickness-chord ratio and more conventional shape.

At supersonic speeds there had been a number of attempts to calculate the effect of thickness. These attempts are discussed in refs. T29, 30, 31, 34, 35 and ref. T30 describes a method of calculation, which is thought to be generally superior in accuracy to the others. Although the method is applicable to arbitrary frequency, and aerofoil profile the results given refer mainly to slow oscillations of an aerofoil of arbitrary profile, since comparison with an exact solution indicates that terms of higher order than the second can be neglected.

In the supersonic theory just mentioned the effect of thickness alone is all that is considered, and it is of interest to note that this effect can be either stabilising or destabilising depending on axis position, but is generally small for thickness-chord ratio of the order of 0.05. The correction terms are proportional to the thickness-chord ratio, and added to the "thin-aerofoil theory" result. The nature of the correction thus differs from that for subsonic speeds, where it takes the form of a positive factor, and again since the "thin aerofoil theory" gives a tendency to unstable $m_{\dot{\theta}}$ derivative for forward axis positions the effect of thickness can be in either sense. It may be possible that as experimental data accumulate to adapt Woods' approach to the supersonic problem and so obtain the combined effect of thickness and viscosity. Alternatively the use of an equivalent "thin aerofoil" suggests itself.

All the above refers to two dimensional flow, and its extension to wings of finite aspect ratio is very much an open question. Fortunately, with the trend towards thin wings ($t/c \sim 0.05$) the effects discussed will be small enough to permit of even the crudest estimate of their magnitude, in which case a correction in the form of an additive term or a factor may be all that is required for design purposes.

7 Experimental data and comparison with theory

A number of experimental techniques has been employed to obtain measured values of the derivatives discussed in this note. These are:-

(1) Wind tunnel.
(2) Ground launched rocket models.
(3) Full scale flight tests.
(4) Wing flow model tests.

In (1) and to a lesser extent in (4) the centre of gravity of the aircraft or the axis position can be changed over a fairly wide range. This opens up the possibility of studying the effect of axis position on a certain derivative, say $m_{\dot{\theta}}$, and further to obtain all the derivatives of section 2 independently.[T17] (2) and (3) are generally much less flexible techniques, and in (2) we are often faced with testing at the wrong centre of gravity, and for an unrepresentative moment of inertia coefficient, i_B. It is, therefore,

perhaps appropriate at this point to indicate how derivatives referred to one axis position are related to those at another axis position. From equation (5.5) of ref. T17 we have on separating the real and imaginary parts (these equations are given in this form as 5.5a in R & M version of T17),

$$\left.\begin{aligned} z_\theta &= z_{\theta,0} + \omega^2 z_w h \approx z_{\theta,0} \\ z_{\dot\theta} &= z_{\dot\theta,0} - z_w h \end{aligned}\right\}$$

$$\left.\begin{aligned} m_w &= m_w^{(0)} - z_w h \\ m_{\dot w} &= m_w^{(0)} - z_{\dot w} h \end{aligned}\right\} \qquad (30)$$

$$\left.\begin{aligned} m_\theta &= m_{\theta,0} - (z_{\theta,0} - \omega^2 m_w^{(0)})h - \omega^2 z_{\dot w} h^2 \\ &\approx m_{\theta,0} - z_{\theta,0} h \\ m_{\dot\theta} &= m_{\dot\theta,0} - (z_{\dot\theta,0} + m_w^{(0)})h + z_{\dot w} h^2 \end{aligned}\right\}$$

and hence

$$\left.\begin{aligned} z_q &= z_{q,0} - z_w h \\ m_q &= m_{q,0} - (z_{q,0} + m_w^{(0)})h + z_{\dot w} h^2 . \end{aligned}\right\} \qquad (31)$$

In these equations ω is the reduced frequency, h is the non-dimensional distance between the axes considered positive if the new axis lies aft of the original axis, and the suffix or index (0) denotes derivatives corresponding to the original axis. It is thus clear that a designer may have insufficient data to even assess the order of the damping in pitch of his aircraft from an "ad hoc" test. In terms of the above equations he may have a value of $m_{\theta,0}$ and z_w. To estimate $m_{\dot\theta}$ resort must be made to theory in respect of $z_{\dot\theta,0}$ at any rate, while $m_w^{(0)}$ can be obtained with the necessary accuracy from generalised experimental data, and theory, in the absence of test results for the design being considered.

Before proceeding with a comparison of calculated and measured derivatives we note that all the above experimental techniques have drawbacks. The wind tunnel test has to strike a compromise between adequate scale, and unknown and possibly large tunnel wall constraint corrections. In the ground launched rocket model the disturbance which is analysed as though it occurred at constant forward speed in fact takes place when the model is decelerating. The validity of this analysis is thus open to some doubt. At this stage, limitations of the instrumentation, and the inadequate recording of small unintentional control movements together with any aeroelastic effects set a limit on the accuracy of the flight test results. Lastly, the very small size of the models used in the "wing flow" technique means that the Reynolds number in such tests is so small that without considerably improved understanding of the interaction of shock waves and boundary layer such tests yield results calling for careful interpretation.

7.1 Tests on delta wing tailless aircraft (Avro 707, Fairey 103, BP 111)

Tests using all the above techniques have been made on a "delta" wing tailless aircraft (Avro 707) whose wing planform details are given in Fig.7a. In view of this an extensive set of calculations, the results of which are summarised in Figs. 7 and 8, were undertaken so that a complete comparison is more or less possible for this case. We still lack the complete set of derivatives, but we do have results at two centre of gravity positions and over a range of Mach numbers.

The curves (Fig.7) show, at Mach numbers not near to unity, the parabolic variation with axis position. Near sonic speeds, however, we have this parabolic relationship only at constant ω. On Fig.8 is shown the variation to be expected with axis position, when ω takes the theoretical value corresponding to the given axis position. This value of ω is given approximately by:

$$\omega = \sqrt{-\frac{z_w}{\mu i_B}\left(\frac{m_w}{z_w} - \frac{m_q}{\mu}\right)} \qquad (32)$$

and for the aircraft in question μ is taken as 71.45 and i_B as 0.377 for the firm's test flight data, but with μ increased to 74.49 for the RAE tests. A full delta wing of the same leading edge sweep was used in these calculations.

A slightly modified wing was used in the calculations at supersonic speeds to ease the labour involved. The effect of this change in planform is unknown, but purely on the basis of the very limited extent of the change, is thought to be small enough for our present purpose.

The calculated derivatives, with due allowance at sonic speed for the effect of ω, are compared with those deduced from various tests in Figs. 17, 18, 19. Bearing in mind the limitations on accuracy on both the experimental and theoretical side the agreement is encouraging, as is also the implied agreement of the experimental data.

Another delta wing tailless aircraft with a higher value of sweepback of the leading edge (the Fairey ER103) has also been tested using the "wing flow" technique. Although tests have been made with transition fixed and free only the results from the transition fixed tests are considered as it is considered these will be more representative of behaviour at higher Reynolds Number, and aircraft conditions. Here no direct comparison is possible, but the approximate estimates based on other similar planforms do indicate that more exact calculations would give results in as good agreement with the experimental data as would be expected (see Fig.22).

The 45° swept delta wing of the Boulton-Paul aircraft gives an appreciable reversal in sign of $m_{\dot{\theta}}$ at near sonic speeds. For this case only the subsonic values have been calculated, and these are compared with the flight test data in Fig.16. The agreement of theory and experiment is again reasonably good, and a fairing of the results at subcritical Mach numbers into the sonic value reproduces the measured transonic variation.

Experiments have also been made by Bratt, Rayner, and Townsend on two of the above wings (Avro and BP deltas) in a small high speed wind tunnel at the N.P.L.[24,5], and some of the results are reproduced here in Fig.26. The agreement with the theoretical values is not good in this case. It is difficult to state at this stage the reason for the discrepancy, but it may be noted that no tunnel corrections can be applied, and that the Reynolds Number of the tests was low.

Ref. E20 by Tobak describes wind tunnel tests of oscillating models with delta wings of aspect ratio 4, 3 and 2 fitted with bodies and oscillating about different axes, and covering a range of subsonic and supersonic Mach numbers. The results are summarised here in Figs. 20, 21, and 23, and a limited number of results from theory are shown, for comparison. It is seen that all but the aspect ratio 2 delta wing suffer a reversal in sign of $m_{\dot{\theta}}$, but it must be remembered that the magnitude of the reduced frequency, ω, is quite unrepresentative. At supersonic speeds the estimated values agree well with the test results, but at subsonic speeds there are too few data to deduce much, except perhaps for the aspect ratio 2 case with the axis at 0.567 c_r when the agreement is reasonably good at all speeds.

Some results are available (ref. E28) for a range of frequency parameters and Mach numbers for two delta wings (A = 2 and 4) oscillating about an axis through the midchord point of the root chord. Owing to the fact that the frequency, Mach number, and Reynolds number could not be varied independently it is difficult to isolate the effect of any of these. To fit in with the general scheme of presentation, the results have been plotted against Mach number rather than frequency as in the original paper. As can be seen from Fig.25 there is considerable scatter of the experimental data. The mean values of $m_{\dot{\theta}}$ are some 70% of the theoretical values.

Two sets of experimental results[E10,31] obtained by the use of rocket models, and shown in Fig.24 complete the data for the tailless delta wing configuration. There is considerable scatter of the experimental points, and so little reliance can be placed on the numerical values in both tests. These tests do, however, bear out the general conclusion that for typical centre-of-gravity positions the damping in pitch would show no marked loss at transonic speeds if the leading edge sweep is of the order of 60°.

7.2 Tests on Arrowhead wing configurations (Refs. E6, 7, 8, 14, 17, 18, 21, 22, 24, 25, 29)

Experimental results are also available for arrowhead wings covering a range of shapes within the following limits: $2.24 < A < 5.5$, $37° < \Lambda_{\ell} < 63°$. Of these, five wings have been tested alone or in combination with a body, the remainder are complete models or full scale aircraft.

Looking first at the tailless models we note that for sweepback of the order of 45° and aspect ratio between 3 and 6 there is a marked tendency to a reversal in sign of $m_{\dot{\theta}}$ at transonic speeds (Figs. 26, 27, 29, 30, 31). At subsonic speeds $-m_{\dot{\theta}}$ increases slightly with increase of Mach number thus confirming the trend predicted by theory. Comparison of theory and experiment on a wider basis is difficult, the sonic case being at present unsolved. The supersonic speed case admits of at least approximate solution, and here also the experiment follows fairly closely the trends indicated by theory, see Fig.27. Little can be said about the effect of increasing sweepback and reducing aspect ratio in the absence of both the necessary theoretical results, and test data, but the isolated case of the English Electric wing of aspect ratio 2.88 and $\Lambda_{\ell} = 60°$ suggests that the beneficial effect of both modifications is a general result, see Fig.26.

In Figs. 29 and 30 are shown the results of tests on wings of aspect ratio 3.0, sweepback 35°, and of thickness-chord ratios 0.06 and 0.105. Small and large scale models were tested with smooth and roughened surface at the leading edge. There is some effect of thickness-chord ratio at transonic speeds but it is not easily isolated from other effects. The main point of interest is the large scale effect for free transition as opposed to the comparatively small effect with fixed transition.

The addition of a tailplane has considerable stabilising effect on $m_{\dot{\theta}}$, see Figs. 31, 32 and 33. Therefore it is to be expected that the rocket model

tests of tailed aircraft having wings with a sweep of 45° or more should show little variation of $m_{\dot{\theta}}$ with Mach number at transonic speeds. Of the test data presented in Figs. 31 and 32 the only point that calls for special comment is the small difference that exists in the curves of $m_{\dot{\theta}}$ of Figs. 31(b) and 32(b), at transonic speeds ($0.85 < M < 1.1$), where the first refers to an aircraft with a wing of low aspect ratio and high sweep, and hence presumably with no marked loss of wing damping contribution at transonic speeds, whilst the second is for a wing of moderate sweep and aspect ratio. We may be permitted to deduce that the tailplane contribution to $m_{\dot{\theta}}$ is larger in the latter case, and of such a form that it offsets the loss of damping that would be expected for the wing alone. This is in agreement with the trend indicated in section 4.2, and by calculation for the case of a delta wing-tail combination (see Fig.25).

It should be noted that these model tests refer to elastic models, and so cannot be compared directly with theory in which we assume rigid wing etc. (see Fig.31).

7.3 "Unswept" wings with and without tail (Refs. E11, 12, 19)

Those wings having very little sweep of the mid-chord line will be classed as unswept. Theory and experiment suggest that for representative centre of gravity positions such wings would exhibit a tendency to reversal in sign of $m_{\dot{\theta}}$ at transonic speeds. The only test data available on a wing without tail are presented in Fig.28. However, the addition of a tailplane should give a contribution sufficient to smooth out the drop in $m_{\dot{\theta}}$, and the only available data collected together in Fig.34 show that in this case there is in fact a slight increase in the overall $m_{\dot{\theta}}$ at transonic speeds.

7.4 Canard aircraft

The canard, or tail ahead of the wing, layout has not been studied to anything like the same extent as the more conventional tail aft layout. In the normal canard design the foreplane lies sufficiently ahead of the wing to be virtually free of the wing's induced velocity field. The contribution of the foreplane is thus almost entirely to the m_q derivative, and can in most cases be calculated on the simplified basis discussed in section 4. This layout of the aircraft implies a centre of gravity well forward on, or often ahead, of the wing, which means that the value of the wing contribution to $-m_{\dot{\theta}}$ is appreciably larger than for the centre of gravity positions associated with tailless or tail aft designs. This can be seen from equations (30) (since the $z_w h^2$ becomes the dominant term in the expression for $m_{\dot{\theta}}$), or from any of the figures showing the effect of axis position on $m_{\dot{\theta}}$ (Figs. 4 to 7). Not all this wing contribution will be realised in practice, since our argument does not allow for the interference effect of the foreplane on the mainplane. Nevertheless the canard design would be expected to give greater damping in pitch. This is borne out by the solitary experiment (Ref. E38, Vitale and McFall) comparing the two layouts for a given wing, and tail geometry.

8 Discussion and conclusions

In the preceding sections we have discussed mainly the damping for oscillations around a very small, or zero, mean incidence, and for a very limited range of amplitudes. Oscillation about a high mean incidence and over a larger amplitude can have pronounced effects on the damping (see Figs. 37, 34, 22, 19 and refs. E16, 20).

The appreciable effect of the amplitude of the oscillation is confined mainly to the transonic speed range, and may be associated with shock wave movement and separation of the flow behind the shock. At low Mach number this effect is only slight.

The limited data of ref. E16 (Beam) (see also Fig.37) point to large variations in the damping-in-pitch derivative, $m_{\dot{\theta}}$, with increase in the mean incidence, but because the severity of these variations is more marked at lower Reynolds number, and at transonic Mach numbers, and the fact that a large change results from roughening the wing leading edge at smaller Reynolds number, it is doubtful whether such large effects would be present in full scale flight.

It may be possible to make some allowance for such effects theoretically by use of methods such as discussed in section 6, cf. ref. T20. The three-dimensional problem is, however, an extremely complicated one as regards the formulation of equivalent thin wings.

A third effect not so far brought out is the effect of changes in the frequency of the oscillation. No general trend is apparent in the data available at present (see Figs. 19, 22, 25 and ref. E16 (Beam)).

Another feature of the test results examined which calls for comment is the fact that in tests of certain wings (e.g. Figs. 37b, 20, 21, 22) the damping becomes markedly non-linear with angle of incidence. For the tests related to Figs. 20 and 21, the damping is stabilising at an incidence of 5° or so, but is reduced as incidence is reduced leading to a steady oscillation of amplitude ±1° at an incidence of 1°. Such a steady oscillation could be an embarrassment for all classes of aircraft. A plausible explanation based on the assumption of a non-linear variation of the steady pitching moment (caused by flow separation arising from boundary layer shock wave interaction) is put forward by Beam in ref. E16. It is perhaps of significance that this effect was not observed on the delta wing of aspect ratio 2 of ref. E20 (Tobak).

From the data available from theory and experiment we can draw the following conclusions:-

1. As outlined in the introduction the damping factor of the short period oscillation in pitch is given by

$$\bar{R} = -\tfrac{1}{2}\left(z_w + \frac{m_{\dot{\theta}}}{i_B}\right) \cdot$$

Of the derivatives involved z_w generally retains the same (stabilising) sign throughout the speed range, but for wings of moderate aspect ratio and leading edge sweepback of the order of 55° or less $m_{\dot{\theta}}$ will have its sign reversed at transonic speeds, whilst for wings of lower aspect ratios and higher sweepback there is no such reversal. The addition of a tailplane to the former set of wings seems to bring about a similar improvement.

When the sign of $m_{\dot{\theta}}$ becomes destabilising the effect of a change in i_B is in the opposite sense to the usual, that is, decrease in i_B now causes the damping to be reduced. Since outside the transonic speed range the effect of changing i_B is normal this means a more pronounced loss of damping at these speeds (see Figs. 35, 36).

2. The present knowledge of the effects of amplitude, mean incidence and frequency (which are most marked at transonic speeds), is insufficient and future test programmes need to be planned accordingly.

3. The discrepancy between the simple approximation for the tailplane contribution based on "delay of steady flow downwash" and the more exact calculations given here is sufficiently large to call for an experimental check. Moreover, the highly complicated pattern of the separated flows around wings of considerable sweepback at moderate to large incidence will necessitate the testing of a number of up and down tailplane positions.

4. The comparison of available experimental results with theory is encouraging inasmuch as the theory gives a sufficiently accurate estimate at subsonic and supersonic speeds while indicating trends at transonic speeds.

5. From (4) it is concluded that an attempt should be made to extend the sonic theory to cover all planforms, and that a systematic set of calculations should be undertaken to provide a basis for the preparation of estimation charts. This calls for the use of automatic computing machinery to bring the time taken for the task within reasonable limits.

6. As is to be expected Multhopp's approach to the subsonic unsteady flow problem becomes unreliable at stream Mach numbers near unity, but the calculations for the limiting case of zero aspect ratio indicate that his general method of solving steady flow load distribution problems (to which the unsteady problem can be generally reduced) can be used with practically no restriction. It, thus, seems that we have the means available of obtaining solutions throughout the speed range, and where required for any frequency.

It must be stressed that while the existence of these solutions shows that linearisation of the problem is possible at transonic speeds, their interpretation in terms of results for wings of finite thickness, in a viscous fluid, and with shock waves present requires care. All that can be hoped is that they will indicate trends with change in wing planform, and that they will form some kind of bound to the values of the derivatives for actual wings. The results presented in the comparison of theory and experiment indicate that the sonic solutions given there do assist the designer in this way.

List of Symbols

A	aspect ratio
a	lift curve slope $\left(\frac{\partial C_L}{\partial \alpha}\right)$
b	wing span (ft)
A_1, B_1, C_1, D_1	coefficients of stability cubic, see equation (2)
C_L	lift coefficient
C_m	pitching moment coefficient
$\bar{c}$	British mean chord $\left(\frac{S}{b}\right)$
$\bar{\bar{c}}$	"Aerodynamic" mean chord
ϑ	downwash function, see equation (II.31)
$h = \frac{x_0}{\bar{c}}$	axis position measured from wing apex in terms of mean chord (positive aft)
i_B	inertia coefficient (about y-axis)
$I = \frac{p - p_\infty}{\rho}$	enthalpy (acceleration potential)

List of Symbols (Contd)

$\frac{2\Delta p}{\rho V^2}$	load coefficient (l_1, l_2, l_3)
M	Mach number
$M_{\dot{w}}$	dimensional pitching moment derivative due to rate of change of w
m_q	(steady) rotary damping derivative in pitch (dimensionless, see R & M 1801 or Appendix III)
$m_{\dot{w}}$	pitching moment derivative due to rate of change of w (dimensionless, see Appendix III)
$m_{\dot{\theta}} = m_q + m_{\dot{w}}$	full rotary damping derivative (dimensionless)
$n = 2\pi f$	frequency of oscillation (sec^{-1})
$\omega = \frac{n\bar{c}}{V}$	reduced frequency
q	rate of pitch (radians per sec)
$\hat{q}$	dimensionless rate of pitch
R	elevator fixed damping factor of short period oscillation (dimensionless)
S	gross wing area (sq ft)
$t = \tau.\hat{t}$	time (secs)
$\hat{t}$	unit of aerodynamic time $\left(\frac{W}{qpSV}\right)$, (secs)
V	velocity of aircraft in undisturbed flight, or free stream velocity (ft/sec)
W	weight of aircraft, lb
w	increment of velocity along z-axis in disturbed flight, ft/sec
$\hat{w}$	dimensionless, increment of incidence in disturbed flight
x,y,z	Cartesian coordinates
Z	force along z-axis of stability system of axes
z_q	z-force derivative due to steady pitching (see Appendix III)
$z_{\dot{w}}$	z-force derivative due to rate of change of $\dot{w}$ (see Appendix III)
$z_{\dot{\theta}} = z_q + z_{\dot{w}}$	full normal force derivative in a rotary oscillation (see Appendix III)
α	wing incidence, radians
ε	downwash angle at the tailplane, radians
θ	angular displacement in pitch from equilibrium position, radians

List of Symbols (Contd)

ϑ	angular displacement in pitch from equilibrium position, in space fixed system of axes, radians
ϑ^o	amplitude of the rotary oscillation, i.e. maximum value of ϑ
Λ_ℓ	leading edge sweepback angle
μ	relative density of aircraft $\left(= \frac{W}{g\rho S\bar{c}}\right)$
ρ	air density, slugs/cu ft
τ	dimensionless aerodynamic time
Ψ	dimensionless coordinate in Appendix I.

To avoid repetition of much of the analysis of the original references the notation of these papers has been used in Appendices I and II so that certain basic relationships can be merely quoted.

REFERENCES

Theory

No.	Author	Title, etc
T1	G. Temple	Modern developments in fluid dynamics. Vol.III, chapter IX. Unsteady Motion. March 1950. ARC 13,024.
T2	John W. Miles	The application of unsteady flow theory to the calculation of dynamic stability derivatives. Aero Physics Lab. Report AL-957. North American Aviation, Inc. Sept. 1950.
T3	W.L. Cowley H. Glauert	The effect of the lag of the downwash on the longitudinal stability of an aeroplane and on the rotary derivative M_q. R & M No. 718. 1921.
T4	S. Neumark	Analysis of short period longitudinal oscillations of an aircraft: interpretation of flight tests. RAE Report No. Aero 2479. R & M 2940. ARC 15,600. September 1952.
T5	H. Multhopp	Methods for calculating the lift distribution of wings (subsonic lifting surface theory). RAE Report No. Aero 2353. R & M 2884. ARC 13,439. January 1950.
T6	H.C. Garner	Multhopp's subsonic lifting surface theory of wings in slow pitching oscillations. ARC 15,096. July 1952.

REFERENCES (Contd)

No.	Author	Title, etc
T7	W.P. Jones	The calculation of aerodynamic derivative coefficients for wings of any planform in non uniform motion. R & M 2470, ARC 10,142. December 1946.
T8	D.E. Lehrian	Aerodynamic coefficients for an oscillating delta wing. R & M 2841. ARC 14,156. July 1951.
T9	D.E. Lehrian	Calculation of stability derivatives for oscillating wings. ARC 15,695. February 1953.
T10	H.R. Lawrence E.H. Gerber	The aerodynamic forces on low-aspect-ratio wings oscillating in an incompressible flow. Cornell Aeronautical Laboratory, Inc. Report No. AF-781-A-1: P40578. January 1952. Or Journal Aeronautical Sciences Vol.19, No.11. November 1952.
T11	W.P. Jones	Oscillating wings in compressible subsonic flow. R & M 2855. ARC 14,336. October 1951.
T12	K.W. Mangler	A method of calculating the short period longitudinal stability derivatives of a wing in linearized unsteady compressible flow. RAE Report Aero 2468. ARC 15,316. June 1952.
T13	S. Neumark	Two-dimensional theory of oscillating aerofoils, with application to stability derivatives. RAE Report Aero 2449. ARC 14,889. November 1951.
T14	J.W. Miles	Unsteady flow theory in dynamic stability. Reader's Forum, Journal of the Aeronautical Sciences, Vol.17, No.1, p.62. 1950.
T15	J.W. Miles	On the compressibility correction for subsonic unsteady flow. Reader's Forum, Journal of the Aeronautical Sciences, Vol.17, No.3, p.181. 1950.
T16	I.C. Statler	Dynamic stability at high speeds from unsteady flow theory. Journal of the Aeronautical Sciences, Vol.17, No.4, p.232. 1950.
T17	S. Neumark A.W. Thorpe	Theoretical requirements of tunnel experiments for determining stability derivatives in oscillatory longitudinal disturbances. RAE Tech Note Aero 2059. ARC 13,667, R & M 2903. June 1950.
T18	W.J.G. Pinsker	A note on the dynamic stability of aircraft at high subsonic speeds when considering unsteady flow. RAE Report Aero 2378. ARC 13,567, R & M 2904. June 1950.
T19	D.E. Lehrian	Calculation of flutter derivatives for wings of general planform. ARC 16,445. January 1954.

REFERENCES (Contd)

No.	Author	Title, etc
T20	F/Lt L.C. Woods	The lift and moment acting on a thick aerofoil in unsteady motion. ARC 15,667. February 1953.
T21	I.C. Statler	Derivation of dynamic longitudinal stability derivatives for subsonic compressible flow from non-stationary flow theory and application to an F-80A airplane. Cornell Aeronautical Laboratory, Inc. TB-495-F-9. March 1949.
T22	H.N. Stone	Aileron characteristics and certain stability derivatives for low-aspect-ratio wings at subsonic speeds. Cornell Aeronautical Laboratory, Inc. Report No. AF-743-A-3. P42291. July 1952.
T23	W.P. Jones	Aerofoil oscillations at high mean incidences. ARC 11,502. R & M 2654. April 1948.
T24	W.E.A. Acum	A brief survey of the present knowledge of the aerodynamic derivatives of wings in unsteady motion at transonic and supersonic speeds. ARC 13,863. CP 85. March 1951.
T25	K.W. Mangler	Calculation of the pressure distribution over a wing at sonic speeds. RAE Report Aero 2439. ARC 14,642, R & M 2888. September 1951.
T26	K.W. Mangler	Improper integrals in theoretical aerodynamics. RAE Report Aero 2424. ARC 14,394. CP 94. June 1951.
T27	T. Nonweiler	Theoretical stability derivatives of a highly swept delta wing and slender body combination. College of Aeronautics, Cranfield Report No.50. ARC 14,597. November 1951.
T28	W.P. Jones	Supersonic theory for oscillating wings of any planform. R & M 2655. ARC 11,559. June 1948.
T29	W.P. Jones	The influence of thickness chord ratio on supersonic derivatives for oscillating aerofoils. R & M 2679. ARC 10,871. September 1947.
T30	M.D. Van Dyke	Supersonic flow past oscillating airfoils including non-linear thickness effects. NACA TN 2982. ARC 16,636. July 1953.
T31	W.E.A. Acum	Note on the effect of thickness and aspect ratio on the damping of pitching oscillations of rectangular wings moving at supersonic speeds. ARC 15,864. CP 151. May 1953.

REFERENCES (Contd)

No.	Author	Title, etc
T32	F.S. Malvestuto K. Margolis H.S. Ribner	Theoretical lift and damping in roll at supersonic speeds of thin sweptback tapered wings with streamwise tips, subsonic leading edges and supersonic trailing edges. NACA Report 970. 1950. NACA TN 1761. January 1949.
T33	F.S. Malvestuto K. Margolis	Theoretical stability derivatives of thin sweptback wings tapered to a point with sweptback or sweptforward trailing edges for a limited range of supersonic speeds. NACA Report 971. 1950.
T34	J.C. Martin N. Gerber	The effect of thickness on airfoils with constant vertical acceleration at supersonic speeds. Ballistic Research Laboratories Report No. 866. P43359. May 1953.
T35	A. Wylly	A second-order solution for an oscillating, two-dimensional, supersonic airfoil. RAND Corp. Rep. 1951.
T36	F.S. Malvestuto D.M. Hoover	Lift and pitching derivatives of thin sweptback tapered wings with streamwise tips and subsonic leading edges at supersonic speeds. NACA TN 2294. February 1951.
T37	F.S. Malvestuto D.M. Hoover	Supersonic lift and pitching moment of thin sweptback tapered wings produced by constant vertical acceleration. Subsonic leading edges and supersonic trailing edges. NACA TN 2315. March 1951.
T38	J.C. Martin M.S. Diederich P.J. Bobbitt	A theoretical investigation of the aerodynamics of wing-tail combinations performing time-dependent motions at supersonic speeds. NACA TN 3072. May 1954.
T39	H.S. Ribner F.S. Malvestuto	Stability derivatives of triangular wings at supersonic speeds. NACA Report 908. 1948.
T40	S.M. Harmon	Stability derivatives at supersonic speeds of thin rectangular wings with diagonals ahead of tip Mach lines. NACA Report 925. 1949. NACA TN 1706. November 1948.
T41	J.C. Martin K. Margolis I. Jeffreys	Calculation of lift and pitching moments due to angle of attack and steady pitching velocity at supersonic speeds for thin sweptback tapered wings with streamwise tips and supersonic leading and trailing edges. NACA TN 2699. June 1952.

REFERENCES (Contd)

No.	Author	Title, etc
T42	A. Robinson J.H. Hunter-Tod	Bound and trailing vortices in the linearized theory of supersonic flow, and the downwash in the wake of a delta wing. College of Aeronautics Cranfield Report No.10. ARC 11,296. R & M 2409. October 1947.
T43	J.C. Martin	The calculation of downwash behind wings of arbitrary planform at supersonic speeds. NACA TN 2135. July 1950.
T44	H.S. Ribner	Time-dependent downwash at the tail and the pitching moment due to normal acceleration at supersonic speeds. NACA TN 2042. 1950.
T45	K.W. Mangler	The short period longitudinal stability derivatives for a delta wing at supersonic speeds. RAE Tech Note Aero 2099. ARC 14,085. March 1951.
T46	I.C. Statler	Effects of non-stationary flow on supersonic dynamic stability characteristics including calculation of tail loads for longitudinal sinusoidal motion. Cornell Aeronautical Laboratory, Inc. Report No. TB-541-F-2. P39530. February 1951.
T47	A. Henderson, Jr.	Pitching moment derivatives C_{m_q} and C_{m_α} at supersonic speeds for a slender-delta-wing and slender-body combination and approximate solutions for broad-delta-wing and slender-body combinations. NACA TN 2553. December 1951.
T48	J.C. Martin N. Gerber	The effect of thickness on pitching airfoils at supersonic speeds. Ballistic Research Laboratories Report 859, P42265. April 1953.
T49	I.E. Garrick	Some research on high-speed flutter. Proceedings of Anglo-American Aeronautical Conference. 1951.

REFERENCES (Contd)

Experiment

No.	Author	Title, etc
E1	C. Scruton L. Woodgate A.J. Alexander	Measurements of the aerodynamic derivatives for a clipped delta wing of low aspect ratio describing pitching and plunging oscillations in incompressible flow. ARC 15,499. December 1952.
E2	G.F. Moss	Low speed wind tunnel measurements of longitudinal oscillatory derivatives on three wing planforms. RAE Tech Note Aero 2208. ARC 15,972. November 1952.
E3	T. Lawrence R. Harmer	The study of stability at transonic speeds by free flying models: Tests on a tailless aeroplane with 45° delta wing (E27/46). RAE Tech Note Aero 2220. ARC 15,589. January 1953.
E4	J.B. Bratt W.G. Raymer J.E.G. Townsend	Measurements of the direct pitching moment derivatives for an Avro B35/46 wing and a DH 108 wing at transonic speeds. ARC 15,486. December 1952.
E5	D.J. Raney J.G. Trebble	Low speed wind tunnel tests on a model of a revised version of a delta wing bomber (Avro B35/46). RAE Aero Report 2416. ARC 14,286. March 1951.
E6	J.B. Bratt W.G. Raymer J.E.G. Townsend	Measurements of the direct pitching moment derivatives for an English Electric transonic wing and a Boulton Paul delta at transonic speeds. ARC 15,206. September 1952.
E7	C. Scruton L. Woodgate A.J. Alexander	Measurements of the aerodynamic derivatives for an arrowhead and a delta wing of low aspect ratio describing pitching and plunging oscillations in incompressible flow. ARC 16,210. October 1953.
E8	W.C. Triplett R.D. Van Dyke	Preliminary flight investigation of the dynamic longitudinal-stability characteristics of a 35° swept-wing airplane. NACA/TIB/2577; NACA RM A50J09a. December 1950.
E9	M. Tobak D.E. Reese B.H. Beam	Experimental damping in pitch of 45° triangular wings. NACA/TIB/2725; NACA RM A50J26. December 1950.
E10	G.L. Mitcham J.E. Stevens H.P. Norris	Aerodynamic characteristics and flying qualities of a tailless triangular-wing airplane configuration as obtained from flights of rocket-propelled models at transonic and low supersonic speeds. NACA/TIB/2644. RM L9L07. February 1950.
E11	C.L. Gillis R.F. Peck A.J. Vitale	Preliminary results from a free-flight investigation at transonic and supersonic speeds of the longitudinal stability and control characteristics of an airplane configuration with a thin straight wing of aspect ratio 3. NACA/TIB/2890; NACA RM L9K25a. February 1950.

REFERENCES (Contd)

No.	Author	Title, etc
E12	C.L. Gillis A.J. Vitale	Wing-on and wing-off longitudinal characteristics of an airplane configuration having a thin unswept tapered wing of aspect ratio 3, as obtained from rocket-propelled models at Mach numbers from 0.8 to 1.4. NACA/TIB/2911. RM L50K16. March 1951.
E13	G.L. Mitcham N.L. Crabhill J.E. Stevens	Flight determination of the drag and longitudinal stability and control characteristics of a rocket powered model of a 60° delta-wing airplane from Mach numbers of 0.75 to 1.70. NACA/TIB/2941. NACA RM L51I04. November 1951.
E14	J.H. Parks A.B. Kehlet	Longitudinal stability, trim, and drag characteristics of a rocket-propelled model of an airplane configuration having a 45° sweptback wing and an unswept horizontal tail. NACA/TIB/3284. NACA RM L52F05. August 1952.
E15	C.T. D'Aiutolo R.N. Parker	Preliminary investigation of the low-amplitude damping in pitch of tailless delta-and-swept-wing configurations at Mach numbers from 0.7 to 1.35. NACA/TIB/3286. NACA RM L52G09. August 1952.
E16	B.H. Beam	The effects of oscillation amplitude and frequency on the experimental damping in pitch of a triangular wing having an aspect ratio of 4. NACA/TIB/3347. NACA RM A52G07. September 1952.
E17	E.C. Holleman	Longitudinal frequency-response and stability characteristics of the Douglas D-558-II airplane, as determined from transient response, to a Mach number of 0.96. NACA/TIB/3495, NACA RM L52E02. September 1952.
E18	E.E. Angle E.L. Holleman	Longitudinal frequency-response characteristics of the Douglas D-558-I airplane, as determined from experimental transient-response histories, to a Mach number of 0.90. NACA/TIB/3415, NACA RM L51K28. February 1952.
E19	J.C. McFall, Jr. J.A. Hollinger	Longitudinal stability, control effectiveness and drag characteristics at transonic speeds of a rocket propelled model of an airplane configuration having an unswept tapered wing of aspect ratio 3 and NACA 65A004.5 airfoil sections. NACA/TIB/3585, NACA RM L52L04. January 1953.
E20	M. Tobak	Damping in pitch of low-aspect-ratio wings at subsonic and supersonic speeds. NACA/TIB/3686, NACA RM A52L04a. April 1953.
E21	S. Faber J.M. Eggleston	A transonic investigation by the free-fall method of an airplane configuration having 45° sweptback wing and tail surfaces. NACA/TIB/3758. NACA RM L53D10. June 1953.

REFERENCES (Contd)

No.	Author	Title, etc
E22	R.G. Arbic W. Gillespie	Free-flight longitudinal-stability investigation including some effects of wing elasticity from Mach numbers of 0.85 to 1.34 of a tailless missile configuration having a 45° sweptback wing of aspect ratio 5.5. NACA/TIB/3845, NACA RM L53F18. August 1953.
E23	C.L. Gillis R. Chapman, Jr.	Summary of pitch-damping derivatives of complete airplane and missile configurations as measured in flight at transonic and supersonic speeds. NACA RM L52K20. 1953.
E24	A.J. Vitale	Effects of wing elasticity on the aerodynamic characteristics of an airplane configuration, having 45° sweptback wings, as obtained from free-flight rocket-model tests at transonic speeds. NACA/TIB/3606, NACA RM L52L30. January 1953.
E25	W.B. Kemp, Jr. R.E. Becht	Damping-in-pitch characteristics at high subsonic and transonic speeds of four 35° sweptback wings. NACA/TIB/3922. - RM L53G29a. October 1953.
E26	A. Henderson, Jr.	Investigation at Mach numbers of 1.62, 1.93 and 2.41 of the effect of oscillation amplitude on the damping in pitch of delta-wing-body combinations. NACA/TIB/3940. NACA RM L53H25. October 1953.
E27	E. Widmayer S.A. Clevenson S.A. Leadbeatter	Some measurements of aerodynamic forces and moments at subsonic speeds on a rectangular wing of aspect ratio 2 oscillating about the midchord. NACA/TIB/3860, NACA RM 53F19. ARC 16,757. August 1953.
E28	S.A. Leadbeatter S.A. Clevenson	Some measurements at subsonic speeds of the aerodynamic forces and moments on two delta wings of aspect ratios 2 and 4 oscillating about the midchord. NACA/TIB/4039, NACA RM L53J26A. December 1953.
E29	J. Vitale J.C. McFall, Jr. J.D. Morrow	Longitudinal stability and drag characteristics at Mach numbers from 0.75 to 1.5 of an airplane configuration having a 60° swept wing of aspect ratio 2.24 as obtained from rocket-propelled models. NACA/TIB/3435, NACA RM L51K06. April 1952.
E30	J.R. Hall	Free-flight investigation of longitudinal stability and control of a rocket-propelled missile model having cruciform, triangular inline wings and tails. NACA/TIB/3071. NACA RM L51J17. March 1952.
E31	M.T. Moul H.T. Baber	The longitudinal stability and control characteristics of a 60° delta wing missile having half-delta tip controls as obtained from a free-flight investigation at transonic and supersonic speeds. NACA/TIB/3398, NACA RM L52H14. October, 1952.

REFERENCES (Contd)

No.	Author	Title, etc
E32	R.F. Peck J.L. Mitchell	Rocket-model investigation of longitudinal stability and drag characteristics of an airplane configuration having a 60° delta wing and a high unswept horizontal tail. NACA/TIB/3546, NACA RM L52K04a. January 1953.
E33	R. Chapman, Jr. J.D. Morrow	Longitudinal stability and drag characteristics at Mach numbers from 0.70 to 1.37 of rocket-propelled models having a modified triangular wing. NACA/TIB/3105, NACA RM L52A31. May 1952.
E34	C.A. Sandahl J.R. Hall	Free-flight investigation of the longitudinal stability and control of a rocket-propelled missile model having cruciform, triangular, interdigitated wing and tails. NACA/TIB/3134, NACA RM L51B15. July 1951.
E35	J.H. Parks A.B. Kehlet	Longitudinal stability and trim of two rocket-propelled airplane models having 45° sweptback wings and tails with the horizontal tail mounted in two positions. NACA/TIB/4032, NACA RM L53J12a. December 1953.
E36	T.H. Kerr	Flight investigation of the short period longitudinal oscillation on a 45° delta aircraft (Boulton Paul P111). RAE - to be published.
E37	J.Jukes K. Smith	Flight measurements of the short period longitudinal oscillation of a 50° delta aircraft (Avro 707A) at high Mach number. RAE Tech Note 2319. ARC 17,289. July 1954.
E38	A.J. Vitale J.C. McFall	Longitudinal stability characteristics at transonic speeds of a canard configuration having a 45° sweptback wing of aspect ratio 6.0 and NACA 65A009 airfoil section. NACA/TIB/4490. NACA RM L54I01. November 1954.

Attached:- Appendices I, II and III
Tables I, II and III
Drgs. 32316S - 32353S
Detachable Abstract Cards

Advance Distribution

PDSR(A)	
ADARD(Res)	Aotion
ADSR(Rec)	
DGTD(A)	
TPA3/TIB	150+90
DARD	
DDARD	
ARD(Structures)	
PDGWRD	
PDRD(Aircraft)	
DMARD(RAF)	
DMARD(RN)	
ADRDL1	
ADRDL2	
ADRDN	
ARD(Proj)	
DCARD	
ADRDAC1	
ADRDAC2	
A & AEE	
MAEE	
NPL(Aero Div)	
RTO at A.V. Roes Ltd	
RTO at Boulton Paul Aircraft Co.	

APPENDIX I

Asymptotic Expansions for the Influence Functions of Multhopp's Subsonic Theory

In this appendix we shall derive expansions for the influence functions i, j, ii, and jj which apply for large distances from the wing in the longitudinal direction, but without any definite restriction of the lateral coordinates. These expansions enable us to discuss the behaviour of the influence functions under these conditions, and in addition provide an alternative means of evaluating the influence functions, thus opening up perhaps a simpler approach to the general problem of downwash.

To avoid making the discussion unduly long reference will be made to results obtained in ref. T6.*

Our starting point is equation (T6.41) from which we have,

$$-\frac{\bar{w}_2(x,y)}{V} = \frac{\omega}{8\pi(1-M^2)V}\iint_S \frac{\bar{\epsilon}(x',y')}{(y-y')^2} \times\left[\int_{-\infty}^{x}\left\{1+\frac{x_o-x_o'}{\sqrt{(x_o-x')^2+(1-M^2)(y-y')^2}}\right\}dx_o\right]dx'dy'. \quad (I.1)$$

Performing the integration with respect to x_o we obtain,

$$-\frac{\bar{w}_2(x,y)}{V} = \frac{\omega}{8\pi(1-M^2)V}\iint_S \frac{\bar{\epsilon}(x',y')}{(y-y')^2}\left\{(x-x')+\sqrt{(x-x')^2+(1-M^2)(y-y')^2}\right\}dx'dy'. \quad (I.2)$$

Inserting for $\bar{\epsilon}$ from (T6.42) gives,

$$-\frac{\bar{w}_2(x,y)}{V} = \frac{\omega}{\pi^2 V(1-M^2)}\iint_S \frac{c(\eta')d\eta'}{(\eta-\eta')^2} \times\left[\left\{\gamma(\eta')\cot\frac{\varphi}{2}+4\mu(\eta')\left(\cot\frac{\varphi}{2}-2\sin\varphi\right)\right\}\frac{g(x'y')}{c(\eta')}\right]d\left(\frac{x'}{c(\eta')}\right)$$

where $$\frac{g(x',y')}{c(y')} = \frac{1}{c(y')}\left\{(x-x')+\sqrt{(x-x')^2+(1-M^2)(y-y')^2}\right\}. \quad (I.3)$$

Comparing (I.3) with (T6.45) we then see that,

$$ii(x,y) = \frac{2}{\pi}\int_0^1 \cot\frac{\varphi}{2}\left[\frac{x-x'}{c_\nu}+\frac{1}{c_\nu}\sqrt{(x-x')^2+(1-M^2)(y-y')^2}\right]d\left(\frac{x'}{c_\nu}\right). \quad (I.4)$$

* The reference will take the form (T6.41) where the second set of numbers is the number of the relevant equation of ref. T6.

Introducing the usual non-dimensional coordinates,

$$X = \frac{x-x_\ell}{c(y')} \quad \text{and} \quad Y = \frac{(y-y')(1-M^2)^{\frac{1}{2}}}{c(y')},$$

and the relationship between X' and φ,

$$X' = \tfrac{1}{2}(1 - \cos\varphi),$$

we can rewrite the equation (I.4) thus,

$$ii(X,Y) = \frac{1}{\pi}\int_0^\pi (1+\cos\varphi)\left\{(X-\tfrac{1}{4}) + \left(\frac{2\cos\varphi - 1}{4}\right)\right\} d\varphi$$

$$+ \frac{1}{\pi}\int_0^\pi (1+\cos\varphi)\left[\left\{(X-\tfrac{1}{4}) + \left(\frac{2\cos\varphi-1}{4}\right)\right\}^2 + Y^2\right]^{\frac{1}{2}} d\varphi . \qquad (I.5)$$

Introducing new coordinates,

$$X_{\frac{1}{4}} = (X-\tfrac{1}{4}), \quad \text{and} \quad \psi = \frac{Y}{X-\frac{1}{4}},$$

we can write equation (I.5), after some reduction, as

$$ii(X_{\frac{1}{4}},\psi) = X_{\frac{1}{4}} + \frac{X_{\frac{1}{4}}}{\pi}\int_0^\pi (1+\cos\varphi)\left[(1+\psi^2) + \frac{f}{X_{\frac{1}{4}}}\left(2 + \frac{f}{X_{\frac{1}{4}}}\right)\right]^{\frac{1}{2}} d\varphi \qquad (I.6)$$

where $$f = \frac{2\cos\varphi - 1}{4}.$$

For large values of $X_{\frac{1}{4}}$ we can expand the integrand in the second term to give,

$$ii(X_{\frac{1}{4}},\psi) = X_{\frac{1}{4}} + \frac{X_{\frac{1}{4}}(1+\psi^2)^{\frac{1}{2}}}{\pi}\int_0^\pi (1+\cos\varphi)\left\{1 + \frac{1}{1+\psi^2}\cdot\frac{f}{X_{\frac{1}{4}}} + \frac{\psi^2}{2(1+\psi^2)^2}\left(\frac{f}{X_{\frac{1}{4}}}\right)^2\right.$$

$$\left. - \frac{\psi^2}{2(1+\psi^2)^3}\left(\frac{f}{X_{\frac{1}{4}}}\right)^3 \cdots\right\} d\varphi . \qquad (I.7)$$

The integrals involved in (I.7) are of the type,

$$I_n = \int_0^\pi (1+\cos\varphi)\left(\frac{2\cos\varphi - 1}{4}\right)^n d\varphi$$

which for $n = 1, 2, 3$ gives,

$$I_1 = 0, \quad I_2 = \frac{\pi}{16}, \quad \text{and} \quad I_3 = -\frac{\pi}{64} \quad \text{respectively.}$$

Inserting in equation (I.7) we finally obtain the following asymptotic development of the influence function ii,

$$ii(X,\psi) = (X-\tfrac{1}{4})\left(1+\sqrt{1+\psi^2}\right) + \frac{(X-\tfrac{1}{4})\,\psi^2}{32(1+\psi^2)^{3/2}}\cdot\frac{1}{(X-\tfrac{1}{4})} + \frac{\psi^2}{128(1+\psi^2)^{5/2}}\cdot\frac{1}{(X-\tfrac{1}{4})^2} + \ldots \qquad (I.8)$$

From this we see that as $X \to \infty$, $ii \to 2(X-\frac{1}{4})$, and further that by comparing with the expansion of the influence function i, given below, that for large values of X we may approximate by writing,

$$ii \approx Xi \approx \frac{X}{\sigma_\nu}\left[1 + \frac{1}{(1+\psi^2)} + \ldots\right]$$

This approximation plays an important role in the development of the simple relation for the tailplane increment in $m_{\dot\theta}$, see Appendix II.

We can, of course, expand the function jj similarly. Again, comparing with equation (T645) we have for jj, the influence function associated with μ,

$$jj = \frac{8}{\pi}\int_0^1 (\cot\tfrac{\varphi}{2} - 2\sin\varphi)\left[\frac{x-x'}{\sigma_\nu} + \frac{\{(x-x')^2 + (1-M^2)(y-y')^2\}^{\frac{1}{2}}}{\sigma_\nu}\right]\frac{dx'}{\sigma_\nu}$$

$$= \frac{4}{\pi}\int_0^\pi (\cos\varphi + \cos 2\varphi)\left\{(X-\tfrac{1}{4}) + \frac{2\cos\varphi - 1}{4}\right\}d\varphi$$

$$+ \frac{4}{\pi}\int_0^\pi (\cos\varphi + \cos 2\varphi)\left\{(1+\psi^2) + \frac{f}{X_{\frac{1}{4}}}\left(2 + \frac{f}{X_{\frac{1}{4}}}\right)\right\}^{\frac{1}{2}} d\varphi \,. \qquad (I.9)$$

Of the first integral the coefficient of $(X-\frac{1}{4})$ is zero, and

$$\int_0^\pi (\cos\varphi + \cos 2\varphi)(2\cos\varphi - 1)\,d\varphi = \pi \,.$$

Expanding the second integral we obtain integrals of the type

$$I'_n = \int_0^\pi (\cos\varphi + \cos 2\varphi)\left(\frac{2\cos\varphi - 1}{4}\right)^n d\varphi$$

which for $n = 1$, 2, and 3 gives $\frac{\pi}{4}$, $-\frac{\pi}{16}$ and $\frac{3\pi}{64}$ respectively.

This yields the following expansion for large values of $X_{\frac{1}{4}}$,

$$jj(X_{\frac{1}{4}},\psi) = 1 + \frac{4X_{\frac{1}{4}}}{\pi}(1+\psi^2)^{\frac{1}{2}}\left\{\frac{I'_1}{(1+\psi^2)X_{\frac{1}{4}}} + \frac{\psi^2}{2(1+\psi^2)^2}\cdot\frac{I'_2}{X^2_{\frac{1}{4}}} - \frac{\psi^2}{2(1+\psi^2)^3}\cdot\frac{I'_3}{X^3_{\frac{1}{4}}} + \ldots\right\} \qquad (I.10)$$

Inserting the values of I_1', I_2', I_3' we have finally,

$$jj(X,\psi) = \left\{1 + \frac{1}{(1+\psi^2)^{\frac{1}{2}}}\right\} - \frac{\psi^2}{8(1+\psi^2)^{3/2}} \cdot \frac{1}{(X-\frac{1}{4})} - \frac{3\psi^2}{32(1+\psi^2)^{5/2}} \cdot \frac{1}{(X-\frac{1}{4})^2} - \ldots, \qquad (I.11)$$

so that as $X \to \infty$, $jj(X,Y) \to 2$.

Returning to the downwash equation for steady flow we can readily deduce similar expansions for the influence functions, that then occur, i and j. These are,

$$i(X,\psi) = \left\{1 + \frac{1}{(1+\psi^2)^{\frac{1}{2}}}\right\} - \frac{3\psi^2}{32(1+\psi^2)^{5/2}} \cdot \frac{1}{(X-\frac{1}{4})^2} - \ldots, \qquad (I.12)$$

of which the first term clearly corresponds to concentration of the load at the quarter-chord point, and,

$$j(X,\psi) = \frac{\psi^2}{(1+\psi^2)^{3/2}} \cdot \frac{1}{(X-\frac{1}{4})} + \frac{3\psi^2}{8(1+\psi^2)^{5/2}} \cdot \frac{1}{(X-\frac{1}{4})^2} - \ldots . \qquad (I.13)$$

It is easily shown that these expansions are equivalent to those given by Multhopp.

From the form of the above expansions it is reasonable to suppose that for the purpose of calculating downwash at an appreciable distance behind the wing (e.g. at tailplane) the first terms only would be adequate approximations to the functions. These approximations are presented graphically in Fig.9, and calculations of downwash referred to elsewhere in the text indicate that they are in fact good approximations.

APPENDIX II

Downwash behind a wing performing low pitching oscillations of small amplitude, and tailplane contributions to $z_{\dot\theta}$ and $m_{\dot\theta}$

1. Subsonic Flow

To simplify the analysis, we assume the wing and tailplane to be coplanar. Furthermore, we shall assume no distortion of the trailing vortex sheet. Taken together with the restriction of small amplitude, as is appropriate in a linearised theory, these assumptions imply that we may set $z = 0$ in the general equation for the downwash. Accordingly our starting point is equation (T6.36,37) which states that the upwash at a point $(x,y,0)$ is given by,

$$w = R\ell\left[\bar{w}\, e^{i\omega\left(t + \frac{x}{V}\cdot\frac{M^2}{1-M^2}\right)}\right] \qquad \bar{w} = \frac{\bar{w}}{V}$$

where

$$\bar{w} = \frac{V(1-M^2)}{8\pi}\int_{-\infty}^{x}\left\{\iint_S \frac{\bar{\ell}(x',y')\,dx'dy'}{\left[(x_o-x')^2 + (1-M^2)(y-y')^2\right]^{3/2}}\right\} e^{\frac{i\omega(x_o-x)}{V(1-M^2)}}\,dx_o \qquad \text{(II.1)}$$

It is admissible for slow oscillations (or retaining only the first power of ω) to approximate to equation (II.1) by expanding the exponential term. We can then write

$$\bar{w} = \bar{w}_1 + i\bar{w}_2$$

where

$$\bar{w}(x,y) = \frac{V(1-M^2)}{8\pi}\int_{-\infty}^{x}\left\{\iint_S \frac{\bar{\ell}(x',y')\,dx'dy'}{\left[(x_o-x')^2 + (1-M^2)(y-y')^2\right]^{3/2}}\right\} dx_o$$

$$-\bar{w}_2(x,y) = \frac{\omega}{8\pi}\int_{-\infty}^{x}(x-x_o)\left\{\iint_S \frac{\bar{\ell}(x',y')\,dx'dy'}{\left[(x_o-x')^2 + (1-M^2)(y-y')^2\right]^{3/2}}\right\} dx_o \qquad \text{(II.2)}$$

The loading $\bar{\ell}(x',y')$ is made up of a number of terms, which if we retain as the amplitude of oscillation, can be written (in notation of ref.T6),

$$\bar{\ell}(x',y') = \delta^*\left(\bar{\ell}_1 + \frac{i\omega\bar{\sigma}}{V}\bar{\ell}'\right) \qquad \text{(II.3)}$$

with

$$\bar{\ell}' = -\frac{x_o}{\bar{\sigma}}\bar{\ell}_1 + \left(\frac{1-2M^2}{1-M^2}\right)\bar{\ell}_2 + \left(\frac{1}{1-M^2}\right)\bar{\ell}_3 \qquad \text{(II.3a)}$$

where,

$\bar{\ell}_1$ is the loading due to uniform incidence,

$\bar{\ell}_2$ is the loading due to unit steady pitching about the wing apex or incidence equal to $\frac{x}{c}$,

and $\bar{\ell}_3$ is the loading which arises from downwash delay, and gives rise to the $\dot{w}$ derivatives.

The corresponding incidence is given by equation (64).

The integrals of (II.2) are evaluated numerically after introduction of the influence functions, i, j, ii, and jj (see ref.6), giving the summations,

$$-\frac{\bar{w}_1}{V} = b_{\nu\nu}\left(\bar{i}_{\nu\nu}\bar{\gamma}_\nu + \bar{j}_{\nu\nu}\bar{\mu}_\nu\right) - \sum_{-\frac{1}{2}(m-1)}^{\frac{1}{2}(m-1)}{}' b_{\nu n}\left(i_{\nu n}\bar{\gamma}_n + j_{\nu n}\bar{\mu}_n\right)$$

and,

$$\frac{V(1-M^2)}{\omega\bar{c}}\cdot\frac{\bar{w}_2}{V} = b_{\nu\nu}\frac{c_\nu}{\bar{c}}\left(\overline{ii}_{\nu\nu}\bar{\gamma}_\nu + \overline{jj}_{\nu\nu}\bar{\mu}_\nu\right) - \sum_{-\frac{1}{2}(m-1)}^{\frac{1}{2}(m-1)}{}' b_{\nu n}\frac{c_n}{\bar{c}}\left(ii_{\nu n}\bar{\gamma}_n + jj_{\nu n}\bar{\mu}_n\right) \qquad \text{(II.4)}$$

where the prime on the summation symbol indicates that the term for which $n = \nu$ is excluded, and where $\bar{\gamma}_n$ and $\bar{\mu}_n$ correspond to the loading $\bar{\ell}$.

Replacing $\bar{\ell}$ by the loading $\bar{\ell}_1$, $\bar{\ell}_2$ and $\bar{\ell}_3$ according to equations (II.3) we now write,

$$\frac{\bar{w}_1}{V\vartheta^*} = \left(1 - \frac{i\omega x_o}{V}\right)\frac{\bar{w}_{11}}{V} + \left(\frac{1-2M^2}{1-M^2}\right)\frac{i\omega\bar{c}}{V}\cdot\frac{\bar{w}_{12}}{V} + \frac{i\omega\bar{c}}{V(1-M^2)}\cdot\frac{\bar{w}_{13}}{V}$$

and

$$\frac{\bar{w}_2}{V\vartheta^*} = \frac{\omega\bar{c}}{V(1-M^2)}\left\{\frac{\bar{w}_{21}}{V}\cdot\frac{V(1-M^2)}{\omega\bar{c}}\right\} \quad \text{neglecting terms in } \omega^2 \text{ and higher order.} \qquad \text{(II.5)}$$

The second suffix denotes the loading functions to which the particular contribution is related, e.g. $\frac{\bar{w}_{11}}{V}$ is obtained by inserting $\bar{\gamma}_1$ and $\bar{\mu}_1$ for $\bar{\gamma}$ and $\bar{\mu}$ in the first of equations (II.4). To evaluate the upwash we approximate to the first part of equation (II.1) thus,

$$\frac{w}{V} = R\ell\,\frac{\bar{w}}{V}\,e^{i\omega t}\left\{1 + \frac{i\omega x}{V}\cdot\frac{M^2}{(1-M^2)}\right\}, \qquad \text{(II.6)}$$

and also write,

$$\frac{\bar{w}}{V} = \vartheta^* \left\{F_1 + \frac{i\omega\bar{c}}{V} F_2\right\} \qquad (II.7)$$

where, by virtue of (II.5)

$$F_1(x,y) = \frac{\bar{w}_{11}}{V},$$

and is in fact the <u>upwash</u> for uniform incidence in a steady flow;

$$F_2(x,y) = \left[-\frac{x_o}{\bar{c}} \cdot \frac{\bar{w}_{11}}{V} + \left(\frac{1-2M^2}{1-M^2}\right)\frac{\bar{w}_{12}}{V} + \frac{1}{(1-M^2)} \cdot \frac{\bar{w}_{13}}{V} + \frac{\bar{w}_{21}}{V} \cdot \frac{V}{\omega\bar{c}}\right].$$

Inserting from equation (II.7) in equation (II.6) we have

$$\frac{w}{V} = R\ell\ \vartheta^*\ e^{i\omega t}\left\{F_1(x,y) + \frac{i\omega\bar{c}}{V}\left[F_2(x,y) + \frac{x}{\bar{c}} \cdot \frac{M^2}{(1-M^2)} F_1(x,y)\right]\right\}$$

$$= \vartheta\ F_1(x,y) + \dot{\vartheta}\frac{\bar{c}}{V}\left\{F_2(x,y) + \frac{x}{\bar{c}} \cdot \frac{M^2}{(1-M^2)} F_1(x,y)\right\}. \qquad (II.8)$$

It thus follows that the effective incidence at a point (x,y,0), which is the sum of the geometric incidence and the upwash as given by (II.8), is

$$\theta(x,y,0) = (1+F_1)\vartheta + \frac{\ell}{V}\dot{\vartheta} + \frac{\bar{c}}{V}\dot{\vartheta}\left\{F_2 + \frac{x}{\bar{c}} \cdot \frac{M^2}{(1-M^2)} F_1\right\}, \qquad (II.9)$$

Now for the calculation of forces and moments on the aircraft we shall assume that tailplanes are generally sufficiently small that the distribution of incidence defined by (II.9) may be replaced by a mean value, obtained by taking a mean of F_1 and F_2. These mean values will be denoted by bars over the symbol. We therefore write,

$$\bar{\vartheta}_t = (1+\bar{F}_1)\vartheta + \left[\frac{\ell}{V} + \frac{\bar{c}}{V}\left\{\bar{F}_2 + \frac{x}{\bar{c}} \cdot \frac{M^2}{(1-M^2)}\bar{F}_1\right\}\right]\dot{\vartheta} \qquad (II.10)$$

from which we have, to the order of accuracy of the remainder of the calculation,

$$\dot{\bar{\vartheta}}_t = (1+\bar{F}_1)\dot{\vartheta}. \qquad (II.11)$$

The increment in the force along the z-axis due to the tailplane is,

$$\Delta Z = \left(\frac{\partial Z}{\partial\dot{\vartheta}}\right)_t \dot{\bar{\vartheta}}_t + \left(\frac{\partial Z}{\partial\vartheta}\right)_t \bar{\vartheta}_t.$$

Substituting for $\dot{\bar{\vartheta}}_t$ and $\bar{\vartheta}_t$, and reducing to the usual non-dimensional derivative form we see that,

$$\Delta z_{\dot\theta} = \frac{S_t}{S}\frac{\bar c_t}{\bar c}\left[(1+\bar F_1)\, z_{\dot\theta_t} + \frac{\bar c}{\bar c_t}\left\{\frac{\ell}{\bar c} + \bar F_2 + \frac{x}{\bar c}\cdot\frac{M^2}{(1-M^2)}\bar F_1\right\} z_{\theta_t}\right]. \tag{II.12}$$

This may be simplified to yield the approximate forms (equations 18,20) discussed in the main text of the paper. The simplest of those (cf. equation 14) calls perhaps for a somewhat more detailed discussion here, but this is deferred until after the calculation of the pitching moment contribution. The increment in the pitching moment is,

$$\Delta M = \ell Z_t + M_{\dot\theta_t}\dot\theta_t + M_{\theta_t}\theta_t .$$

From this we readily deduce,

$$\Delta m_{\dot\theta} = \frac{S_t}{S}\left(\frac{\bar c_t}{\bar c}\right)\left(\frac{\ell}{\bar c}\right)\left[(1+\bar F_1) z_{\dot\theta_t} + \frac{\bar c}{\bar c_t}\left\{\frac{\ell}{\bar c} + \bar F_2 + \frac{x}{\bar c}\cdot\frac{M^2}{(1-M^2)}\bar F_1\right\} z_{\theta_t}\right]$$
$$+ \frac{S_t}{S}\left(\frac{\bar c_t}{\bar c}\right)^2\left[(1+\bar F_1) m_{\dot\theta_t} + \left\{\frac{\ell}{\bar c} + \bar F_2 + \frac{x}{\bar c}\cdot\frac{M^2}{(1-M^2)}F_1\right\} m_{\theta_t}\right]. \tag{II.13}$$

In both (II.12) and (II.13) z_{θ_t}, $z_{\dot\theta_t}$ etc. refer to the derivatives of the isolated tail.

Returning now to the approximate forms for $\Delta z_{\dot\theta}$ and $\Delta m_{\dot\theta}$ we note that retention of the terms in z_{θ_t} only implies a consideration of the bracket

$$\left\{\frac{\ell}{\bar c} + \bar F_2 + \frac{x}{\bar c}\cdot\frac{M^2}{(1-M^2)}\bar F_1\right\}.$$

At first sight there may seem little connection between this and the simple expression (equation 14) given in the section on the tailplane contributions, but we assume that the tail and wing are far apart, so retain only terms of highest order in ℓ or x. Then of the terms in $\bar F_2$ the only one which we need consider further is that involving $\bar w_{21}$. From Appendix I we see that we can approximate to ii by $\frac{x}{c_\nu}$ i, and jj by 2 for sufficiently large values of x. Ignoring the terms in μ we are thus led to the approximation

$$\frac{\bar w_{21}}{V}\cdot\frac{V}{\omega\bar c} \approx -\frac{x}{\bar c}\cdot\frac{1}{(1-M^2)}\cdot\frac{\bar w_{11}}{V}. \tag{II.14}$$

Introducing this approximation, and combining it with the term in $\bar F_1$ we see that the bracket above can be written approximately as,

$$\frac{\ell}{\bar c} - \frac{x}{\bar c}\cdot\frac{\bar w_{11}}{V} \approx \frac{\ell}{\bar c}\left(1 + \frac{d\varepsilon}{d\alpha}\right) \tag{II.15}$$

with $x \approx \ell$, and introducing the more familiar notation for the downwash for steady uniform incidence. This leads to the well-known approximation without further restrictions on M.

2. Sonic Flow (Delta Wings)

We have dealt with the problem of a tailplane-wing combination of any planform at subsonic speeds. At transonic speeds there is certain to be a marked effect on the downwash at the tailplane, and hence on Δz_ϑ and Δm_ϑ, due to the presence of shock-waves on the wing. No analytical approach can at present deal with this extremely complex problem, but it is possible, as mentioned in the main text, to formulate the linearised inviscid flow theory (excluding shock-waves) in such a manner that we can include sonic speed. At this limit the theory becomes appreciably less unwieldy and the solution has been obtained for delta wings by Mangler[T12*]. We shall now proceed to evaluate the downwash field of such a wing, and hence the contributions to z_ϑ and m_ϑ. In general, for any wing we have that the upwash at a point $(x,y,0)$ is given by,[T12]

$$\frac{w}{V} = \frac{\bar{w}}{V} e^{int} = (w_r + i\omega w_i) e^{int} \qquad \text{(II.16)}$$

where

$$w_r(x,y) = \frac{1}{4\pi} \iint_S L_r(x',y') \frac{dx'dy'}{(y-y')^2} \qquad \text{(II.16a)}$$

and,

$$w_i(x,y) = \frac{1}{4\pi} \iint_{S+S_w} L_i(x',y') \frac{dx'dy'}{(y-y')^2} - F(x,y) \qquad \text{(II.16b)}$$

in which,

$$F(x,y) = \frac{\vartheta^*}{2\pi\bar{o}} (x-x_t) \int_{-s}^{s} \frac{\sqrt{s^2-y'^2}}{(y-y')^2} dx'dy' + \frac{1}{4\pi} \iint_S \left[\int_{x_\ell}^{x'} L_r(\xi,y') \frac{d\xi}{2\bar{o}} \right] \frac{dx'dy'}{(y-y')^2}$$

$$+ F_1(x,y) \qquad \text{(II.16c)}$$

and,

$$F_1(x,y) = \frac{1}{4\pi} \iint_S L_r(x',y') \frac{1}{\omega} \sin \frac{\omega(y-y')^2}{2\bar{o}(x-x')} \cdot \frac{dx'dy'}{(y-y')^2}$$

$$\approx \frac{1}{4\pi} \iint_S L_r(x',y') \frac{dx'dy'}{2\bar{o}(x-x')}, \qquad \text{(II.16d)}$$

since (x,y) lies outside the wing and so we may replace the sine by its argument. S is wing area and S_w area of wake ahead of $(x,y,0)$.

* The more general case of the cropped delta wing has been considered by Mangler and Thomas but the (unpublished) solutions so far obtained are either in error by some unknown amount (probably not very pronounced) or whilst essentially correct indicate that the higher order terms in ω may have coefficients involving terms like $\ell n\lambda$ and $1/\lambda$ (λ = taper ratio) so rendering some expansions unsuitable for use at the small values of λ, normally used for cropped delta wings.

Now for the particular family of wings we are considering, we have the following solutions for the modified loadings L_r, and L_i,[T12]

$$L_r(x',y') = 4\vartheta^* \frac{\partial}{\partial x'} \sqrt{s_\ell^2 - y'^2}$$

$$L_i = L_{i0} + L_{i1} + L_{iq} ,$$

where,

$$L_{i0}(x',y') = \frac{2\vartheta^*}{\bar{c}} \sqrt{s_\ell^2 - y'^2} ,$$

$$L_{i1}(x',y') = -2\vartheta^* \cot^2\Lambda_\ell \frac{\partial}{\partial x'} \left\{ -\frac{x'}{\bar{c}} \sqrt{s_\ell^2 - y'^2} \, \ell n \frac{\gamma\omega x'}{8\bar{c}} \cot^2\Lambda_\ell \right\}$$

and, finally,

$$L_{iq}(x',y') = 4\vartheta^* \frac{\partial}{\partial x'} \left\{ \frac{x' - x_0}{\bar{c}} \sqrt{s_\ell^2 - y'^2} \right\} .$$

The functions are now introduced into equations (II.16) and (II.16a,b,c,d) and the resulting integrals evaluated. We begin by considering an integral of the form,

$$H(x,y) = \frac{1}{4\pi} \int_{-s}^{s} \int_{x_\ell}^{c_r} \frac{\partial}{\partial x'} \left\{ f(x') \sqrt{s_\ell^2 - y'^2} \right\} \frac{dx'dy'}{(y-y')^2}$$

$$= \frac{1}{4\pi} \int_{-s}^{s} \frac{dy'}{(y-y')} \left[f(x') \sqrt{s_\ell^2 - y'^2} \right]_{x_\ell = |y'| \tan\Lambda_\ell}^{c_r}$$

$$= \frac{f(c_r)}{4\pi} \int_{-s}^{s} \frac{\sqrt{s^2 - y'^2}}{(y-y')^2} \, dy' . \qquad \text{(II.17)}$$

We have to take the principal value of this integral which can be shown to be $-\pi$ for $y < s$ (Mangler, ref.T26), a condition usually satisfied by a point anywhere on a tailplane.

As a special case we deduce that $w_r = -\vartheta^*$ for all positive values of $x > c_r$ and for $y < s$. The next stage is to evaluate the various contributions to $w_i(x,y)$. To calculate $F(x,y)$ consider the integral,

$$\frac{1}{2\bar{c}} \int_{x_\ell}^{x'} L_r(\xi,y') \, d\xi$$

which becomes,

$$\frac{2\theta^*}{\bar{c}}\sqrt{s_\ell^2 - y'^2}, \qquad \text{(II.18)}$$

Thus

$$\frac{1}{4\pi}\iint_S \left[\frac{1}{2\bar{c}}\int_{x_\ell}^{x'} l_r(\xi,y')d\xi\right]\frac{dx'dy'}{(y-y')^2} = \frac{\theta^*}{2\pi\bar{c}}\iint_S \frac{\sqrt{s_\ell^2-y'^2}}{(y-y')^2}\,dx'dy' . \qquad \text{(II.19)}$$

The area S is now divided into two regions S_1 and S_2 defined by $x' \gtrless |y| \tan \Lambda_\ell$, and so we write,

$$\iint_S \frac{\sqrt{s_\ell^2-y'^2}}{(y-y')^2}\,dx'dy' = \int_0^{|y|\tan\Lambda_\ell} dx' \int_{-s_\ell}^{s_\ell} \frac{\sqrt{s_\ell^2-y'^2}}{(y-y')^2}\,dy' + \int_{|y|\tan\Lambda_\ell}^{c_r} dx' \int_{-s_\ell}^{s_\ell} \frac{\sqrt{s_\ell^2-y'^2}}{(y-y')^2}\,dy' . \qquad \text{(II.20)}$$

We have

$$\int_{-s_\ell}^{s_\ell} \frac{\sqrt{s_\ell^2-y'^2}}{(y-y')^2}\,dy' = \left|-\frac{\sqrt{s_\ell^2-y'^2}}{(y-y')} - \sin^{-1}\frac{y'}{s_\ell}\right|_{-s_\ell}^{s_\ell} - y\int_{-s_\ell}^{s_\ell} \frac{dy'}{\sqrt{s_\ell^2-y'^2}\,(y-y')}$$

$$= -\pi - y\int_{-s_\ell}^{s_\ell} \frac{dy'}{\sqrt{s_\ell^2-y'^2}\,(y-y')} . \qquad \text{(II.21)}$$

In the region S_1, $y < s_\ell$ and the integral on right is zero, but in S_2, $y > s_\ell$ and the same integral has the principal value $-\frac{\pi|y|}{y\sqrt{y^2-s_\ell^2}}$. Thus equation (II.20) can be written,

$$\iint_S \frac{\sqrt{s_\ell^2-y'^2}\,dx'dy'}{(y-y')^2} = -\pi\int_0^{c_r} dx' + \pi|y| \int_0^{|y|\tan\Lambda_\ell} \frac{dx'}{\sqrt{y^2-s_\ell^2}}$$

$$= -\pi\left[c_r - \frac{\pi|y|}{2}\tan\Lambda_\ell\right] . \qquad \text{(II.22)}$$

Combining equations (II.19) and (II.22), we have,

$$\frac{1}{4\pi}\iint_S \left[\frac{1}{2\bar{c}}\int_{x_\ell}^{x'} L_r(\xi,y')d\xi\right]\frac{dx'dy'}{(y-y')^2} = -\vartheta^*\left\{1-\frac{\pi}{4}\frac{|y|}{\bar{c}}\tan\Lambda_\ell\right\}. \qquad (II.23)$$

To complete the calculation of $F(x,y)$ we have to determine the function $F_1(x,y)$.

Now

$$F_1(x,y) \approx \frac{1}{4\pi}\iint_S L_r(x',y')\frac{dx'dy'}{2\bar{c}(x-x')}$$

$$= \frac{1}{4\pi}\int_0^{c_r}\int_{-s_\ell}^{s_\ell}\frac{4\vartheta^* s_\ell \frac{ds_\ell}{dx'}}{\sqrt{s_\ell^2-y'^2}}\cdot\frac{dx'dy'}{2\bar{c}(x-x')}$$

$$= \frac{\vartheta^*}{2\bar{c}}\cot^2\Lambda_\ell\int_0^{c_r}\frac{x'dx'}{(x-x')}$$

$$= -\vartheta^*\cot^2\Lambda_\ell\left\{1+\frac{x}{2\bar{c}}\ell n\left(\frac{x-c_r}{x}\right)\right\}. \qquad (II.24)$$

Collecting terms we have, from (II.23) and (II.24),

$$F(x,y) = -\vartheta^*\left[1+\frac{x-x_t}{2\bar{c}}-\frac{\pi}{4}\frac{|y|}{\bar{c}}\tan\Lambda_\ell+\cot^2\Lambda_\ell\left\{1+\frac{x}{2\bar{c}}\ell n\left(\frac{x-c_r}{x}\right)\right\}\right]. \qquad (II.25)$$

It remains to evaluate the contributions to w_i arising from the loadings associated with L_{i0} and L_{i1}.

Over the wing surface the first of these is simply,

$$w_{i0} = \frac{1}{4\pi}\iint_S L_{i0}(x',y')\frac{dx'dy'}{(y-y')^2} = \frac{\vartheta^*}{2\pi\bar{c}}\int_0^{c_r}\int_{-s_\ell}^{s_\ell}\frac{\sqrt{s_\ell^2-y'^2}\,dx'dy'}{(y-y')^2}$$

$$= -\vartheta^*\left\{1-\frac{\pi}{4}\frac{|y|}{\bar{c}}\tan\Lambda_\ell\right\}, \qquad (II.26)$$

and the second is,

$$w_{11} = \frac{1}{4\pi}\iint_S \frac{L_{11}\,dx'dy'}{(y-y')^2}$$

$$= \frac{\theta^* \cot^2\Lambda_\ell}{2\pi}\int_{-s}^{s}\int_{x_\ell}^{c_r} \frac{\partial}{\partial x'}\left\{\sqrt{s_\ell^2 - y'^2}\,\frac{x}{\bar{c}} - \ell n\,\frac{\gamma\omega x'}{8\bar{c}}\cot^2\Lambda_\ell\right\}\frac{dx'dy'}{(y-y')^2}$$

or by use of equation (II.17),

$$w_{11} = -\theta^* \cot^2\Lambda_\ell\, \ell n\,\frac{\gamma\omega}{4}\cdot\cot^2\Lambda_\ell\,. \qquad \text{(II.27)}$$

Finally, there is the contribution due to the steady pitch load function L_{iq}. This is,

$$w_{iq} = \frac{1}{4\pi}\iint_S L_{iq}\,\frac{dx'dy'}{(y-y')^2}$$

$$= \frac{\theta^*}{\pi}\int_{-s}^{s}\int_{x_\ell}^{c_r}\frac{\partial}{\partial x'}\left\{\left(\frac{x'-x_o}{\bar{c}}\right)\sqrt{s_\ell^2-y'^2}\right\}\frac{dx'dy'}{(y-y')^2}$$

$$= -\theta^*\left(2 - \frac{x_o}{\bar{c}}\right) \quad \text{by use of (II.17).} \qquad \text{(II.28)}$$

From equation (28) of ref.T12 we have,

$$L_r(x',y') = \ell_r(x',y') = 0$$

in the wake, and

$$L_i(x',y') = \ell_i(x',y') - \frac{1}{1+M}\int_{x_\ell}^{x'} \ell_r(\xi',y')\,\frac{d\xi'}{\bar{c}}$$

$$= -\frac{1}{1+M}\int_{x_\ell}^{x_t} \ell_r(\xi',y')\,\frac{d\xi'}{\bar{c}} \quad \text{in the wake}$$

$$= -\frac{2\theta^*}{\bar{c}}\sqrt{s^2-y'^2} \quad \text{for wake of delta wing at sonic speed.}$$

Thus

$$\frac{1}{4\pi}\iint_{S_w} L_i(x',y')\,\frac{dx'dy'}{(y-y')^2} = -\frac{\theta^*}{2\pi\bar{c}}\int_{x_t}^{x} dx' \int_{-s}^{s}\frac{\sqrt{s^2-y'^2}}{(y-y')^2}\,dy'$$

$$= \frac{\theta^*(x-x_t)}{2\bar{c}} = \frac{\theta^*}{2\bar{c}}(x-c_r)\,. \qquad \text{(II.29)}$$

Summing the various contributions to w_i, equations (II.25, 26, 27, 28 and 29) we obtain,

$$w_i(x,y) = -\vartheta^* \left\{ 2 - \left(\frac{x - c_r}{\bar{c}}\right) - \frac{x_o}{\bar{c}} - \cot^2\Lambda_\ell \left(1 + \frac{x}{2\bar{c}} \ln \frac{2-2\bar{c}}{x} - \ln \frac{Y\omega}{4} \cot^2\Lambda_\ell \right)\right\} \quad \text{(II.30)}$$

from which we have for the <u>downwash</u> angle

$$-\frac{w}{V} = -\left(w_r + i n \frac{\bar{c}}{V} w_i\right) e^{int}$$

$$= \vartheta^* e^{int} \left(1 - \frac{in\bar{c}}{V} \cdot \frac{w_i}{\vartheta^*}\right)$$

$$= \vartheta + \dot{\vartheta} \frac{\bar{c}}{V} \delta(x) \quad \text{(II.31)}$$

if we write $-\dfrac{w_i}{\vartheta^*} = \delta(x)$. It is interesting to note that for $y < s$ the downwash depends only on the streamwise position of the point (x,y).

In calculating the tailplane contributions to $z_{\dot{\vartheta}}$ and $m_{\dot{\vartheta}}$ we make the same approximation as before, that is, we replace the incidence distribution given by,

$$\vartheta_t = \vartheta + \frac{\ell\dot{\vartheta}}{V} - \vartheta - \dot{\vartheta}\frac{\bar{c}}{V}\delta(x) = \frac{\bar{c}}{V}\dot{\vartheta}\left(\frac{\ell}{\bar{c}} - \delta(x)\right)$$

by a mean value denoted by a bar over the symbols. Using the suffix t to denote derivatives for the isolated tailplane we have,

$$\Delta z_{\dot{\vartheta}} = \frac{\Delta Z_{\dot{\vartheta}}}{\rho V S \bar{c}} = \frac{S_t}{S}\left(\frac{\ell}{\bar{c}} - \bar{\delta}(x)\right) z_{\vartheta_t} \quad \text{(II.32)}$$

and for the moment derivative,

$$\Delta m_{\dot{\vartheta}} = \frac{\Delta M_{\dot{\vartheta}}}{\rho V S \bar{c}^2}$$

$$\Delta m_{\dot{\vartheta}} = \frac{S_t}{S} \cdot \frac{\ell}{\bar{c}}\left(\frac{\ell}{\bar{c}} - \bar{\delta}(x)\right)\left(z_{\vartheta_t} + \frac{\bar{c}_t}{\ell} m_{\vartheta_t}\right). \quad \text{(II.33)}$$

We have as yet not defined ℓ precisely, or in other words fixed the axis to which the tailplane derivatives refer. If, however, we now choose ℓ to be the distance from the aircraft centre of gravity to the aerodynamic centre of the tailplane we have by virtue of the approximate relations $z_\vartheta \approx z_w$, and $m_\vartheta \approx m_w$,

$$\Delta m_\vartheta = \frac{S_t}{S} \cdot \frac{\ell}{\bar{c}} z_{w_t}\left(\frac{\ell}{\bar{c}} - \bar{\delta}(x)\right) = \frac{\ell}{\bar{c}} \Delta z_{\dot{\vartheta}} . \quad \text{(II.34)}$$

We have already discussed the usual simple approximations and its relation to the results obtained in this Appendix for subsonic conditions. It is possible there to establish such a relationship (see section 1). For sonic speeds equation (II.30) shows that a parallel simplification is of much less significance, as can be seen if we consider the behaviour of $\beta(x)$ as x becomes large. The only terms affected are

$$\frac{x}{2\bar{c}} \ell n \left(\frac{x-2\bar{c}}{x}\right), \quad \text{and} \quad \left(\frac{x-c_r}{\bar{c}}\right).$$

For large values of x we may approximate as follows,

$$\frac{x}{c_r} \ell n \left(\frac{x-c_r}{x}\right) = \frac{x}{c_r} \ell n \left(1 - \frac{c_r}{x}\right)$$

$$= -\frac{x}{c_r}\left(\frac{c_r}{x} + \frac{c_r^2}{2x^2} + \cdots\right)$$

$$\approx -1 + \frac{c_r}{2x}.$$

Thus for large x this term is of order -1, and the other term of order $\frac{\ell}{\bar{c}}$.

It follows, therefore, that provided x is such that we are permitted to linearise with respect to ω, $\beta(x) \to \frac{\ell}{\bar{c}} + \text{const.}$ for large x. The simple Glauert result involves neglecting the constant term as compared with $\frac{\ell}{\bar{c}}$, but as the constant term involves a term in $\ell n \omega$ this approximation is of restricted usefulness.

APPENDIX III

Conversion of American Derivatives etc. to their British Equivalents

American Symbol	Meaning	Equivalent	Equivalent in British Symbols
C_{L_α}	$\frac{\partial C_L}{\partial \alpha}$	$\frac{L}{\frac{1}{2}\rho V^2 S} \approx -\frac{2Z}{\frac{1}{2}\rho V^2 S}$	$\approx -2z_w$
C_{m_α}	$\frac{\partial C_m}{\partial \alpha} = \frac{\frac{\partial M}{\partial \alpha}}{\frac{1}{2}\rho V^2 S \bar{\bar{c}}}$	$\frac{2\frac{\partial M}{\partial w}}{\rho V S \bar{o}} \cdot \frac{\bar{\bar{c}}}{\bar{o}}$	$2\frac{\bar{\bar{c}}}{\bar{o}} m_w$
C_{L_q}	$\frac{\partial C_L}{\partial\left(\frac{q\bar{\bar{c}}}{2V}\right)} = \frac{4L_q}{\rho V S \bar{\bar{c}}}$	$\approx -\frac{4Z_q}{\rho V S \bar{o}} \cdot \frac{\bar{\bar{c}}}{\bar{o}}$	$-4\frac{\bar{\bar{c}}}{\bar{o}} z_q$
C_{m_q}	$\frac{\partial C_m}{\partial\left(\frac{q\bar{\bar{c}}}{2V}\right)} = \frac{4M_q}{\rho V S \bar{\bar{c}}^2}$	$\frac{4M_q}{\rho S V \bar{c}^2}\left(\frac{\bar{c}}{\bar{\bar{c}}}\right)^2$	$4\left(\frac{\bar{c}}{\bar{\bar{c}}}\right)^2 m_q$
$C_{L_{\dot{\alpha}}}$	$\frac{\partial C_L}{\partial\left(\frac{\dot{\alpha}\bar{\bar{c}}}{2V}\right)} = \frac{4L_{\dot{\alpha}}}{\rho S \bar{\bar{c}} V}$	$\approx -\frac{4Z_{\dot{w}}}{\rho S \bar{o}} \cdot \frac{\bar{\bar{c}}}{\bar{o}}$	$-4\left(\frac{\bar{c}}{\bar{\bar{c}}}\right) z_{\dot{w}}$
$C_{m_{\dot{\alpha}}}$	$\frac{\partial C_m}{\partial\left(\frac{\dot{\alpha}\bar{\bar{c}}}{2V}\right)} = \frac{4M_{\dot{\alpha}}}{\rho S \bar{\bar{c}}^2 V}$	$\frac{4M_{\dot{w}}}{\rho S \bar{o}^2}\left(\frac{\bar{c}}{\bar{\bar{c}}}\right)^2$	$4\left(\frac{\bar{c}}{\bar{\bar{c}}}\right)^2 m_{\dot{w}}$
$C_{m_q} + C_{m_{\dot{\alpha}}}$			$4\left(\frac{\bar{c}}{\bar{\bar{c}}}\right)^2 m_{\dot{w}}$

Relation between mean chords

$\bar{o}$ = British Standard Mean Chord = $\frac{S}{b}$

$\bar{\bar{c}}$ = American or so-called Aerodynamic Mean Chord

$$= \frac{\int_{-b/2}^{b/2} c^2\, dy}{\int_{-b/2}^{b/2} c\, dy}.$$

For trapezoidal wings we have,

$$\frac{\bar{\bar{c}}}{\bar{o}} = \frac{4}{3} \cdot \frac{(1+\lambda+\lambda^2)}{(1+\lambda)^2}.$$

TABLE I

SWEPT WING of Ref.E20

Wing Geometry etc,* AR = 3; $\Lambda_{\ell} = 45°$; $\lambda = 0.4$; $\frac{S_t}{S} = 0.15$;

$\frac{x}{c}\frac{\ell}{c} = 2.019$; $\frac{\bar{c}_t}{\bar{c}} = 0.45$; $\frac{x}{c} = 2.925$.

M	$(\Delta z_{\dot{\theta}})_1$	$(\Delta z_{\dot{\theta}})_2$	$(\Delta z_{\dot{\theta}})_3$	$(\Delta m_{\dot{\theta}})_1$	$(\Delta m_{\dot{\theta}})_2$	$(\Delta m_{\dot{\theta}})_3$
0.6	-0.86	-0.84	-0.83	-1.74	-1.69	-1.68
0.8	-0.95	-0.93	-0.94	-1.94	-1.88	-1.89

Variation with CG position

$\frac{x_0}{\bar{c}}$	$(\Delta z_{\dot{\theta}})_1$	$(\Delta z_{\dot{\theta}})_2$	$(\Delta z_{\dot{\theta}})_3$	$(\Delta m_{\dot{\theta}})_1$	$(\Delta m_{\dot{\theta}})_2$	$(\Delta m_{\dot{\theta}})_3$
0	-1.04	-1.02	-1.36	-3.05	-2.98	-3.98
0.906	-0.95	-0.93	-0.94	-1.94	-1.88	-1.89
1.425	-0.90	-0.88	-0.70	-1.37	-1.33	-1.05

TABLE II

BP DELTA with Tailplane

Wing Geometry etc,* AR = 3; $\Lambda_{\ell} = 45°$; $\lambda = \frac{1}{7}$; $\frac{S_t}{S} = 0.0998$

$\frac{\bar{c}_t}{\bar{c}} = 0.316$; $\frac{\ell}{\bar{c}} = \begin{matrix}1.503\\2.202\end{matrix}$; $\frac{x}{\bar{c}} = \begin{matrix}2.498\\3.25.\end{matrix}$

$\frac{x_0}{\bar{c}} = 2.498$

M	$(\Delta z_{\dot{\theta}})_1$	$(\Delta z_{\dot{\theta}})_2$	$(\Delta z_{\dot{\theta}})_3$	$(\Delta m_{\dot{\theta}})_1$	$(\Delta m_{\dot{\theta}})_2$	$(\Delta m_{\dot{\theta}})_3$
0	-0.31	-0.30	-0.41	-0.47	-0.45	-0.61
0.8	-0.37	-0.37	-0.50	-0.57	-0.55	-0.76
0.917	-0.47	-0.47	-0.57	-0.72	-0.71	-0.85

$\frac{x_0}{\bar{c}} = 3.25$

M	$(\Delta z_{\dot{\theta}})_1$	$(\Delta z_{\dot{\theta}})_2$	$(\Delta z_{\dot{\theta}})_3$	$(\Delta m_{\dot{\theta}})_1$	$(\Delta m_{\dot{\theta}})_2$	$(\Delta m_{\dot{\theta}})_3$
0	-0.50	-0.49	-0.58	-1.	-1.09	-1.28
0.8	-0.61	-0.60	-0.73	-1.34	-1.32	-1.61
0.917	-0.71	-0.71	-0.83	-1.58	-1.56	-1.83

* Tail geometry similar to wing.

TABLE III

DELTA WING ($\Lambda_\ell = 45°$) plus cropped delta tail ($\Lambda_\ell = 45°$, $\lambda = 1/7$)

Wing Geometry etc, AR = 4; $\Lambda_\ell = 45°$; $\lambda = 0$; $\frac{S_t}{S} = 0.0998$; $\frac{\bar{c}_t}{\bar{c}} = 0.365$;

$\frac{\ell}{\bar{c}} = 1.36$; $\frac{\bar{x}}{\bar{c}} = 2.498$; $\frac{x_o}{\bar{c}} = 1.028$.

Tail Geometry etc, AR = 3; $\Lambda_\ell = 45°$; $\lambda = 1/7$

M	$(\Delta z_\vartheta')_1$	$(\Delta z_\vartheta')_2$	$(\Delta z_\vartheta')_3$	$(\Delta m_\vartheta')_1$	$(\Delta m_\vartheta')_2$	$(\Delta m_\vartheta')_3$
0.88	-0.32	-0.31	-0.48	-0.45	-0.43	-0.65

M		0.887	1.0	1.0307	1.118	1.25	1.414	1.6008	1.8028	2.2361
Wing Alone	z_ϑ'	-0.41	3.75	5.65	2.17	1.15	0.72	0.19	-0.01	-0.14
	m_ϑ'	-1.08	0.84	2.17	0.58	0.15	-0.002	-0.18	-0.23	-0.24
Wing + Tail	$z_\vartheta' + \Delta z_\vartheta'$	-0.73	3.11	5.05	1.64	0.71	0.36			
	$m_\vartheta' + \Delta m_\vartheta'$	-1.52	-0.03	1.28	-0.02	-0.45	-0.54			

TABLE IV

DELTA WING ($\Lambda_\ell = 60°$) plus cropped delta tail ($\Lambda_\ell = 45°$, $\lambda = 1/7$)

Wing Geometry etc, AR = 2.31; $\Lambda_\ell = 60°$; $\lambda = 0$; $\frac{S_t}{S} = 0.0998$;

$\frac{\bar{c}_t}{\bar{c}} = 0.277$; $\frac{\ell}{\bar{c}} = 1.278$; $\frac{\bar{x}}{\bar{c}} = 2.498$; $\frac{x_o}{\bar{c}} = 1.136$.

Tail Geometry etc, AR = 3; $\Lambda_\ell = 45°$; $\lambda = 1/7$

M	$(\Delta z_\vartheta')_1$	$(\Delta z_\vartheta')_2$	$(\Delta z_\vartheta')_3$	$(\Delta m_\vartheta')_1$	$(\Delta m_\vartheta')_2$	$(\Delta m_\vartheta')_3$
0.6	-0.23	-0.23	-0.39	-0.31	-0.29	-0.50

M		0.6	1.0	1.0307	1.118	1.25	1.414	1.6008	1.8028
Wing Alone	z_ϑ'	-1.12	-0.36	+0.09	-0.19	-0.26	-0.21	-0.07	-0.03
	m_ϑ'	-0.47	-0.45	-0.30	-0.38	-0.38	-0.35	-0.28	-0.24
Wing + Tail	$z_\vartheta' + \Delta z_\vartheta'$	-1.35	-0.78	-0.56	-0.78	-0.75	-0.63	-0.40	-0.29
	$m_\vartheta' + \Delta m_\vartheta'$	-0.78	-1.07	-1.25	-1.26	-1.11	-0.96	-0.77	-0.63

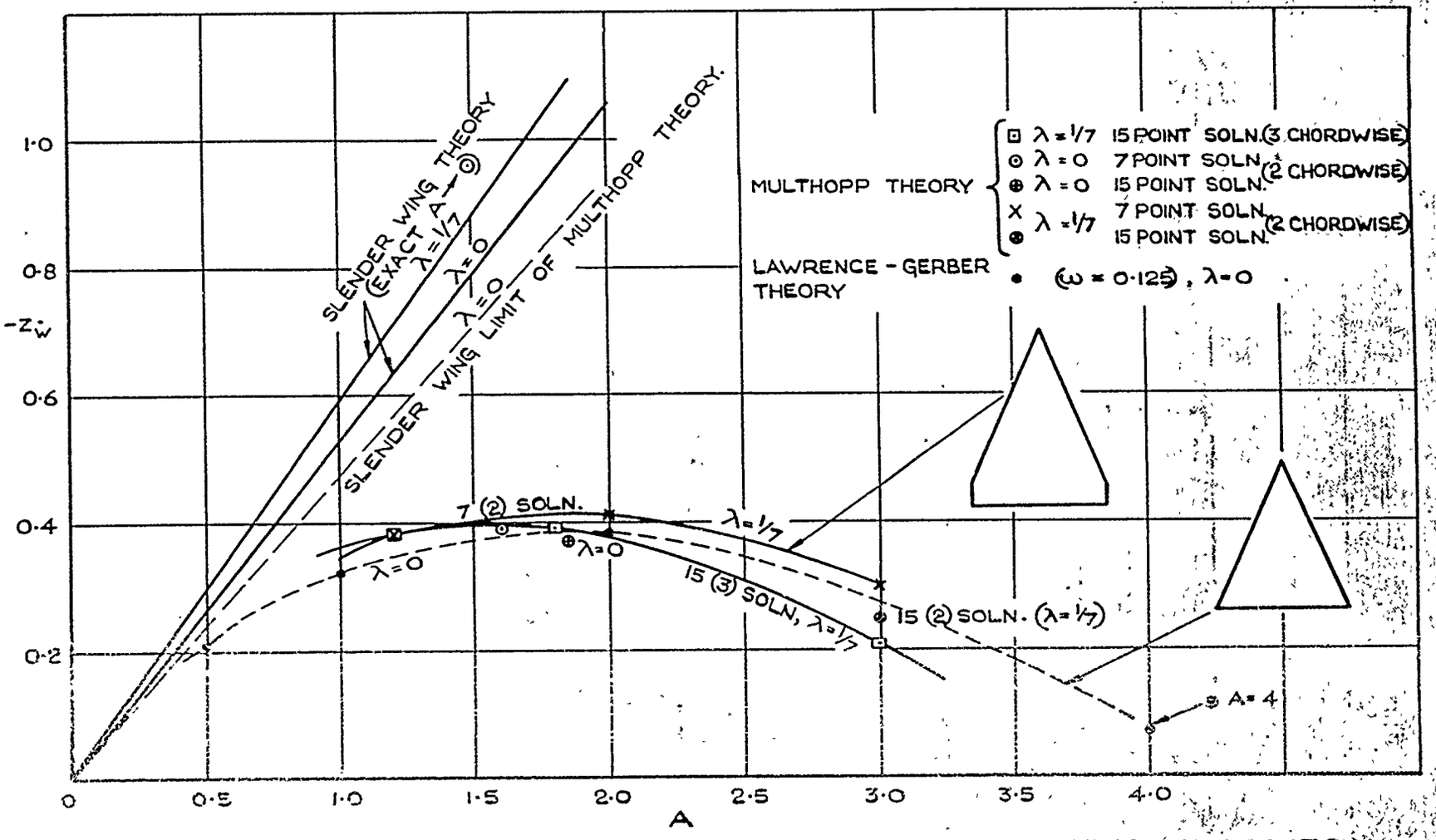

FIG. 1. VARIATION OF $Z_{\dot{w}}$ WITH ASPECT RATIO FOR TWO FAMILIES OF DELTA WINGS. (INCOMPRESSIBLE FLOW)

FIG. 1.

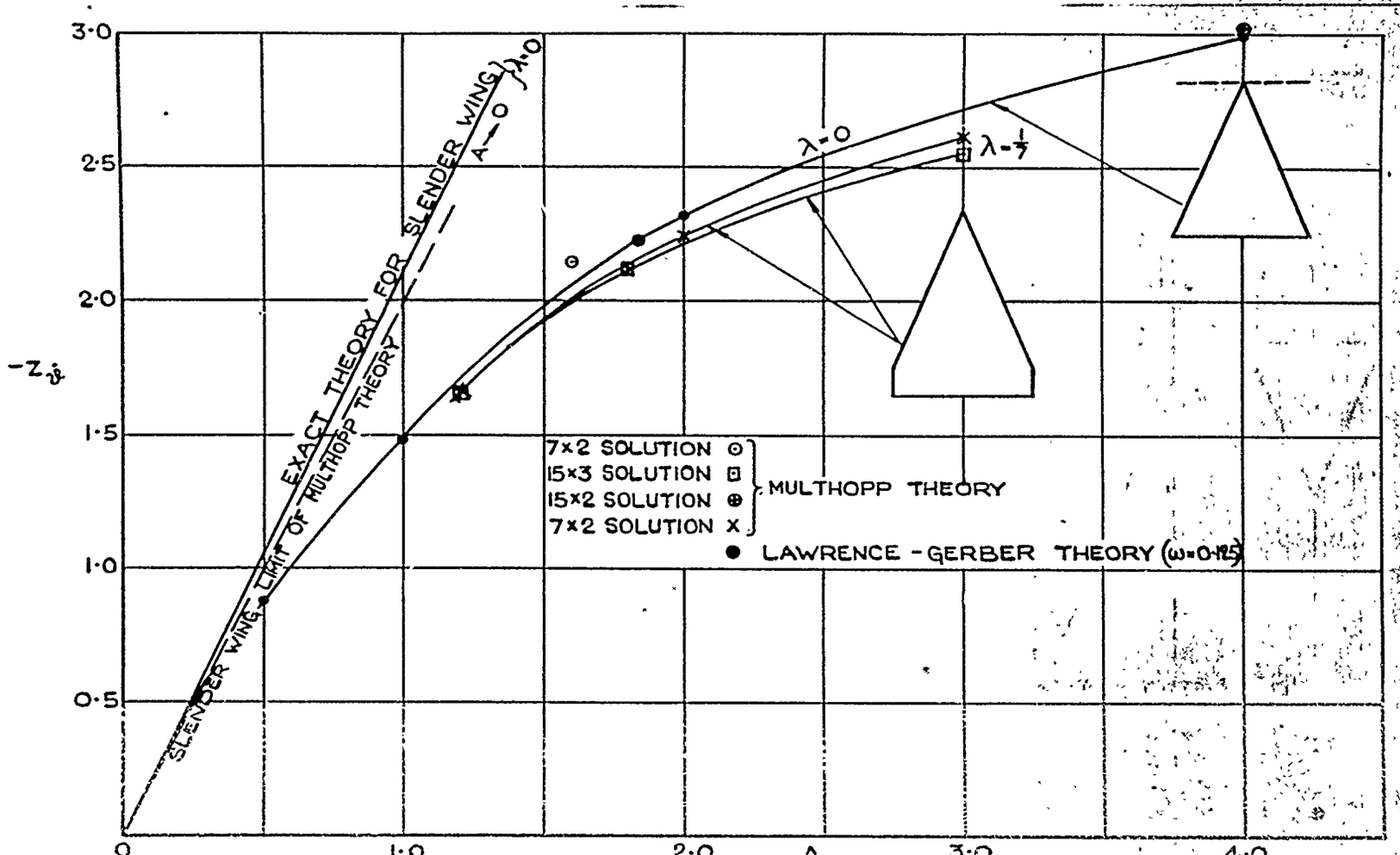

FIG.2. COMPARISON OF $Z_{\dot{\alpha}}$ AS CALCULATED USING VARIOUS THEORIES FOR DELTA WINGS IN INCOMPRESSIBLE FLOW, AND AXIS THROUGH THE WING APEX.

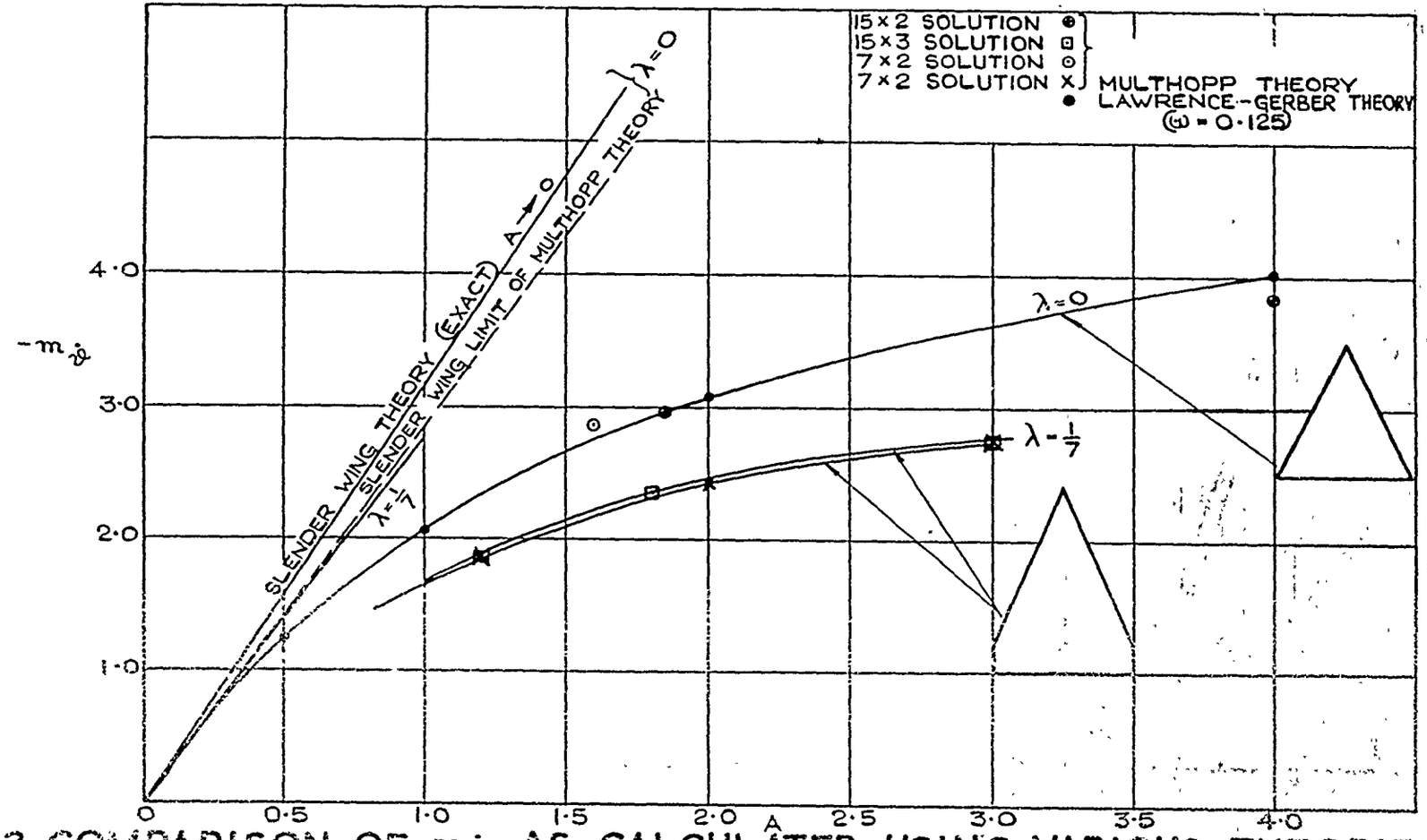

FIG.3. COMPARISON OF $m_{\dot{\vartheta}}$ AS CALCULATED USING VARIOUS THEORIES FOR TWO FAMILIES OF DELTA WINGS OSCILLATING ABOUT AXIS THROUGH WING APEX, IN INCOMPRESSIBLE FLOW.

FIG.3.

FIG. 4.(a&b)

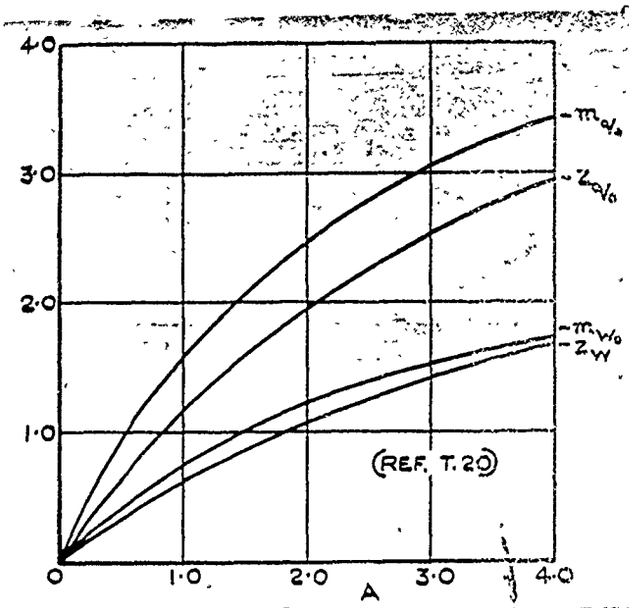

FIG. 4.(a). STEADY AND QUASI-STEADY DERIVATIVES FOR DELTA WINGS, IN INCOMPRESSIBLE FLOW, AND FOR AXIS THROUGH THE WING APEX.

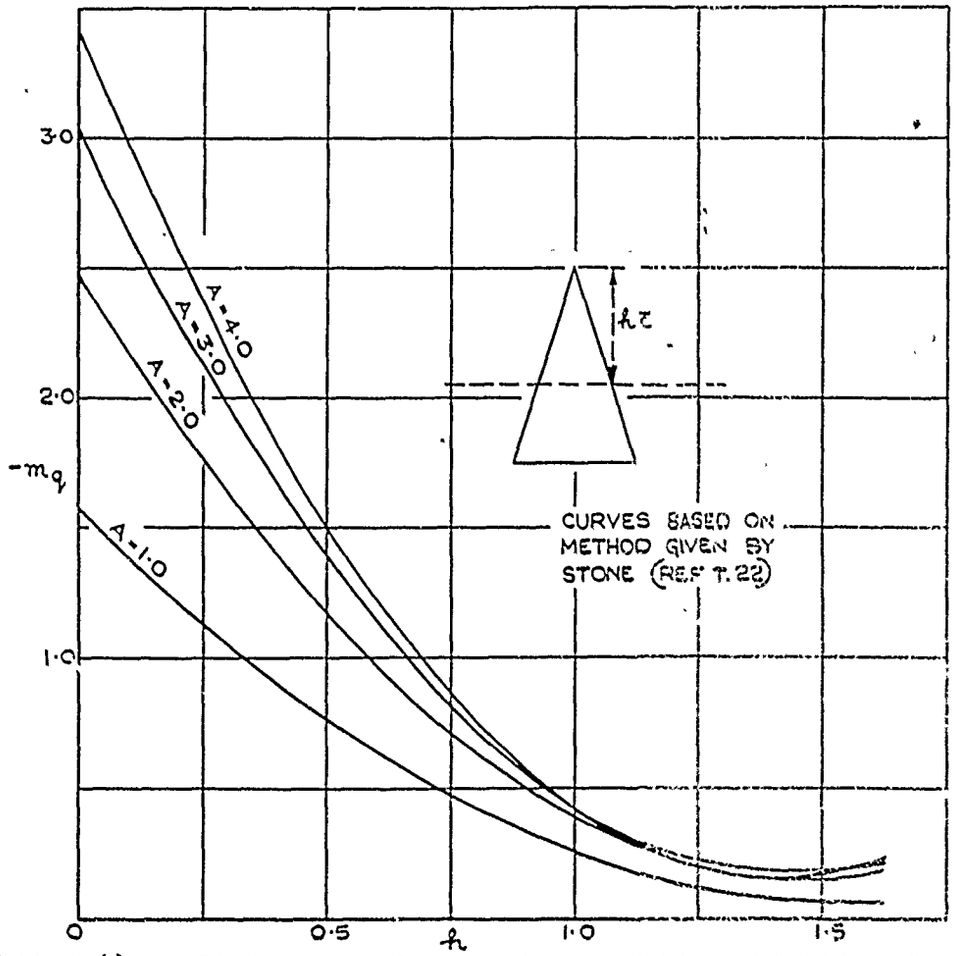

FIG. 4.(b). VARIATION OF m_q WITH AXIS POSITION FOR DELTA WINGS (INCOMPRESSIBLE FLOW).

FIG.5.

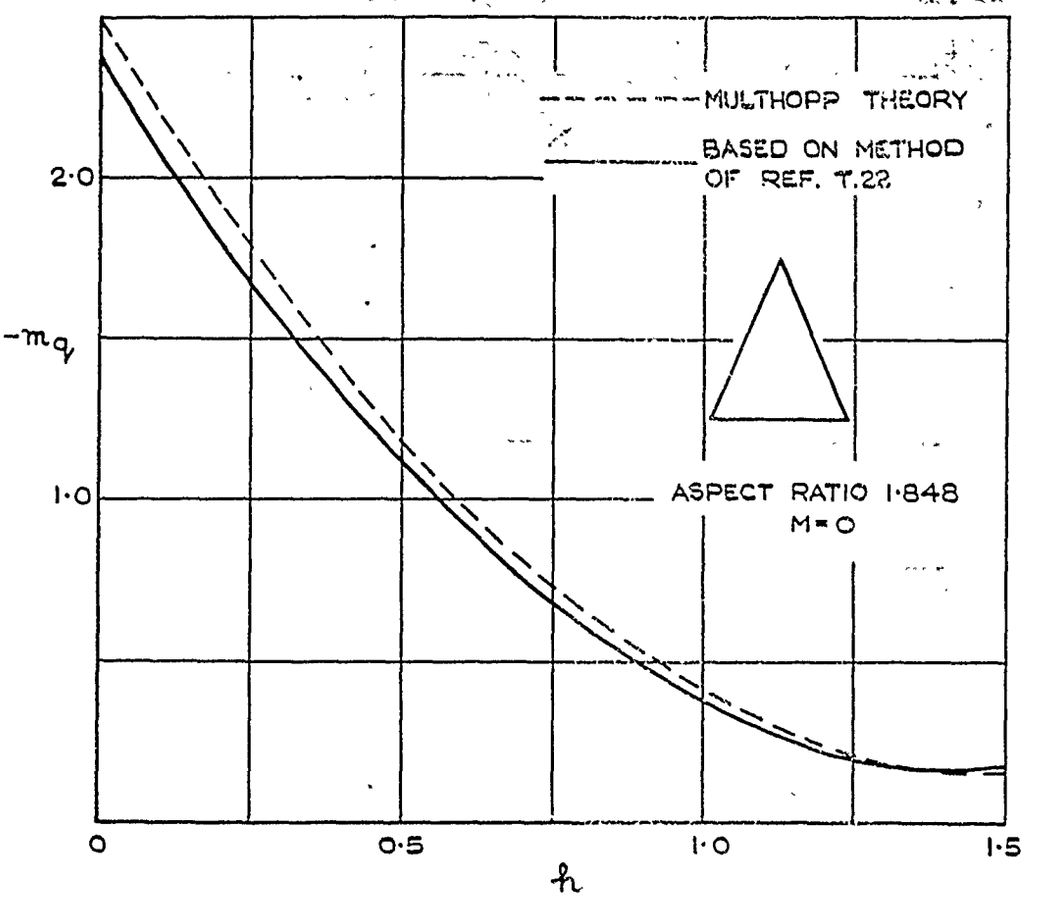

FIG.5. COMPARISON OF m_q AS CALCULATED BY TWO METHODS.

FIG. 6.

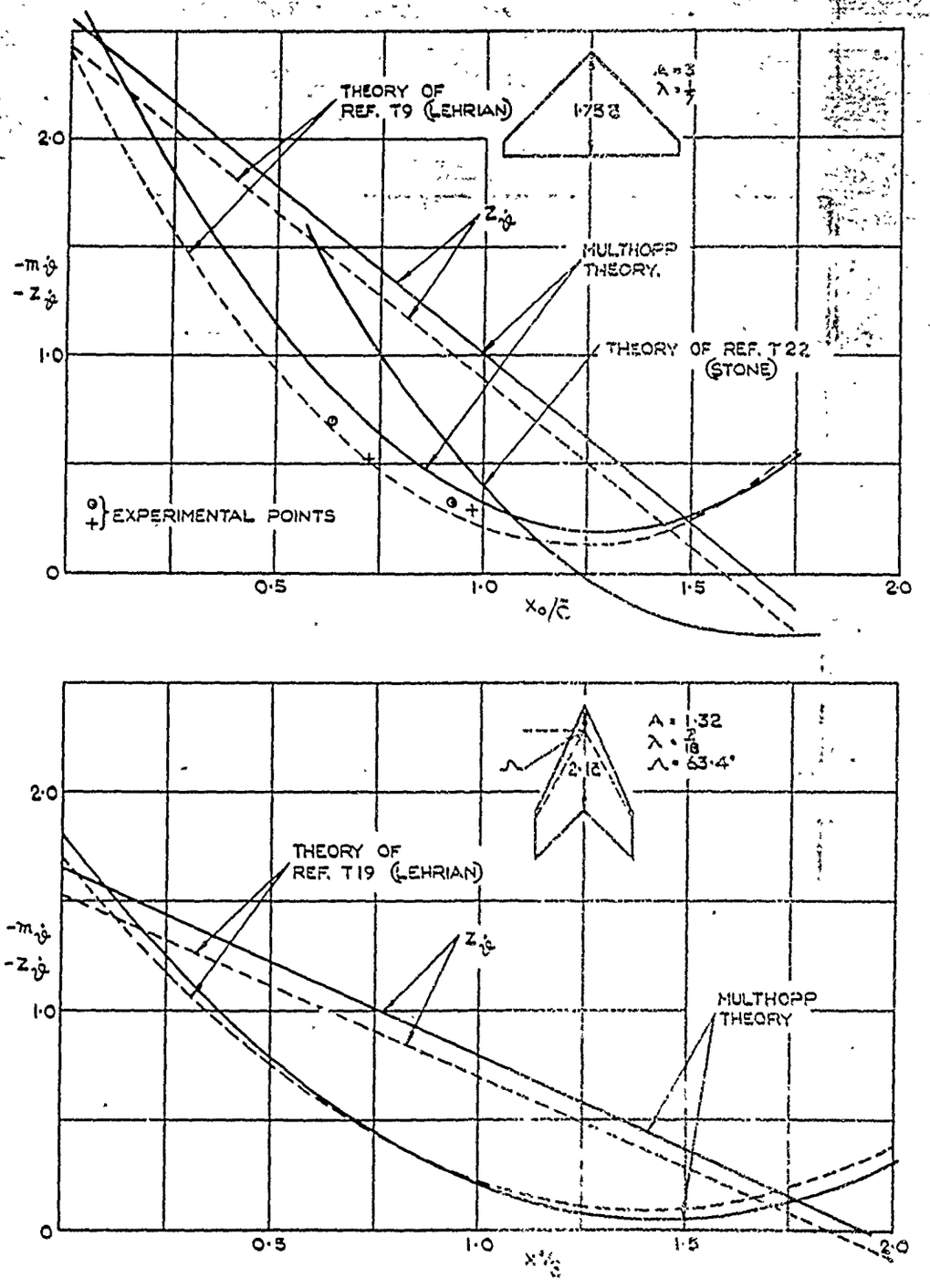

FIG. 6. COMPARISON OF VARIOUS THEORETICAL AND EXPERIMENTAL RESULTS FOR INCOMPRESSIBLE FLOW.

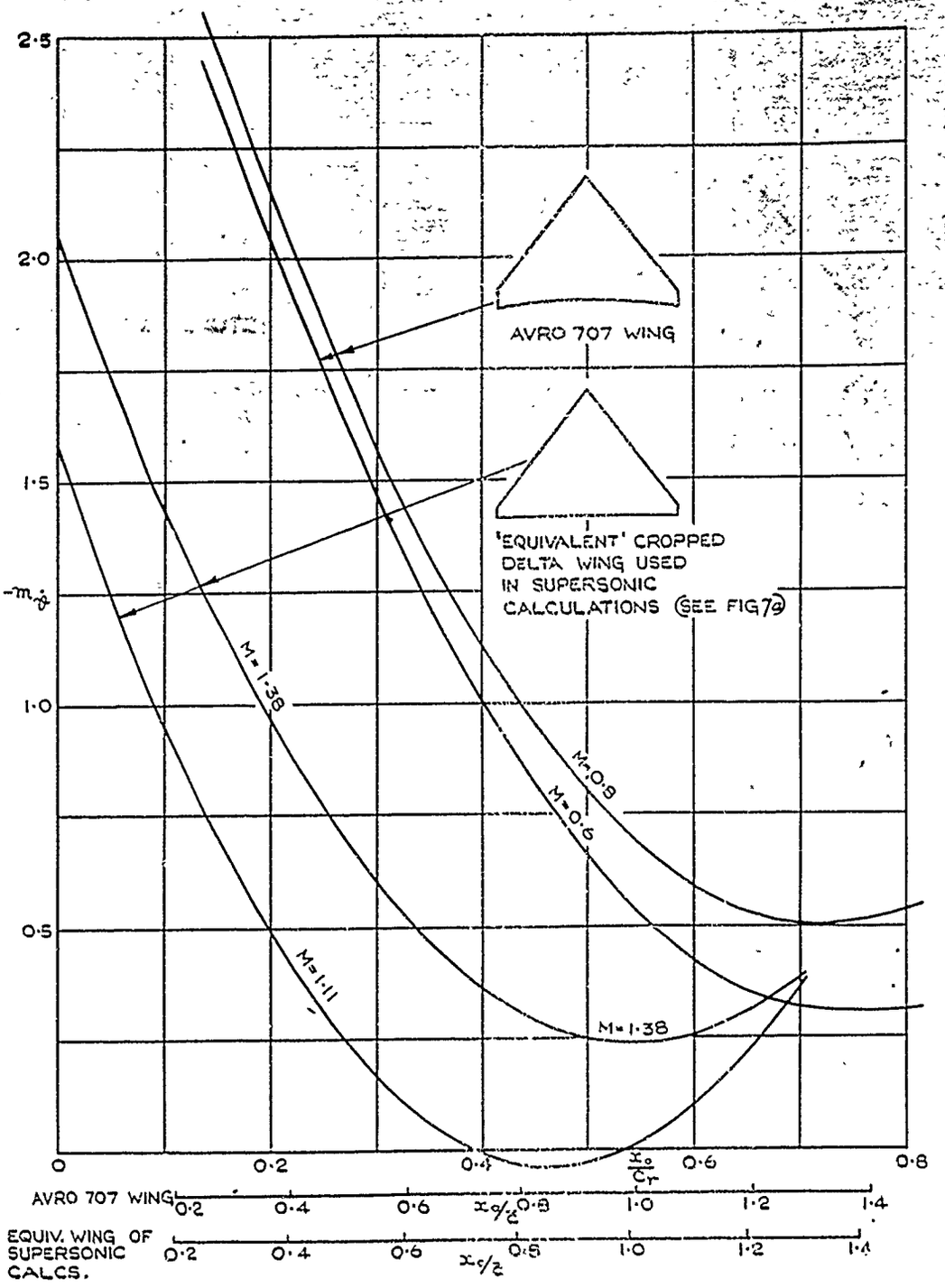

FIG. 7. VARIATION OF $m_{\dot{\alpha}}$ WITH AXIS POSITION AT VARIOUS MACH NUMBERS FOR AVRO 707 WING (APPROXIMATE ONLY FOR M > 1)

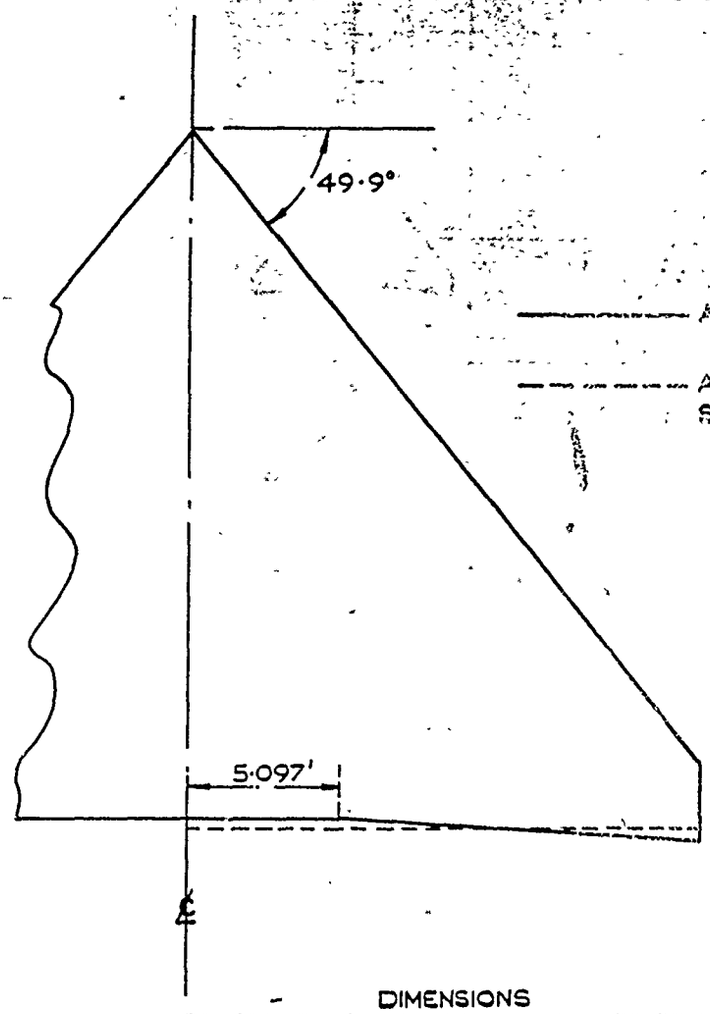

DIMENSIONS

	AVRO 707 WING	EQUIV. WING.
SPAN (FT)	34·167	34·167
ROOT CHORD (FT)	21·826	22·086
TIP CHORD (FT)	2·28	1·799
SWEEP OF OUTER T.E.	3·54°	0°

THE TWO WINGS HAVE SAME L.E. SWEEP, ASPECT RATIO, AND SPAN THEIR MEAN CHORDS ARE THUS EQUAL, BUT SLIGHTLY DISPLACED ONE RELATIVE TO THE OTHER.

FIG. 7@. COMPARISON OF ACTUAL AVRO 707 WING WITH THAT USED IN CALCULATION OF THE DERIVATIVES AT SUPERSONIC SPEEDS.

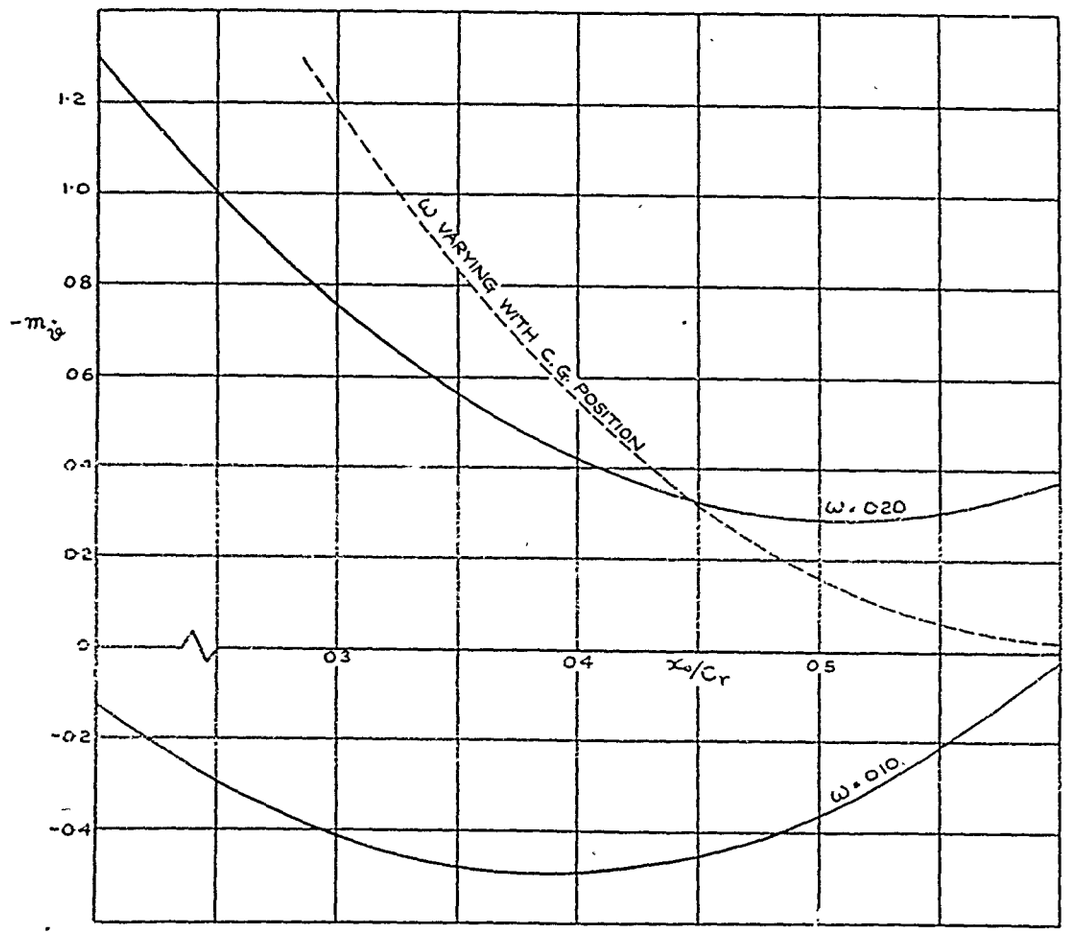

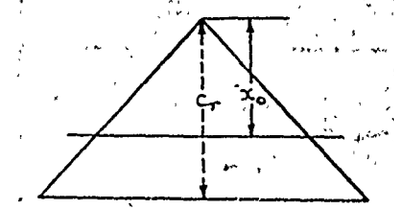

——— CONST. REDUCED FREQUENCY.

– – – – REDUCED FREQUENCY RELATED TO C.G. POSITION.

$$\omega = \sqrt{\frac{z_w}{\mu i_B}\left(\kappa_m - \frac{m_q}{\mu}\right)}$$

FIG.8. VARIATION OF SONIC VALUE OF $m_{\dot{\theta}}$ WITH C.G. POSITION FOR A DELTA WING WITH LEADING EDGE SWEEP OF 49·9°

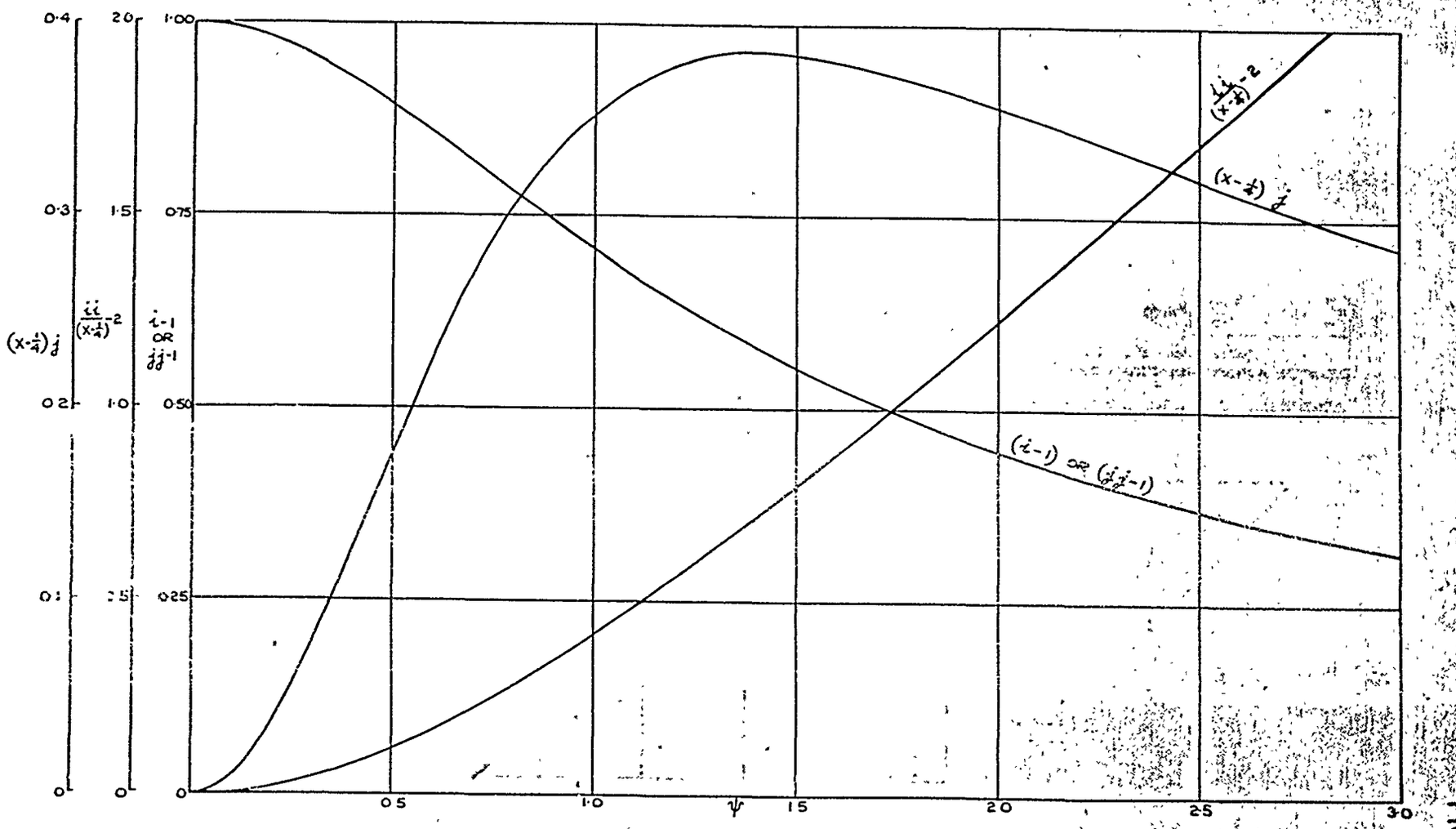

FIG. 9. ASYMPTOTIC APPROXIMATIONS TO THE INFLUENCE FUNCTIONS i, j, ii AND jj.

FIG. 9.

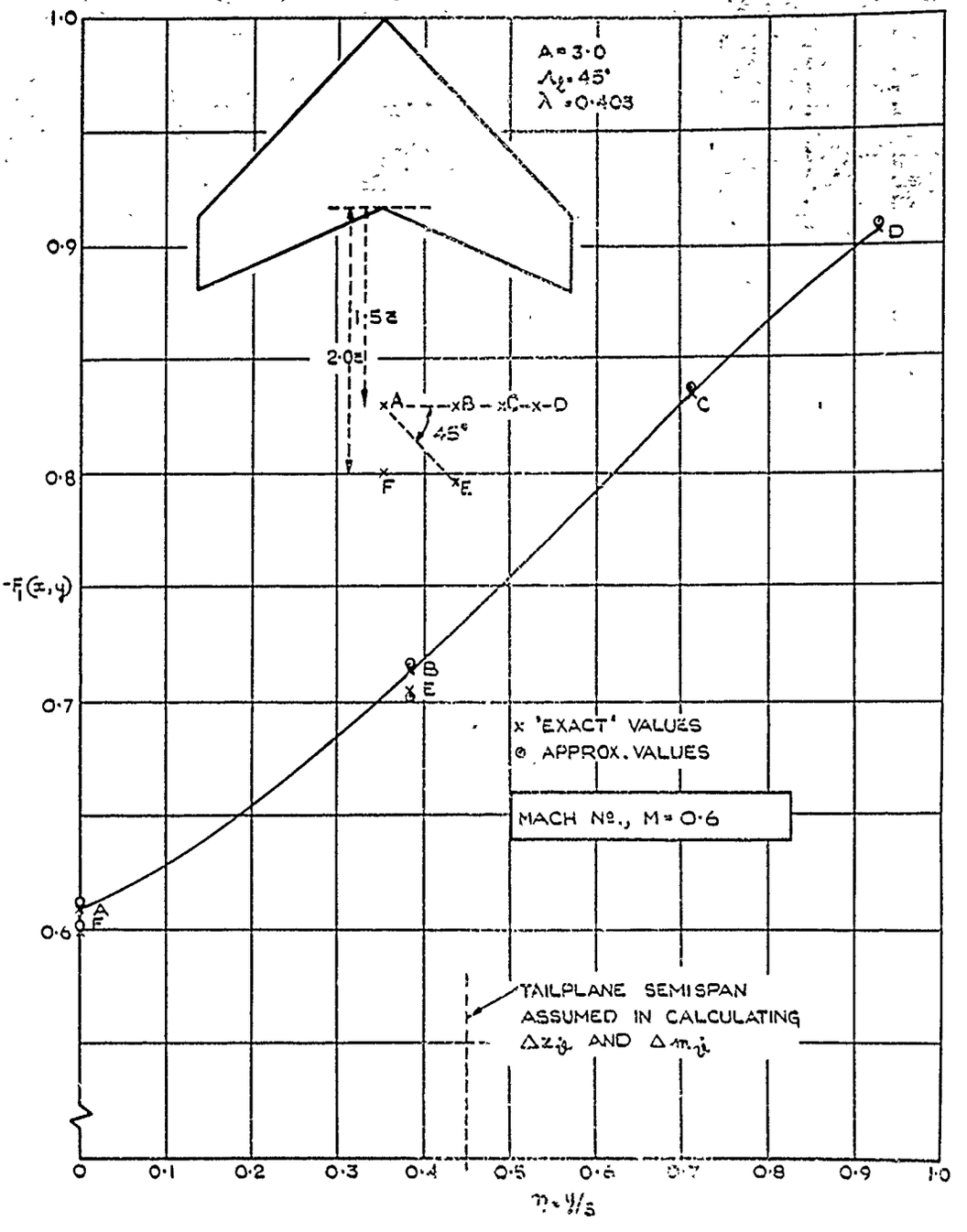

FIG. 10. VARIATION OF THE DOWNWASH FUNCTION $F_1(x,y)$ WITH CHORDWISE AND SPANWISE LOCATION.

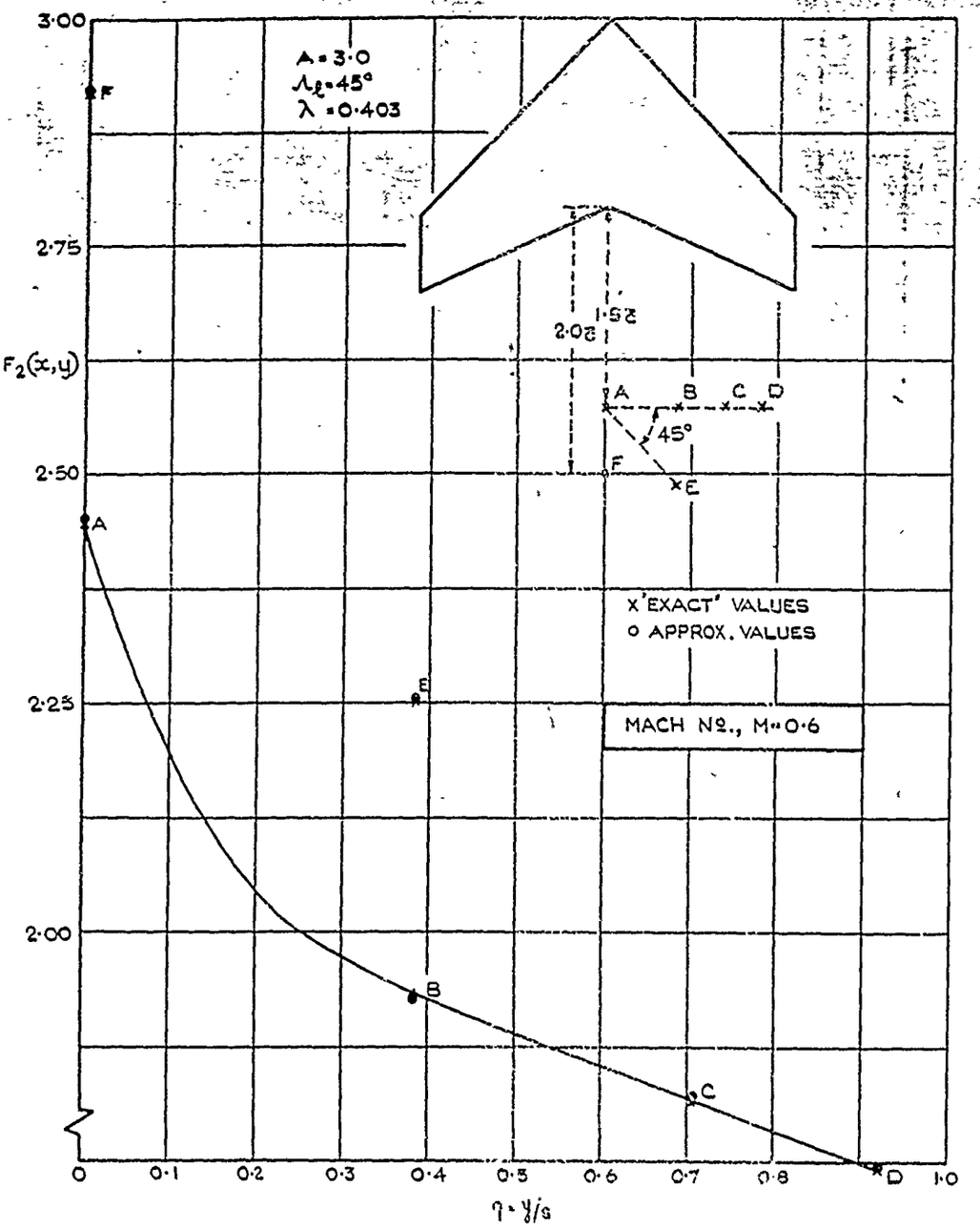

FIG. 11. VARIATION OF THE DOWNWASH FUNCTION $F_2(x,y)$ WITH CHORDWISE AND SPANWISE LOCATION.

FIG. 12.

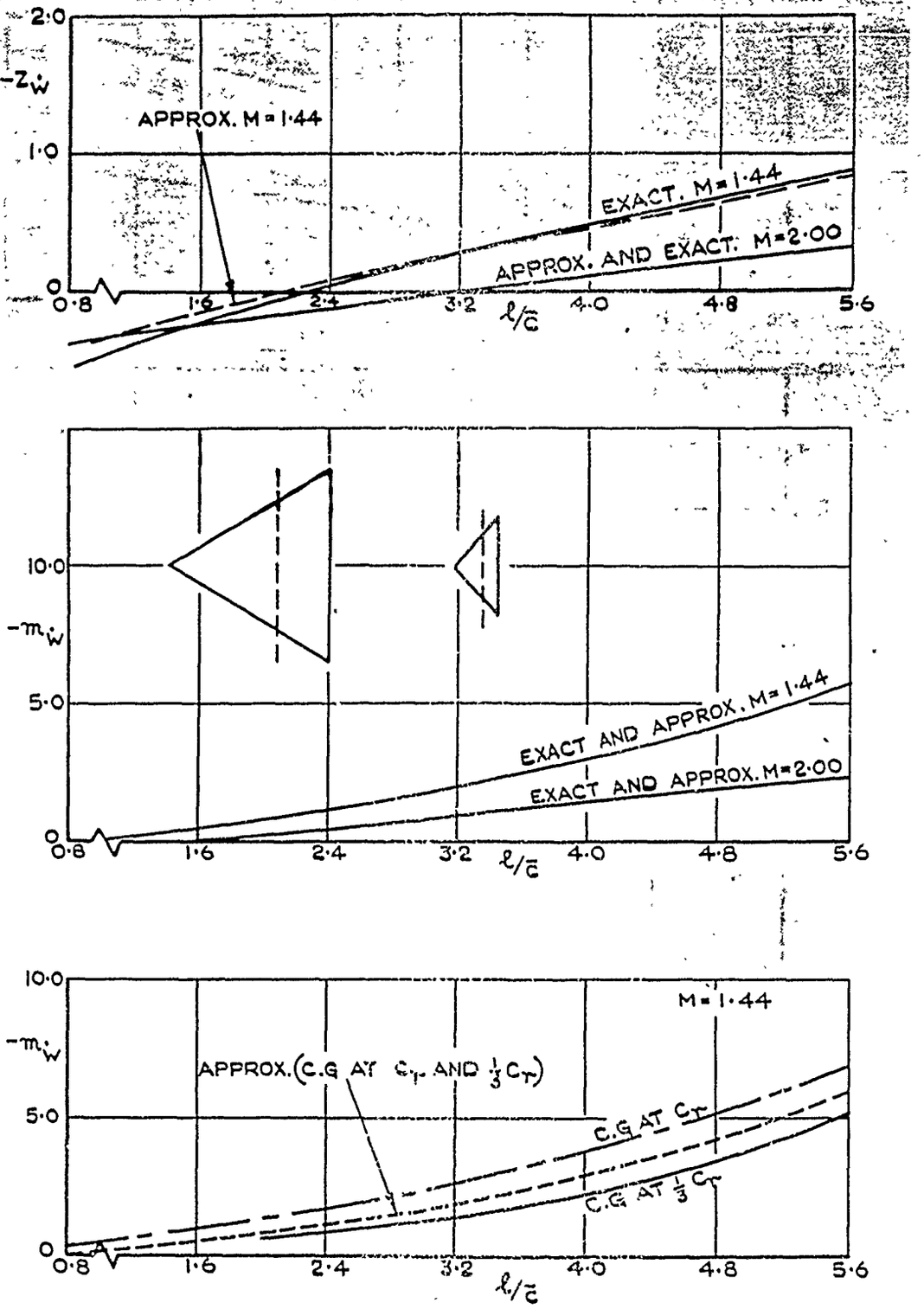

FIG. 12. COMPARISON OF "EXACT" & APPROXIMATE $Z_{\dot{w}}$ & $m_{\dot{w}}$ FOR DELTA WING-TAIL COMBINATIONS AT VARIOUS C.G. POSITIONS, & MACH NUMBERS (FROM REF. T 38)

FIG.13.

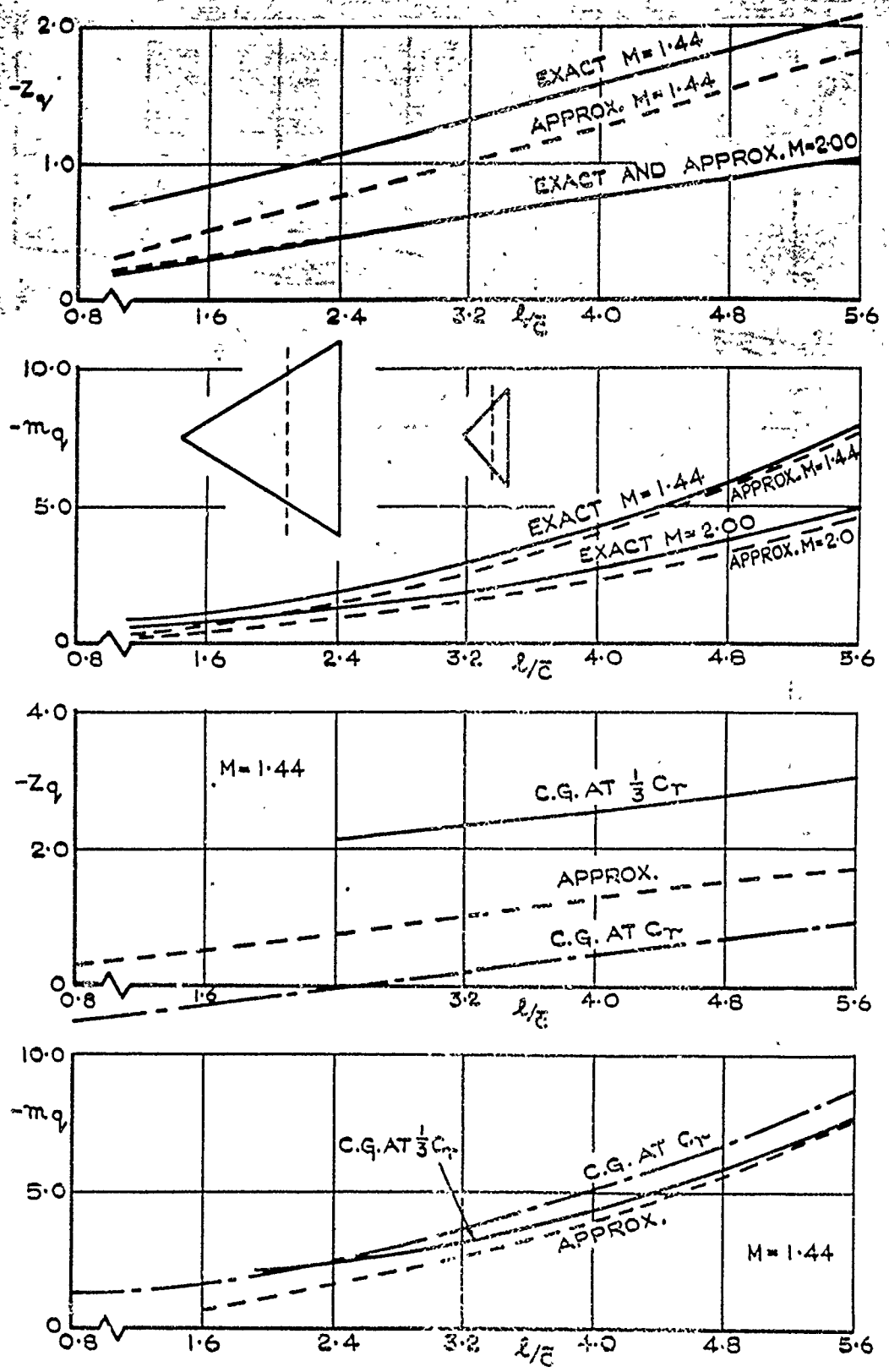

FIG.13. COMPARISON OF "EXACT" AND APPROXIMATE Z_q AND m_q FOR DELTA WING-TAIL COMBINATIONS AT VARIOUS C.G. POSITIONS, AND MACH NUMBERS. (FROM REF. T38).

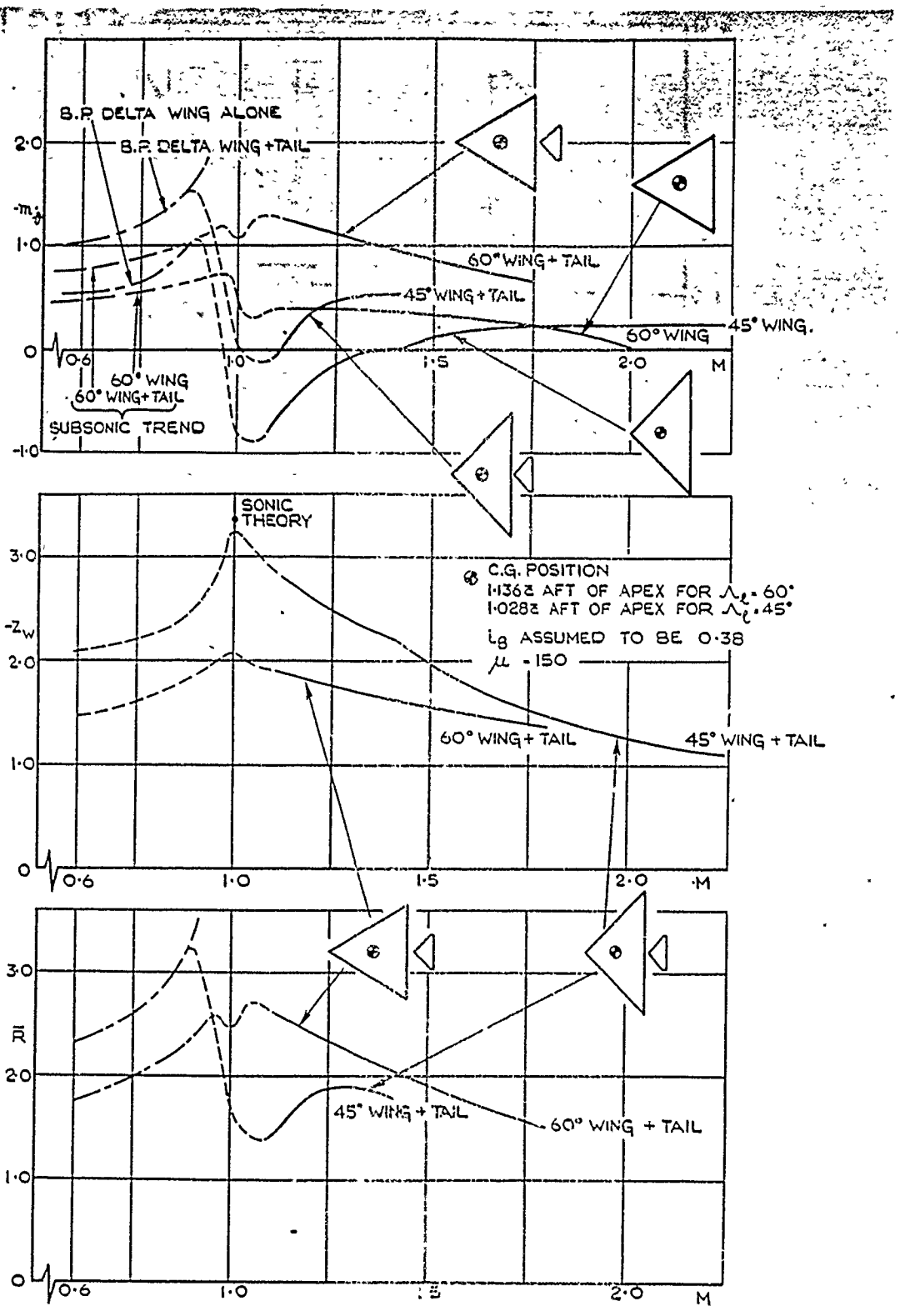

FIG. 14. COMPARISON OF DAMPING FACTOR & DERIVATIVES FOR TAILED DELTA WINGS OF 45° & 60° LEADING EDGE SWEEP.

FIG. 15.

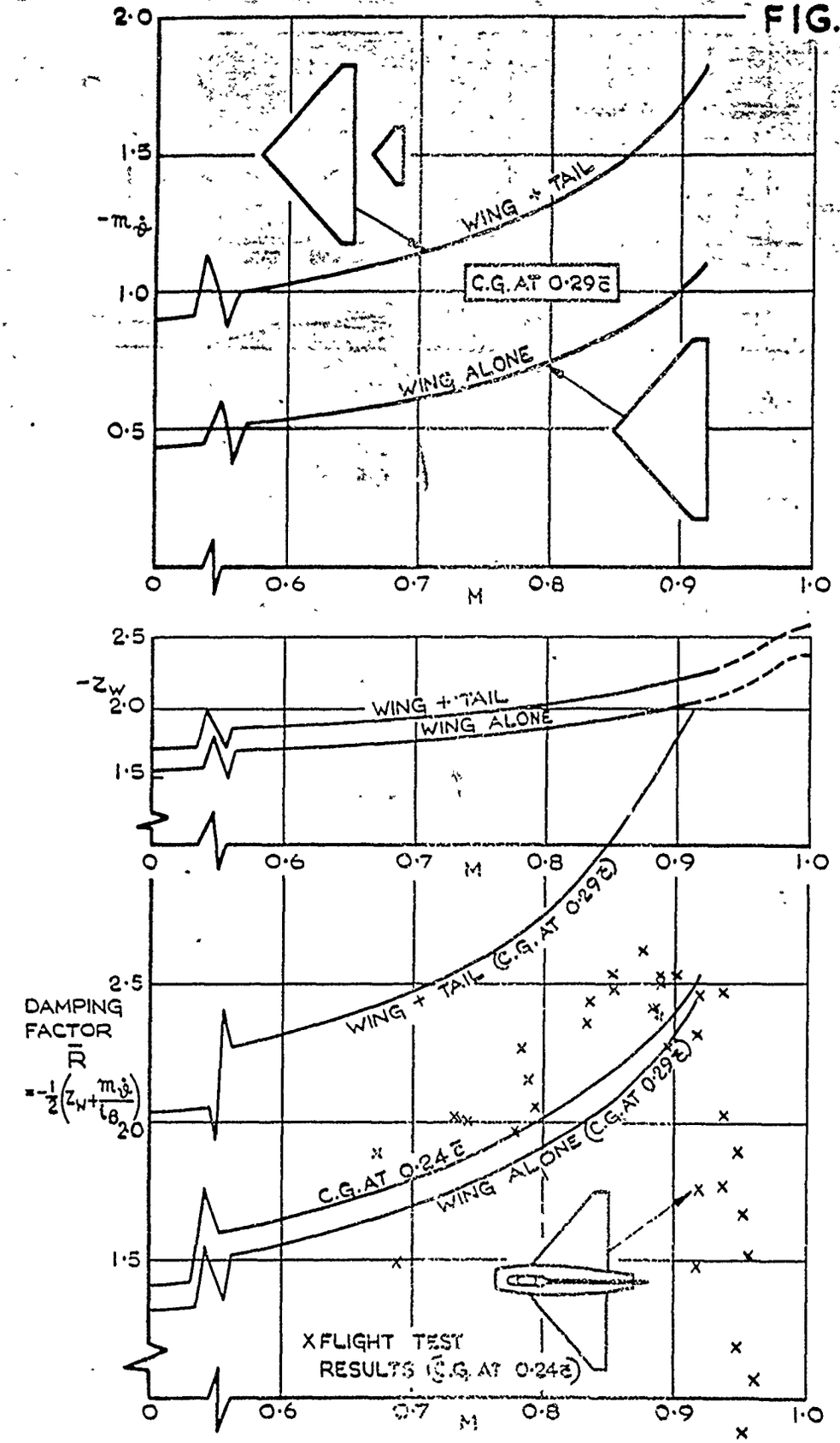

FIG. 15. EFFECT OF ADDING A TAIL ON THE DERIVATIVES. Z_w, $m_{\dot{\theta}}$, AND ON THE DAMPING FACTOR $\bar{R}$, WITH A COMPARISON OF CALCULATED $\bar{R}$ FOR WING ALONE WITH MEASUREMENTS FOR A TAILLESS AIRCRAFT.

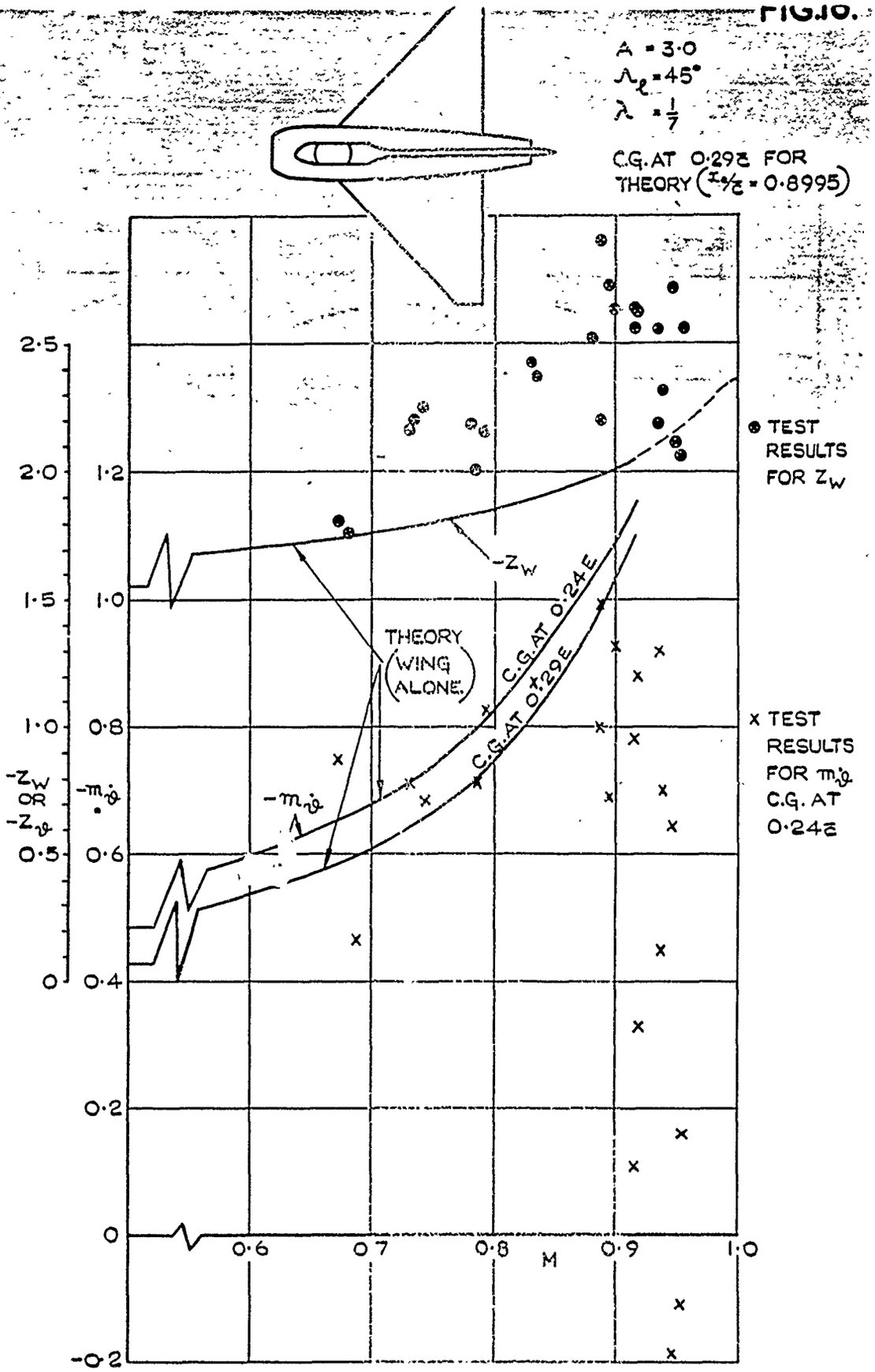

FIG.16. COMPARISON OF MEASURED AND CALCULATED DERIVATIVES FOR BOULTON - PAUL P.111.

FIG. 17. (a & b)

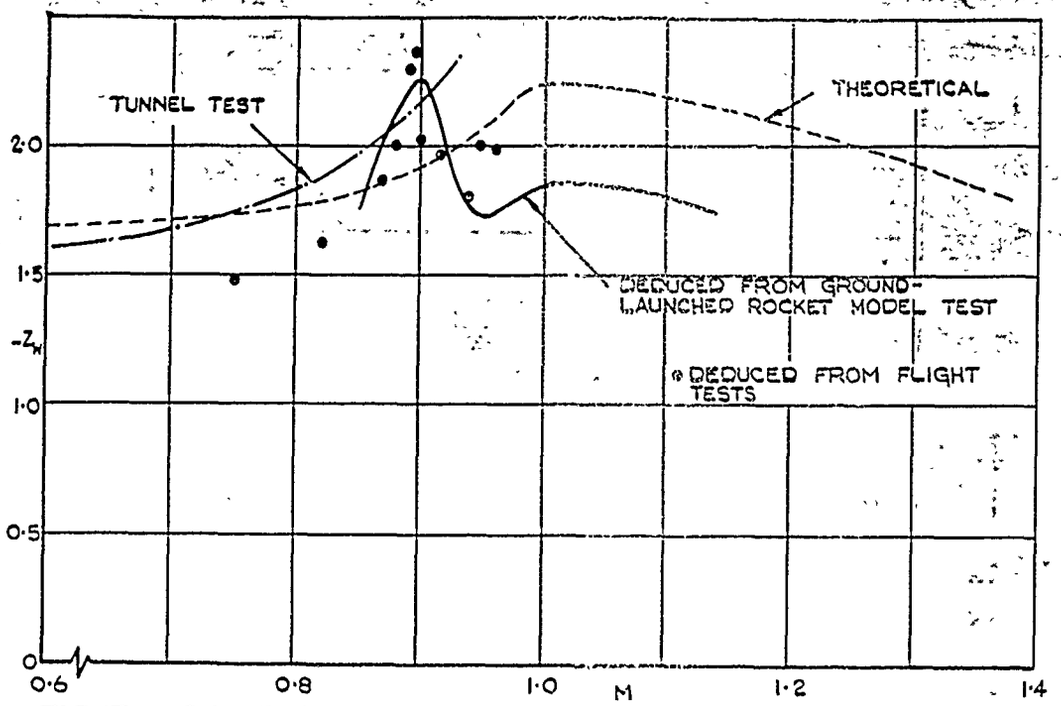

FIG. 17 (a) COMPARISON OF THEORETICAL & EXPERIMENTAL Z_w FOR AVRO 707.

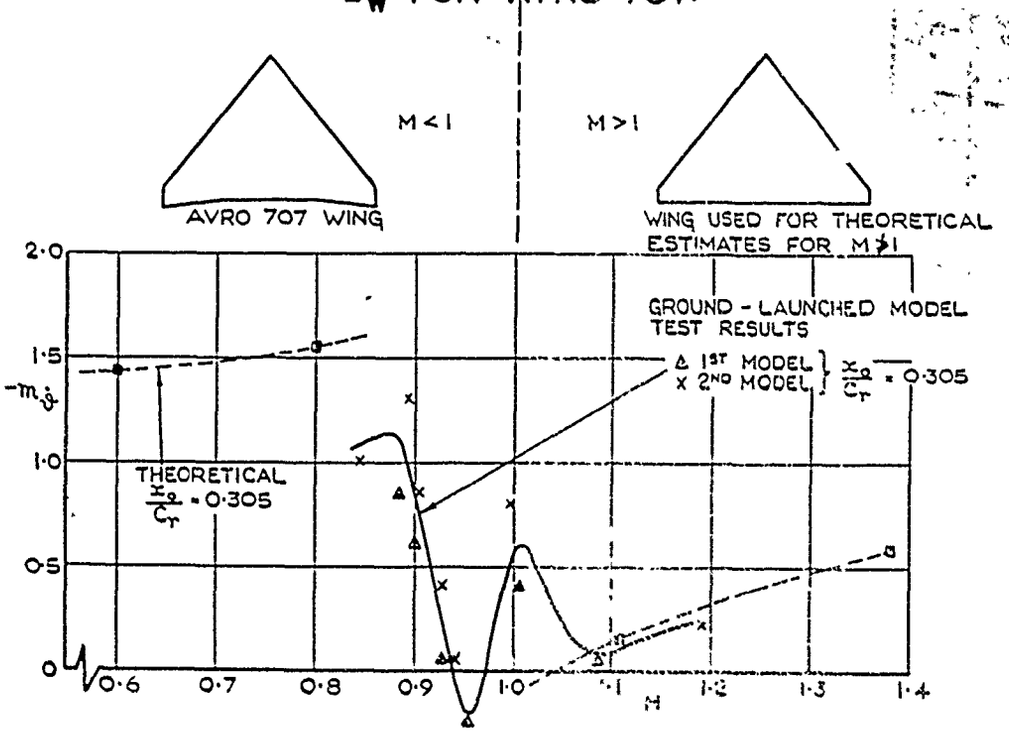

FIG. 17 (b) COMPARISON OF THEORETICAL & EXPERIMENTAL $M_{\dot{\alpha}}$ FOR AVRO 707.

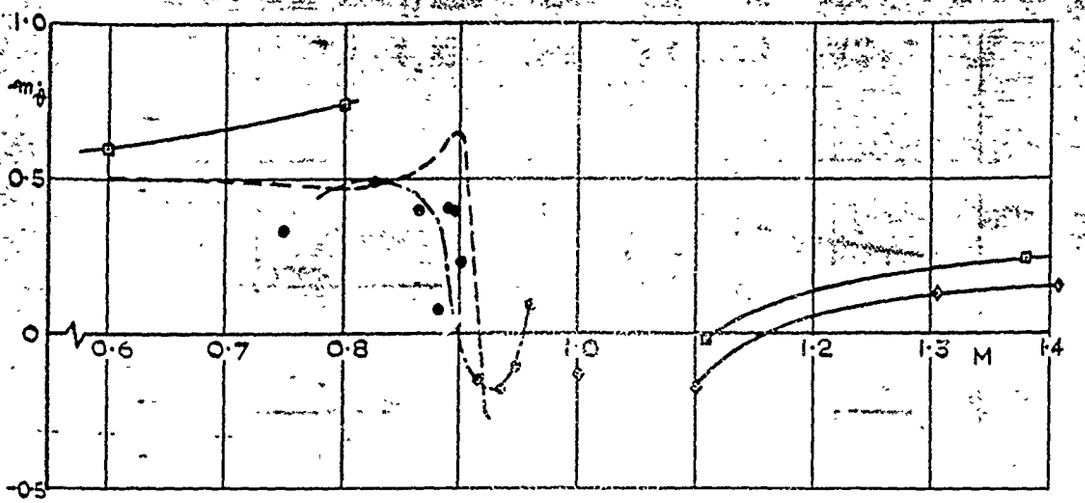

FIG.18(a) COMPARISON OF EXPERIMENTAL AND THEORETICAL $m_{\dot{\theta}}$.

—·—·—·— R.A.E. FLIGHT TEST $x_o/c_r = 0.518$
– – – – AVRO FLIGHT TEST $x_o/c_r = 0.523$
——— THEORY,
——— THEORY FOR UNCROPPED DELTA, WITH $\omega = 0.123$ AT M=1, $x_o/c_r = 0.523$

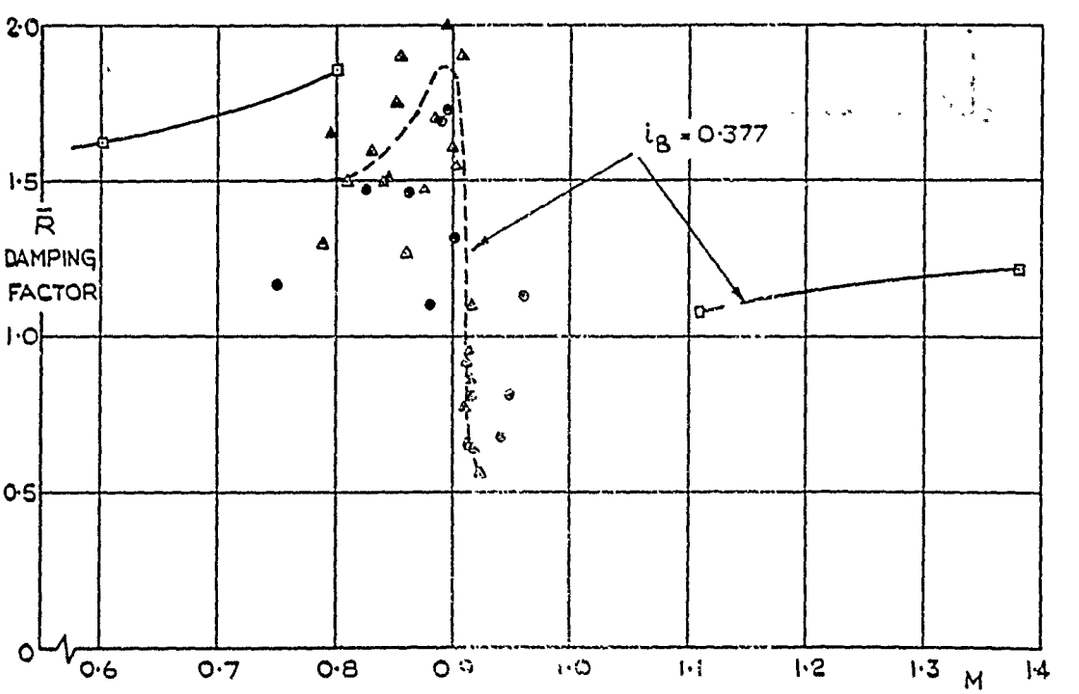

FIG.18(b) COMPARISON OF THEORY WITH FLIGHT TESTS FOR THE DAMPING OF THE SHORT PERIOD OSCILLATION FOR AVRO 707.

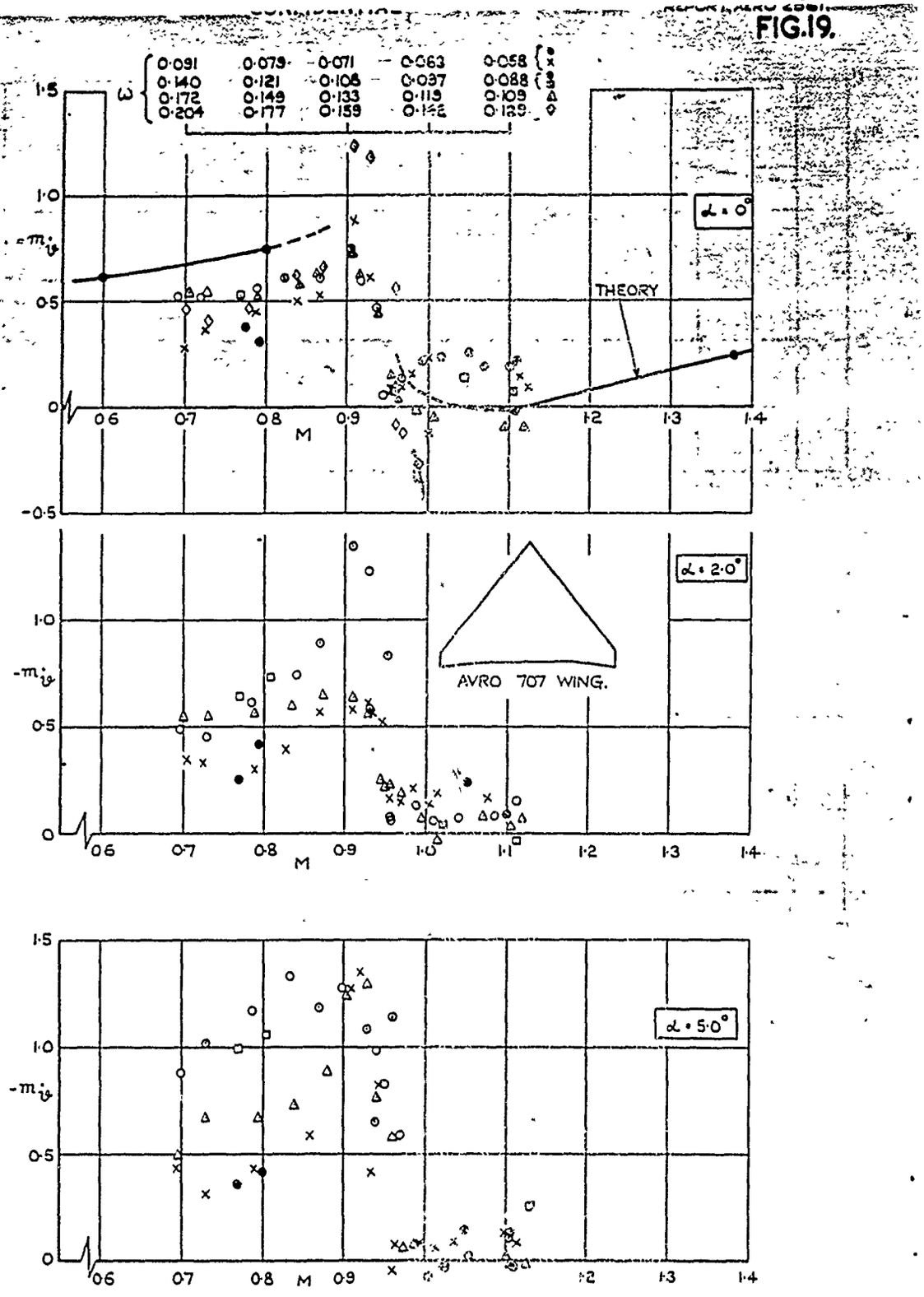

FIG.19. VARIATION OF $-m_q$ WITH MACH NUMBER FOR DIFFERENT MEAN INCIDENCES, AND RANGES OF REDUCED FREQUENCY AS GIVEN BY WING FLOW EXPERIMENTS (AXIS POSITION 0·280 c OR 0·522 C_r)

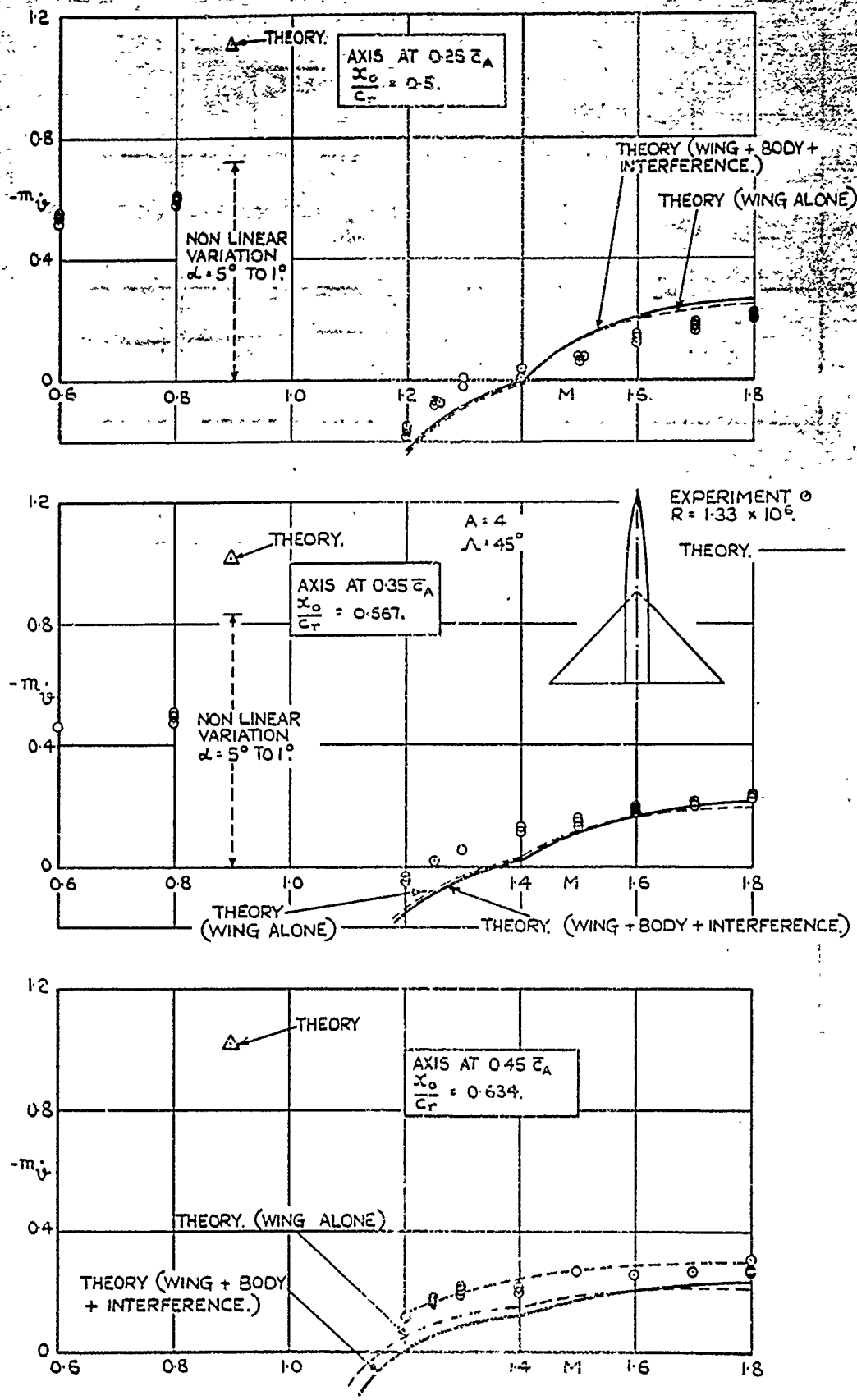

FIG.20. COMPARISON OF THEORY AND WIND TUNNEL TEST RESULTS FOR DELTA WING, A = 4, Λ_ℓ = 45°.

FIG.21.

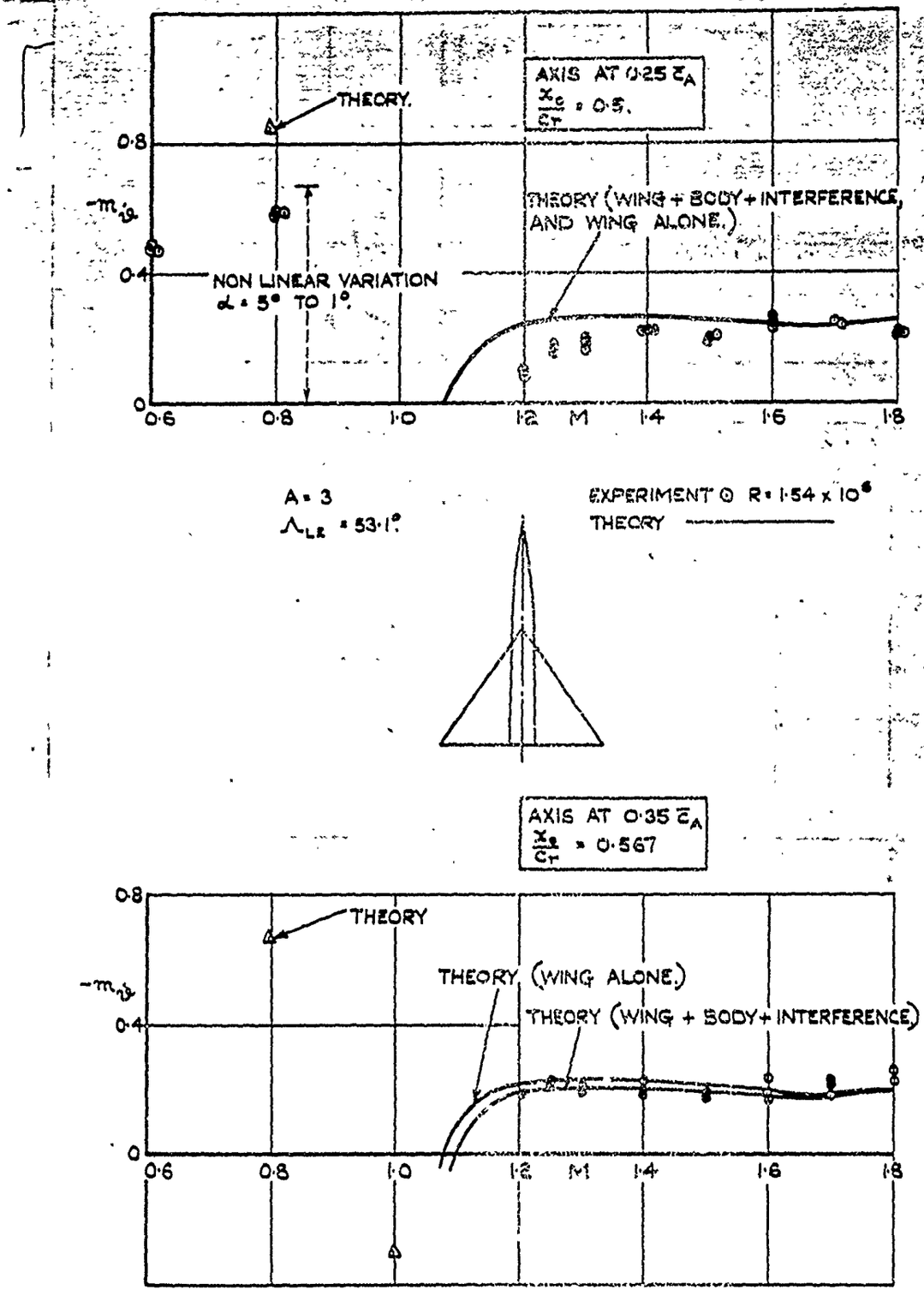

FIG.21. COMPARISON OF CALCULATED $m_{\dot{\alpha}}$ AND WIND TUNNEL TEST RESULTS FOR DELTA WING, A=3, $\Lambda_{\frac{1}{4}}$ = 53·1°.

FIG. 22.

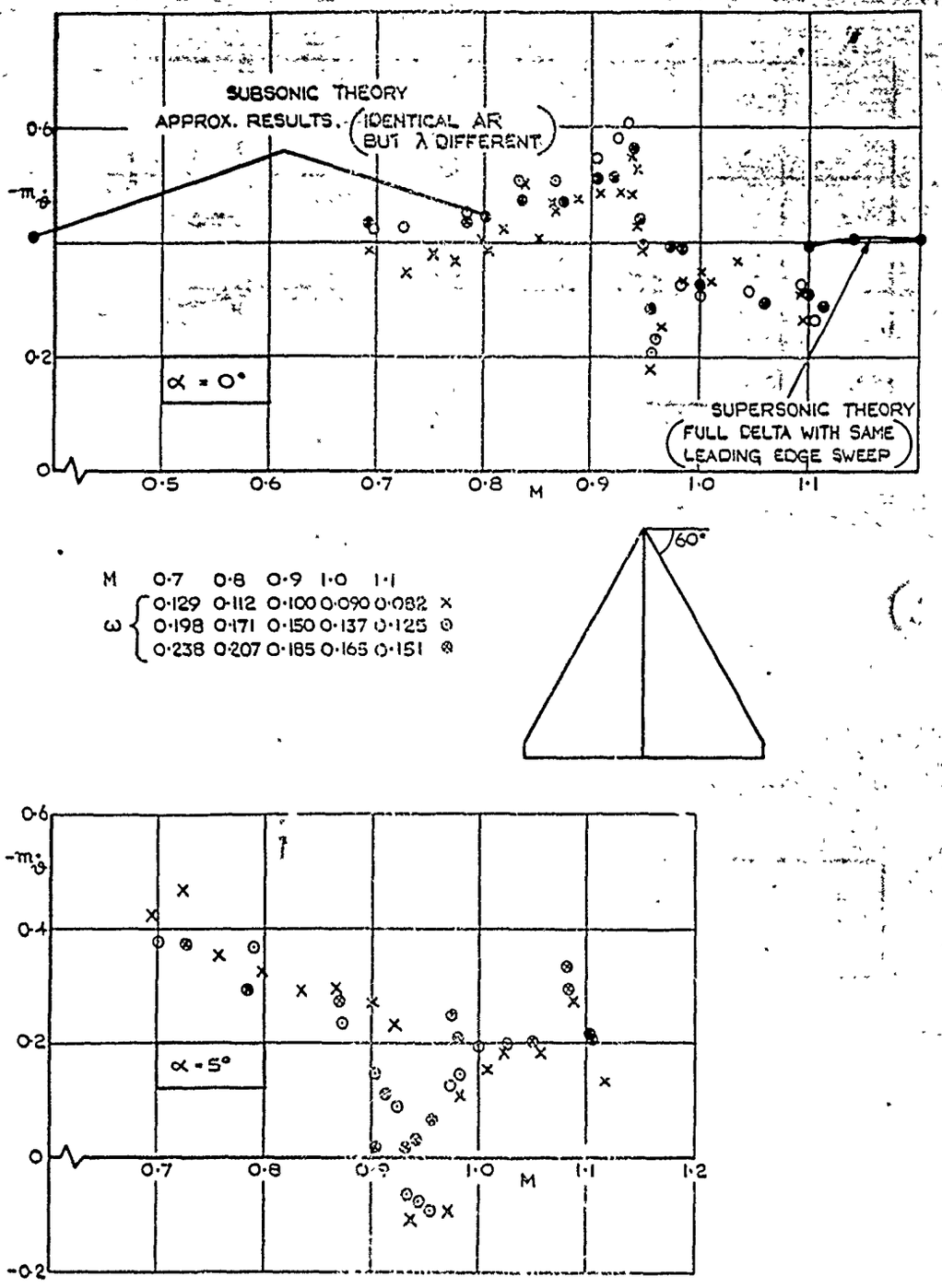

FIG. 22. VARIATION OF $-m_{\dot{\theta}}$ WITH MACH NUMBER FOR FAIREY ER. 103. – TRANSITION FIXED AT 5% CHORD BY SPOILER.

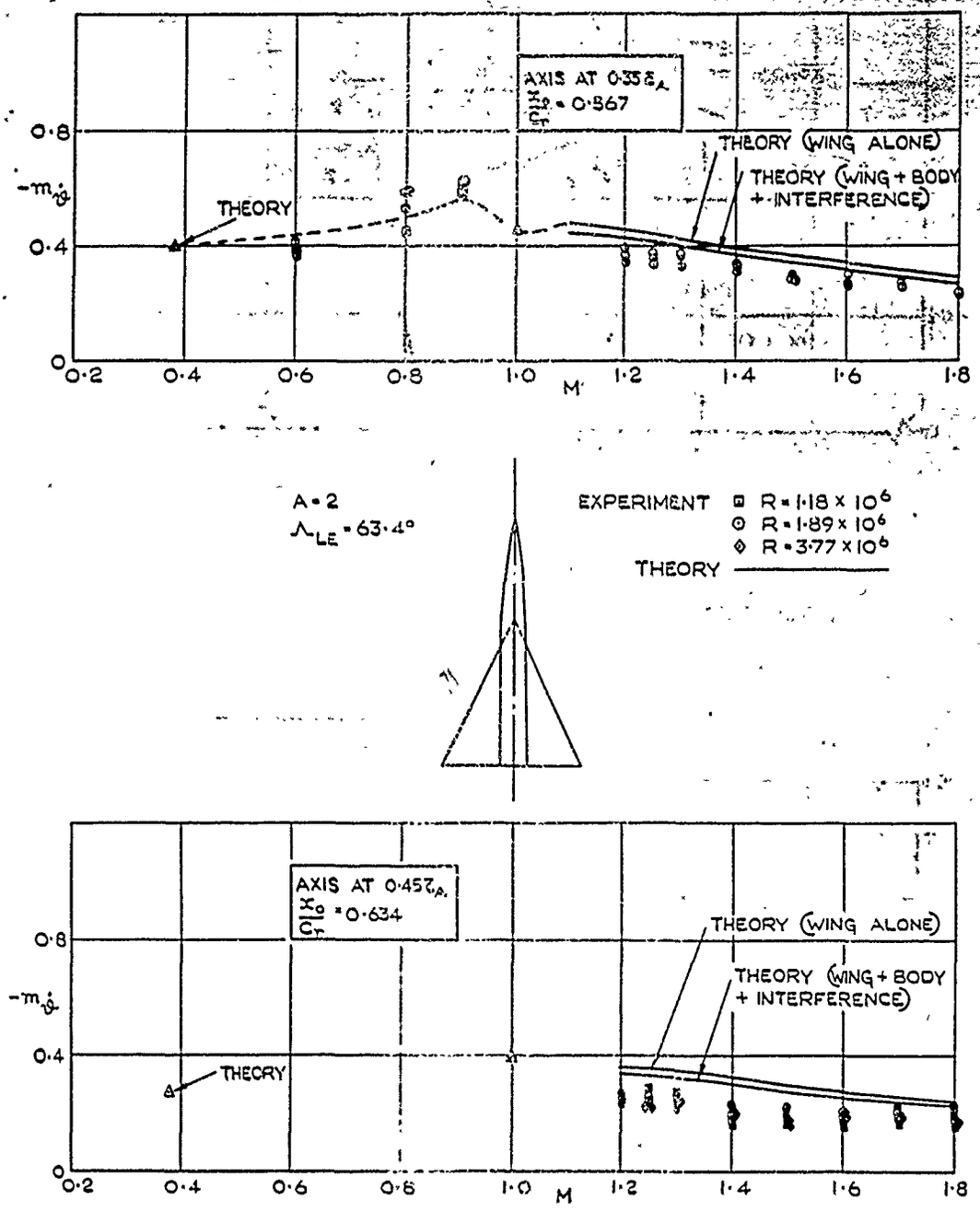

FIG. 23. COMPARISON OF CALCULATED $m_{\dot{\theta}}$ AND WIND TUNNEL TEST RESULTS FOR DELTA WING. A=2, Λ_{LE}=63·4°.

FIG. 24.

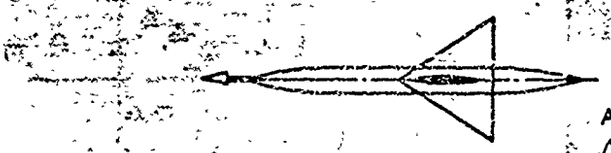

A = 2·35
Λ_ℓ = 59° 32'
k = 0·834

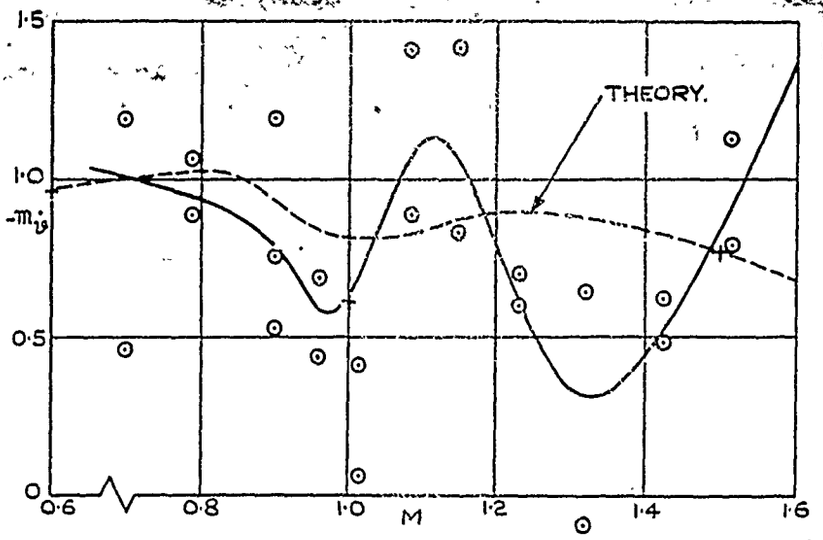

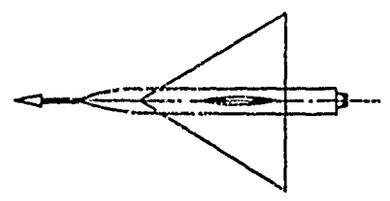

A = 2·31
Λ_ℓ = 60°

⊙ MODEL 1. k = 1·0
⊡ MODEL 2. } k = 0·933.
◇ MODEL 3. }

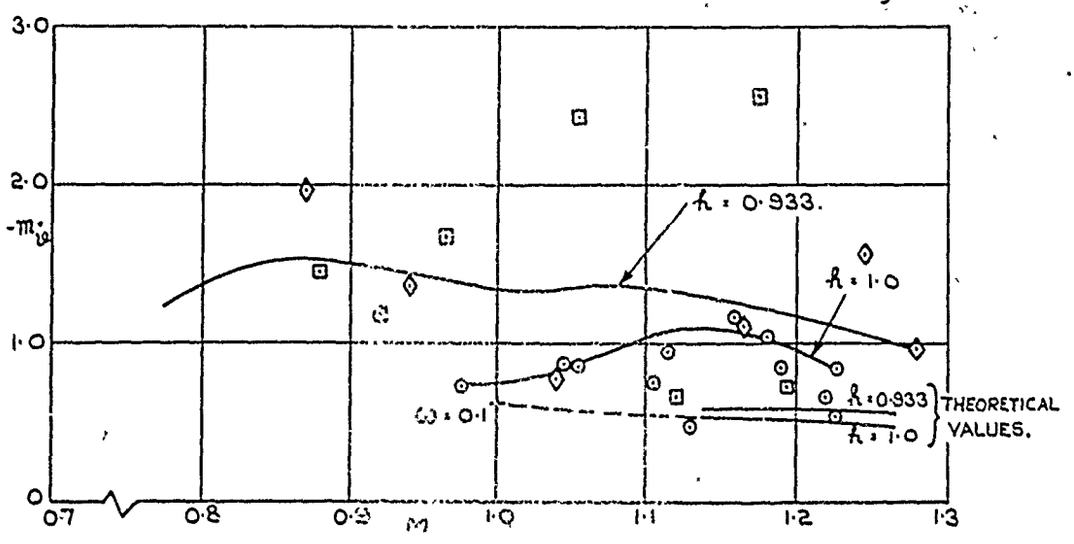

FIG. 24. VARIATION OF $m_{\dot{\theta}}$ WITH M FOR TWO TAILLESS DELTA WING CRUCIFORM MISSILES AS DETERMINED FROM GROUND LAUNCHED ROCKET TESTS.

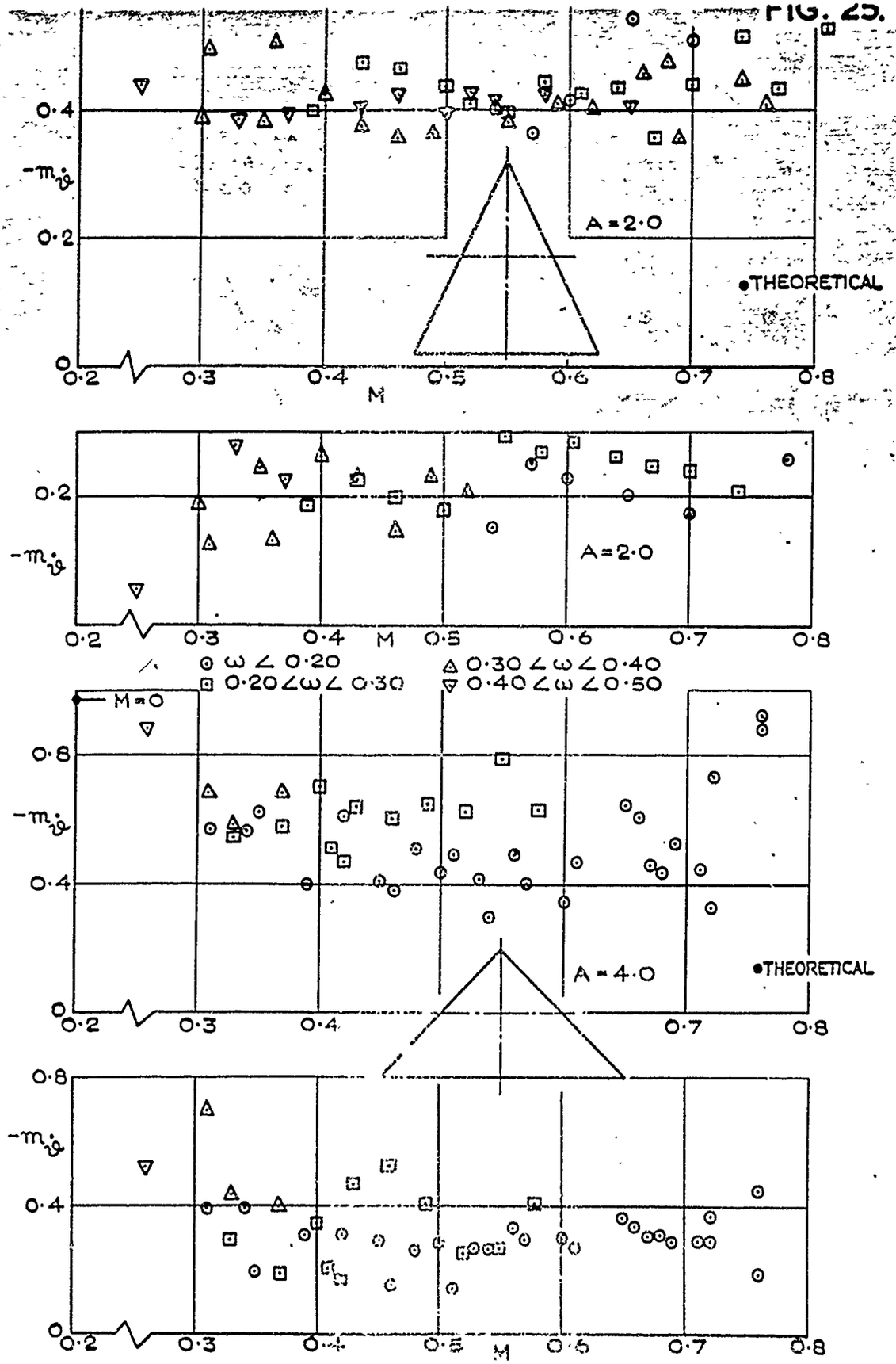

FIG.25. MEASUREMENTS OF $m_{\dot{\theta}}$ & $m_{\dot{\theta}}$ ON TWO DELTA WINGS, ASPECT RATIOS 2 AND 4, OSCILLATING ABOUT AN AXIS THROUGH THE MID-ROOT-CHORD AT SUBSONIC SPEEDS AND VARIOUS VALUES OF THE REDUCED FREQUENCY.

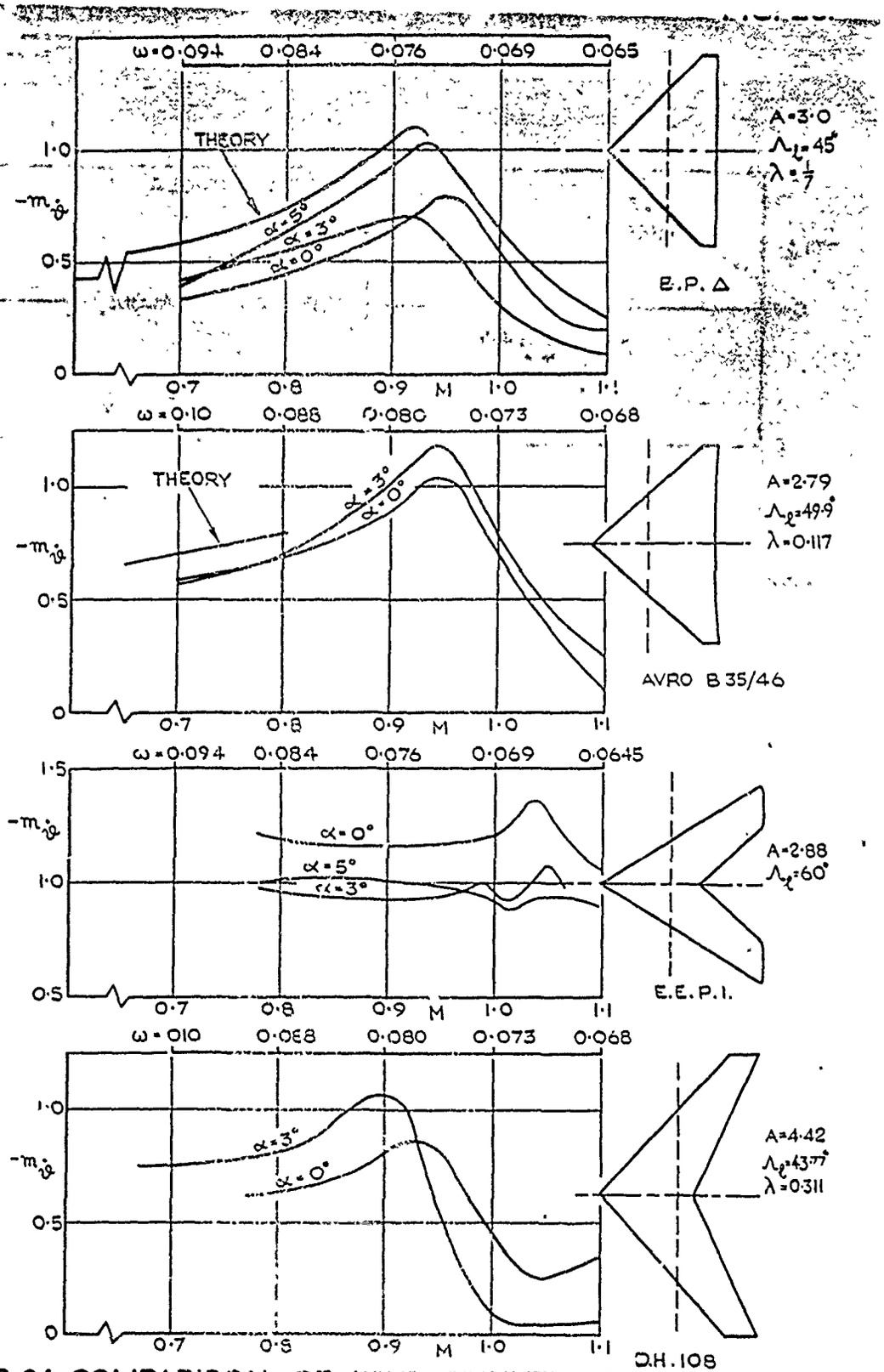

FIG. 26. COMPARISON OF WIND TUNNEL RESULTS FOR FOUR PLANFORMS OSCILLATING ABOUT DIFFERENT MEAN INCIDENCES.

FIG. 27.

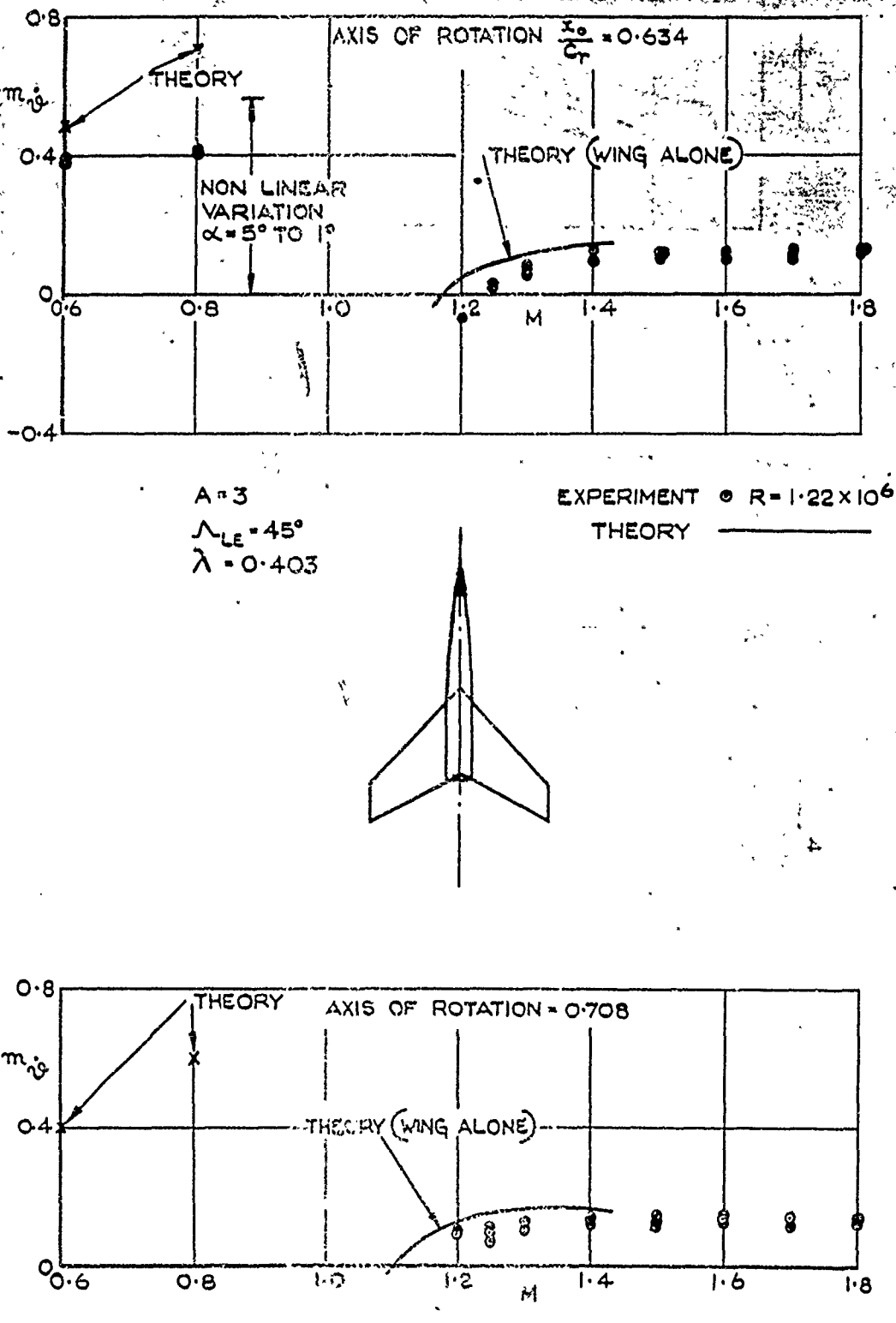

FIG. 27. COMPARISON OF CALCULATED $m_{\dot{\theta}}$ AND WIND TUNNEL TEST RESULTS FOR SWEPT BACK WING, A = 3·0, $\Lambda_{\frac{1}{2}}$ = 45°, λ = 0·4.

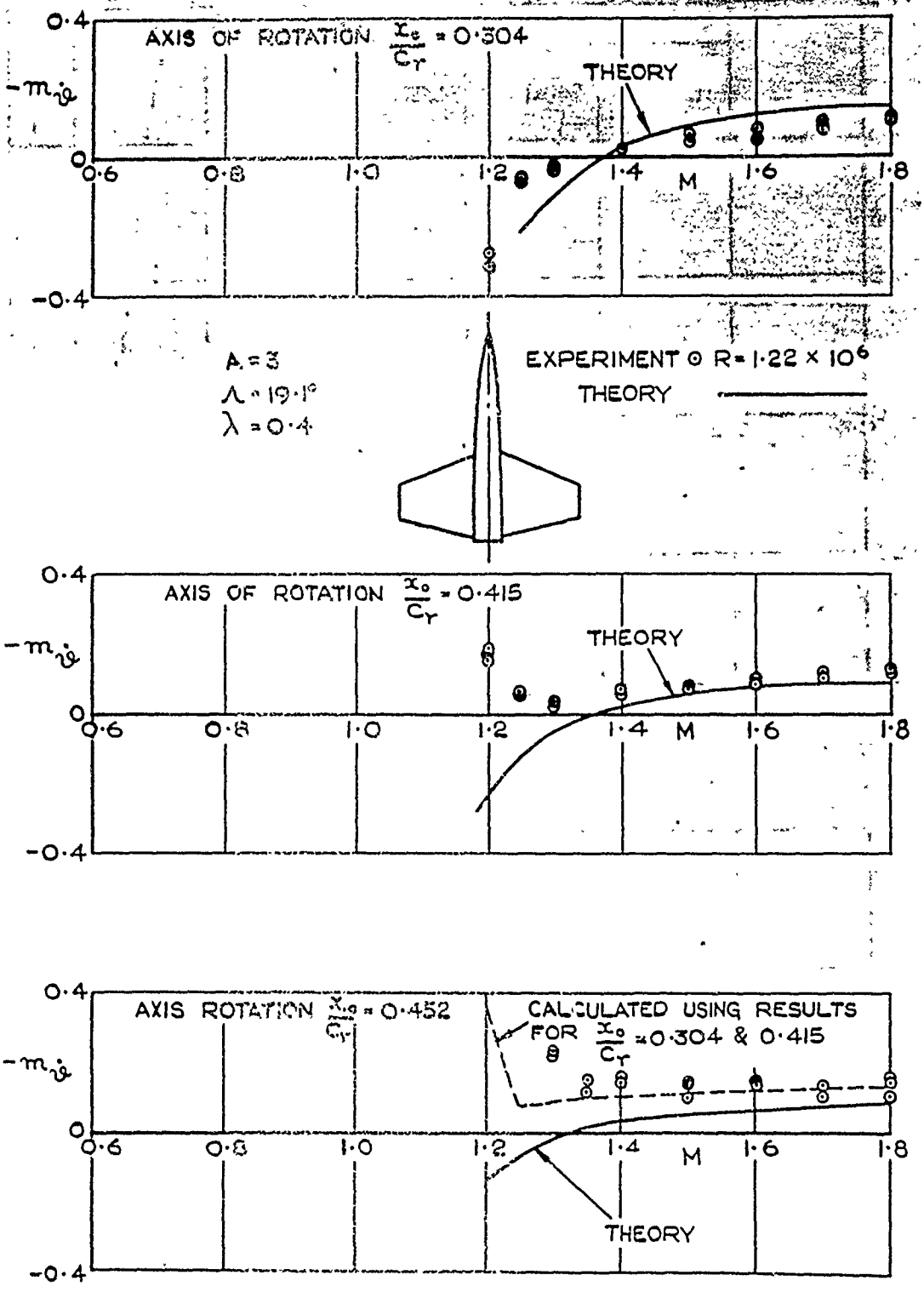

FIG. 28. COMPARISON OF CALCULATED $m_{\dot{\theta}}$ AT SUPERSONIC SPEEDS WITH WIND TUNNEL RESULTS FOR AN "UNSWEPT" WING OF ASPECT RATIO 3.

FIG.29.

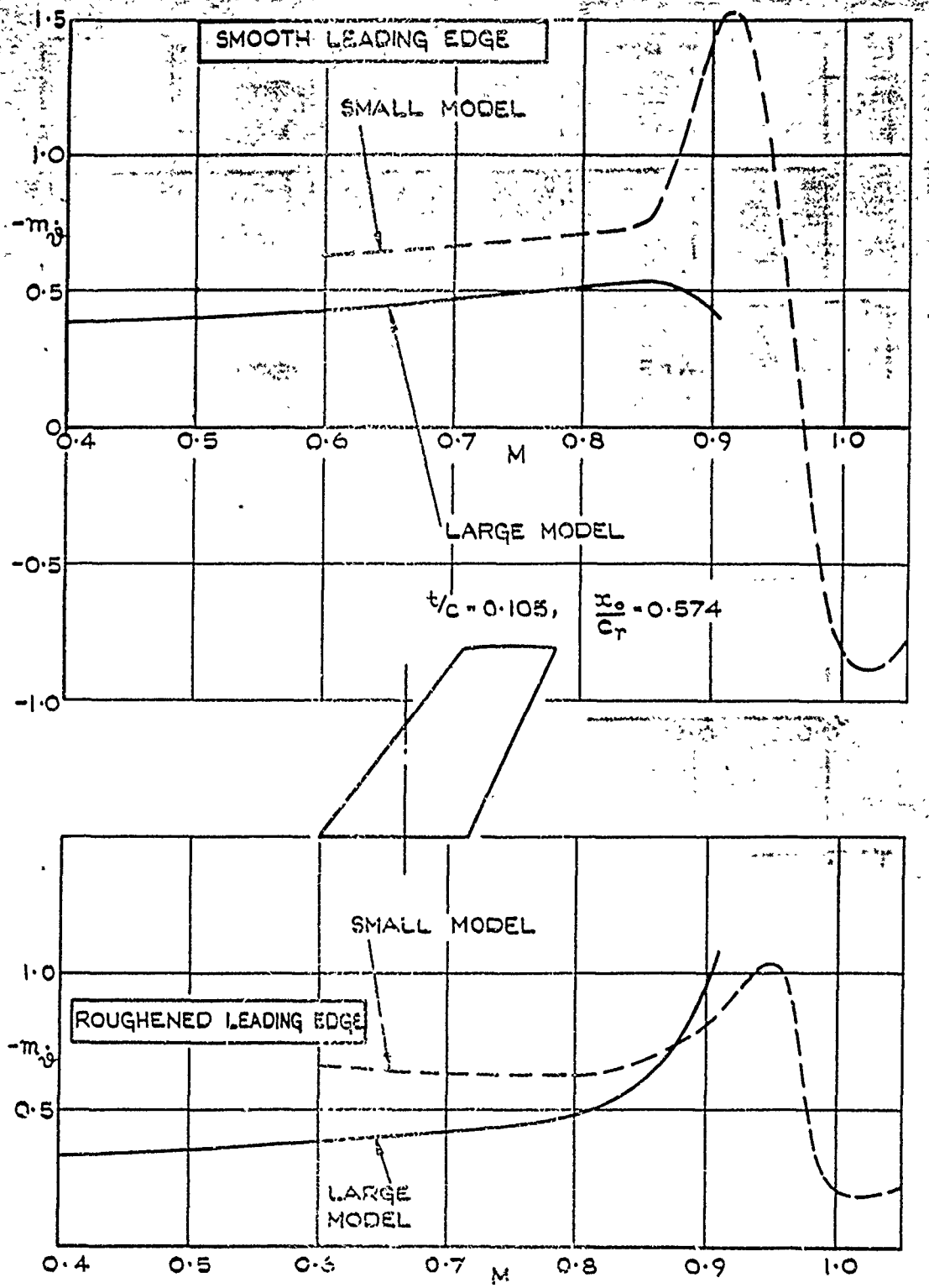

FIG. 29. VARIATION OF $m_{\dot{\theta}}$ WITH MACH NUMBER FOR 35° SWEPT WING ILLUSTRATING SCALE EFFECT FOR TRANSITION FIXED AND FREE.

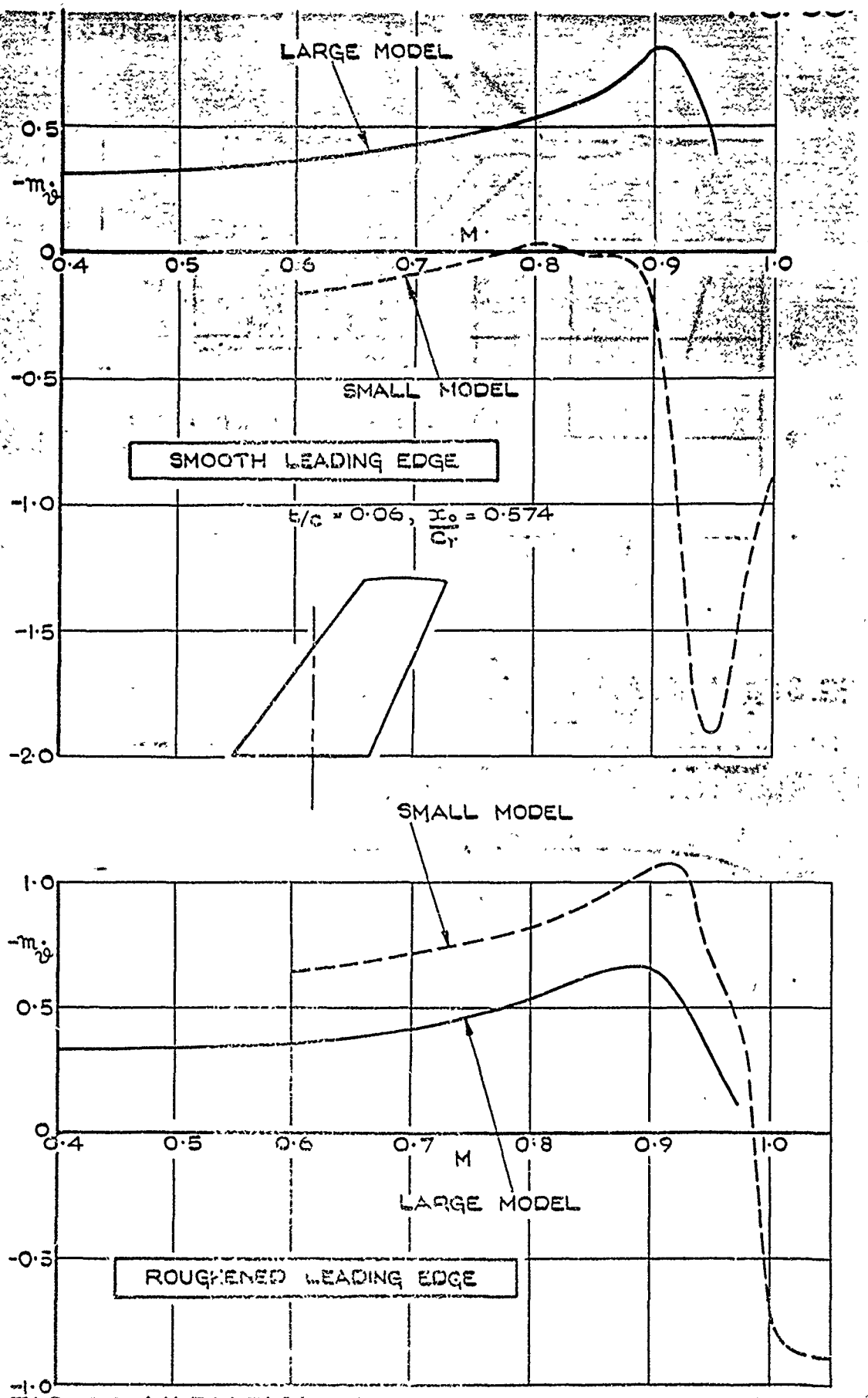

FIG. 30. VARIATION OF $m_{\dot{\theta}}$ WITH MACH NUMBER FOR 35° SWEPT WING ILLUSTRATING SCALE EFFECT FOR TRANSITION FIXED AND FREE.

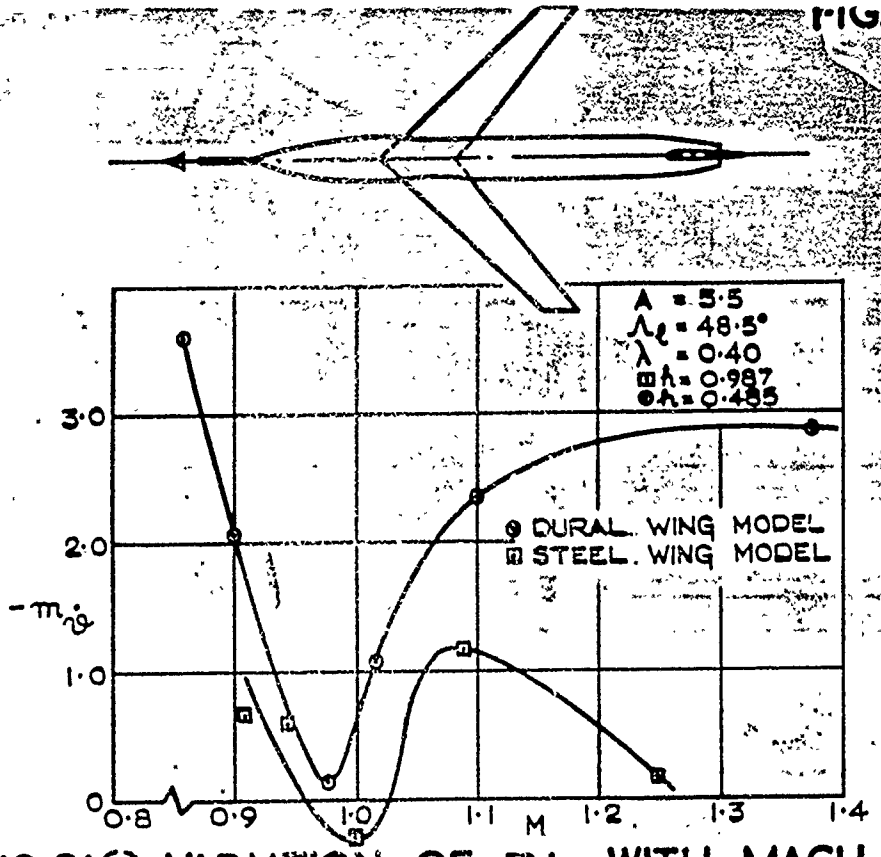

FIG. 31(a). VARIATION OF $m_{\dot{\theta}}$ WITH MACH Nº FOR TAILLESS SWEPT BACK WING MODEL ILLUSTRATING AEROELASTIC EFFECTS.

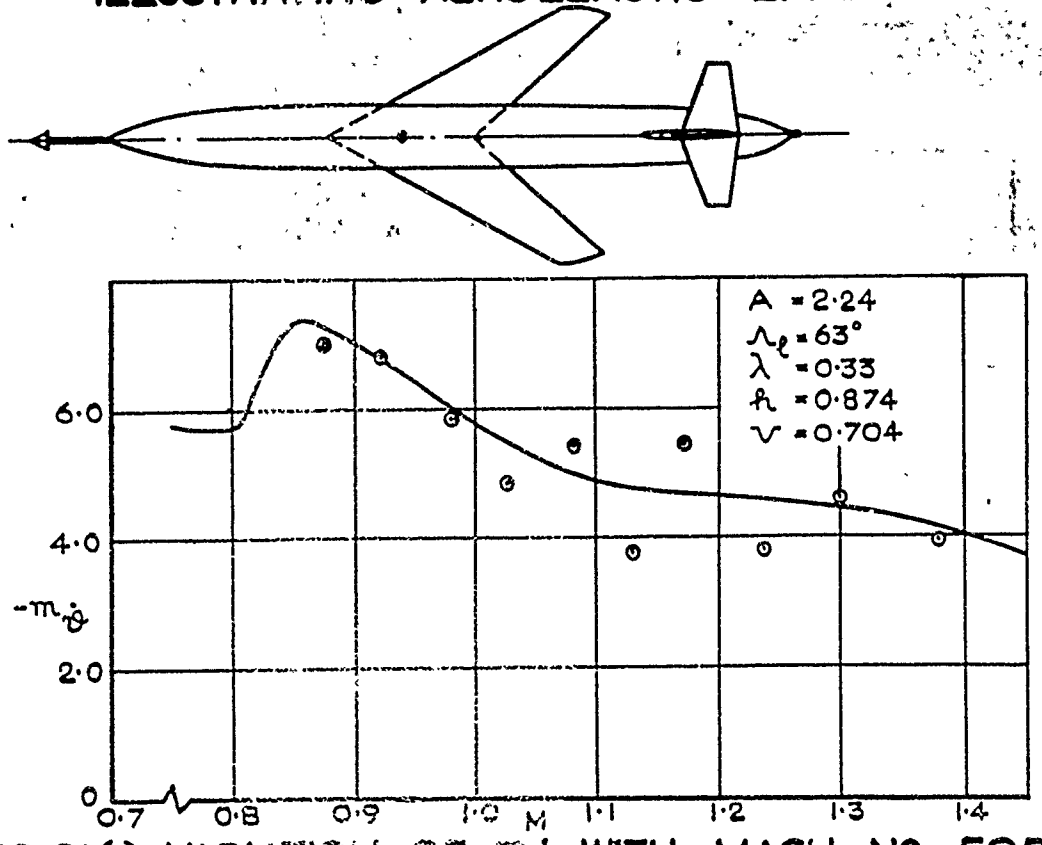

FIG. 31(b) VARIATION OF $m_{\dot{\theta}}$ WITH MACH Nº. FOR AIRCRAFT MODEL WITH SWEPT BACK WING AND UNSWEPT TAILPLANE.

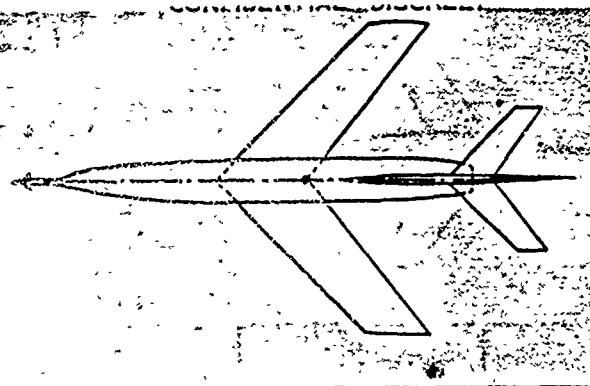

A = 4·0
Λ_{ℓ} = 46·73°
λ = 0·6
h = 1·215
V = 0·470.

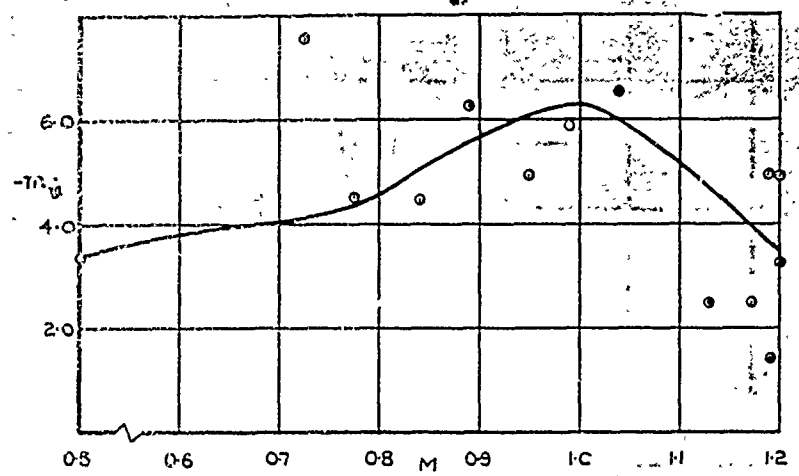

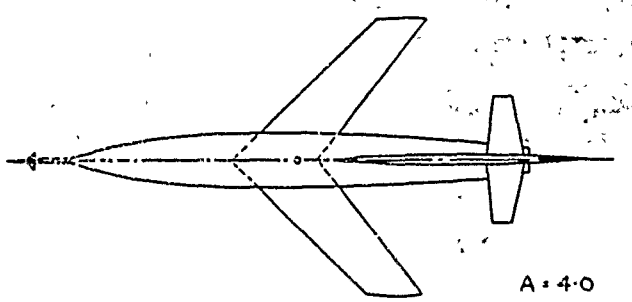

A = 4·0
Λ_{ℓ} = 46. 73°
λ = 0·6
h = 1·484
V = 0·620.

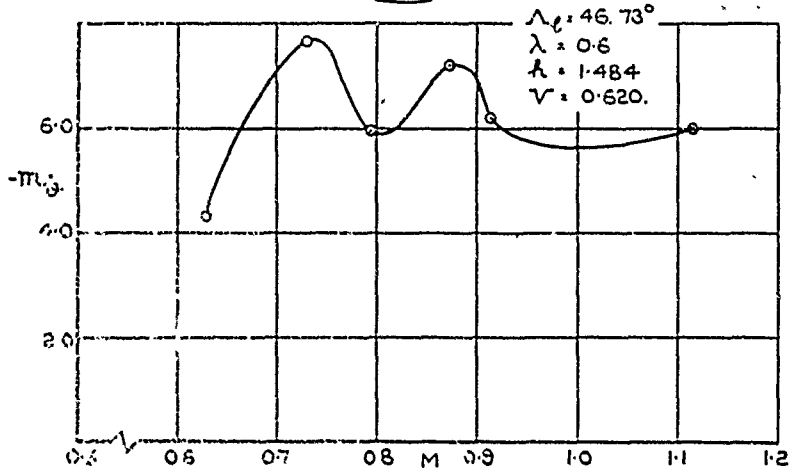

FIG.32. EXPERIMENTALLY DETERMINED $m_{\dot{w}}$ IN TRANSONIC SPEED RANGE FOR TWO MODELS HAVING IDENTICAL SWEPTBACK WINGS BUT TAILPLANES OF DIFFERENT SIZE AND SHAPE.

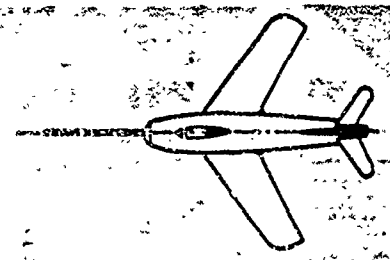

A = 4·79
Λ_{ℓ} = 37·0°
λ = 0·51
h = 0·564
V = 0·284

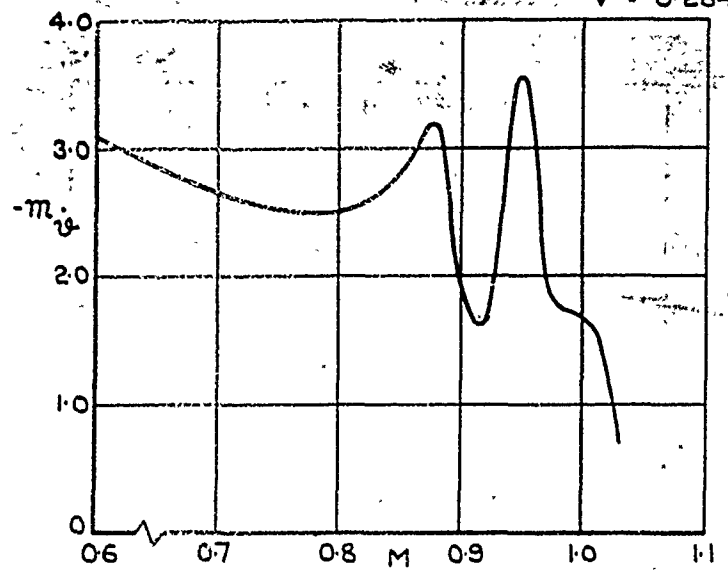

FIG.33 (a) DAMPING-IN-PITCH DERIVATIVE $m_{\dot{\theta}}$ FOR SWEPTBACK WING TAILED AIRCRAFT AS OBTAINED FROM FLIGHT TESTS.

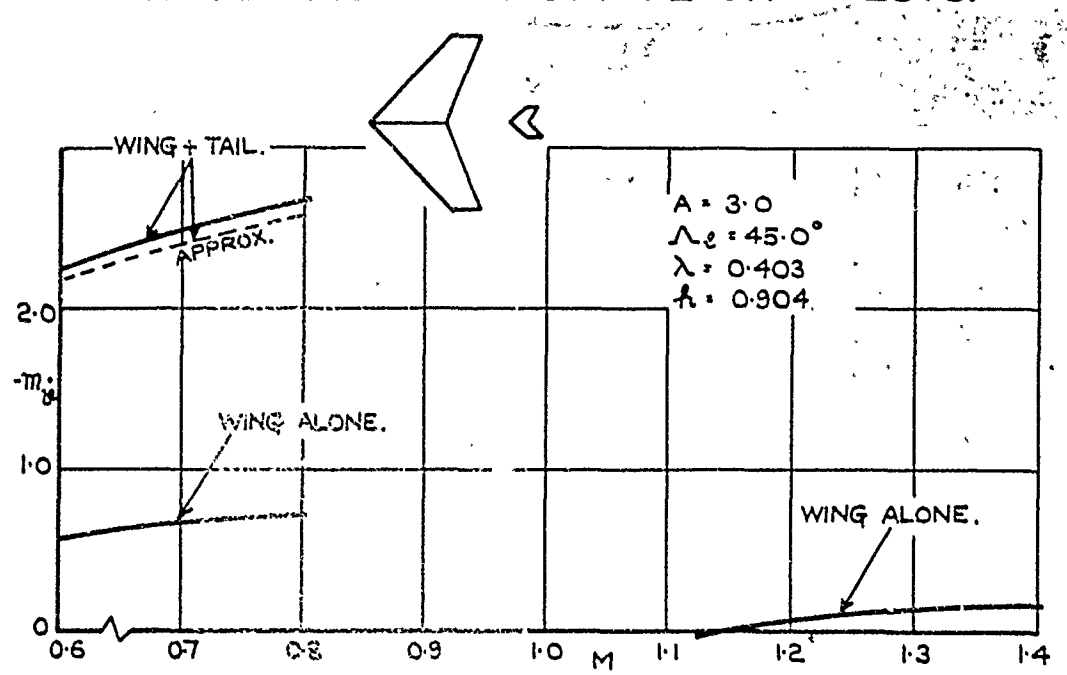

FIG.33 (b) CALCULATED VARIATION OF $m_{\dot{\theta}}$ WITH MACH Nº. FOR SWEPTBACK WING AND SWEPTBACK WING AND TAIL COMBINATION.

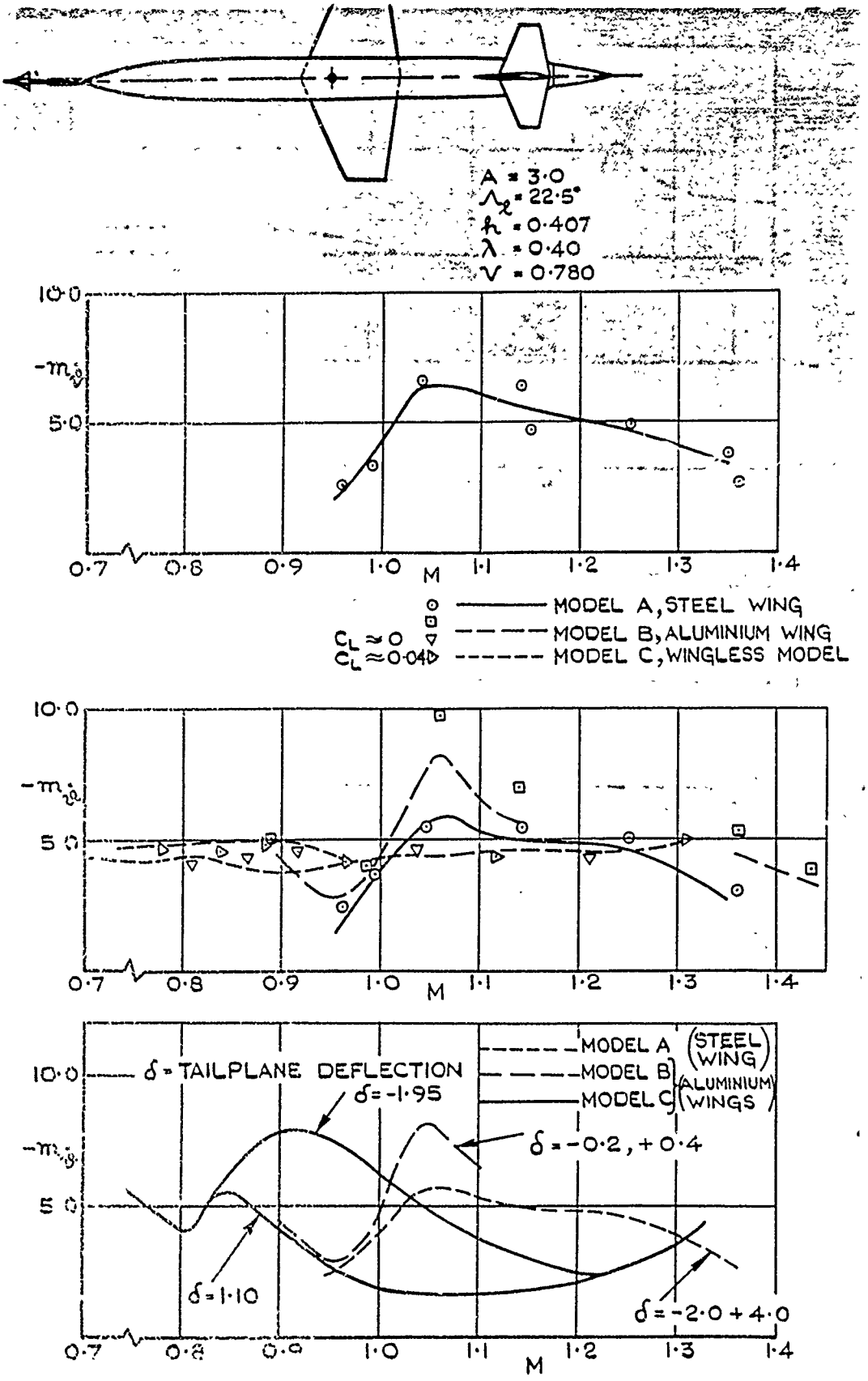

FIG. 34. VARIATION OF $m_{\dot{\theta}}$ WITH MACH Nº IN TRANSONIC SPEED RANGE FOR STRAIGHT WING TAILED AIRCRAFT FOR DIFFERENT MODEL CONSTRUCTION AND TEST CONDITIONS.

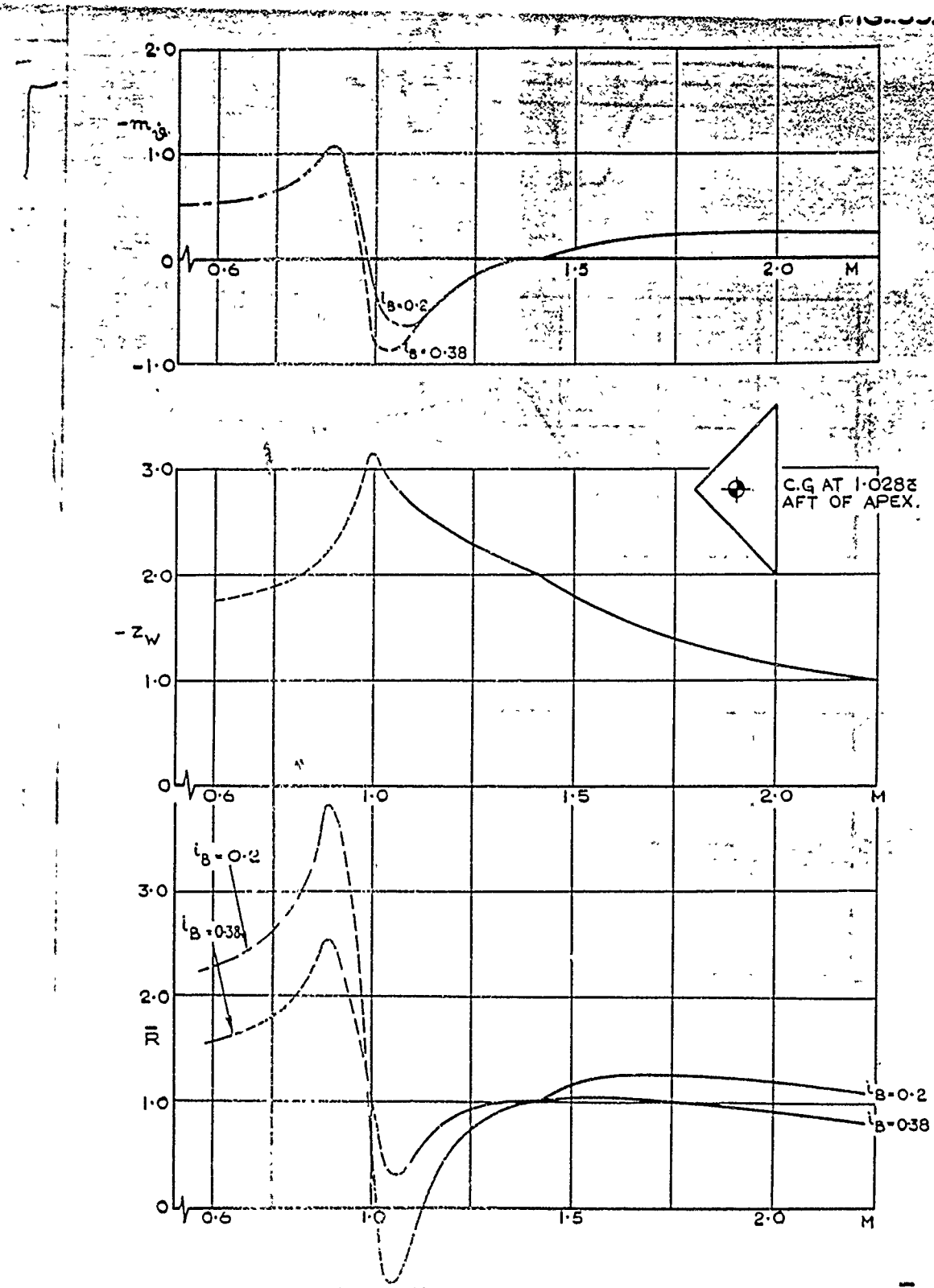

FIG. 35. VARIATION OF $m_{\dot{\alpha}}$, z_w, AND DAMPING FACTOR $\bar{R}$ WITH MACH NUMBER FOR A TAILLESS DELTA AIRCRAFT ($\Lambda_{LE}=45^\circ$) AND FOR TWO VALUES OF i_B.

FIG. 36 (a & b)

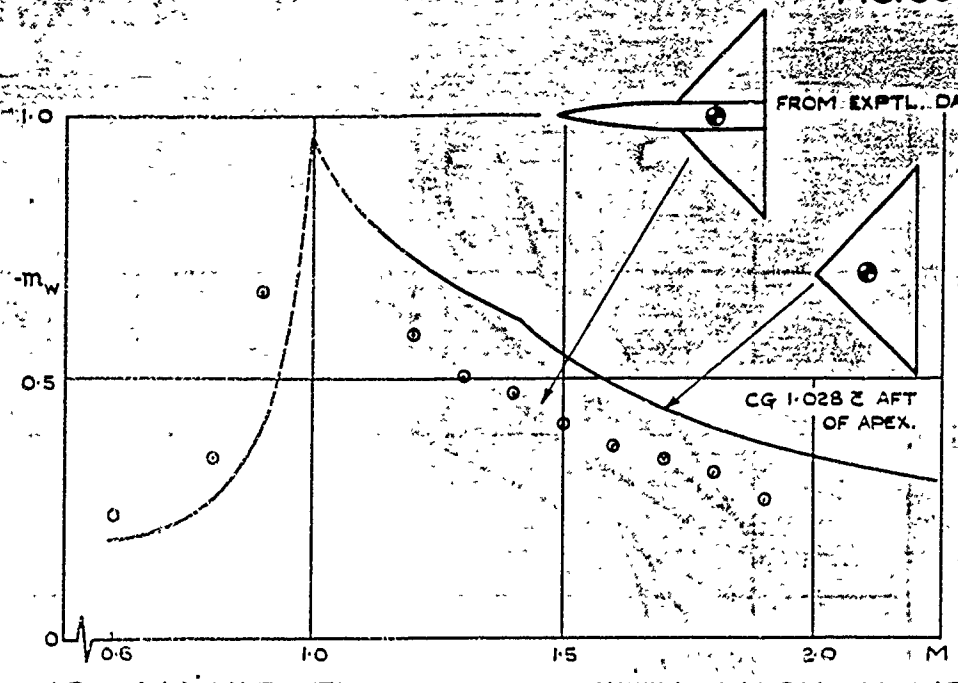

FIG. 36(a) VARIATION OF m_w WITH MACH NUMBER FOR DELTA WING OF ASPECT RATIO 4.

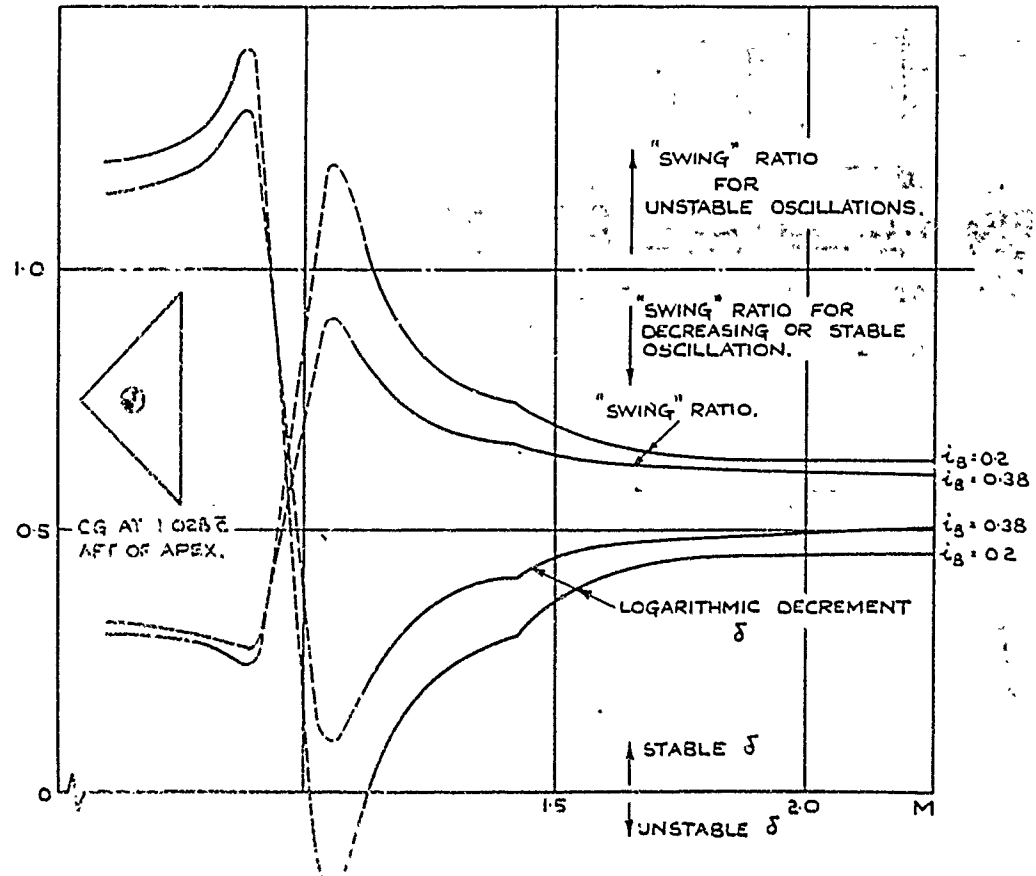

FIG. 36(b) EFFECT OF CHANGING THE MOMENT OF INERTIA IN PITCH ON THE CHARACTERISTICS OF THE SHORT PERIOD PITCHING OSCILLATIONS OF A TAILLESS DELTA WING AIRCRAFT ($\Lambda_\ell = 45°$)

FIG. 37(a & b)

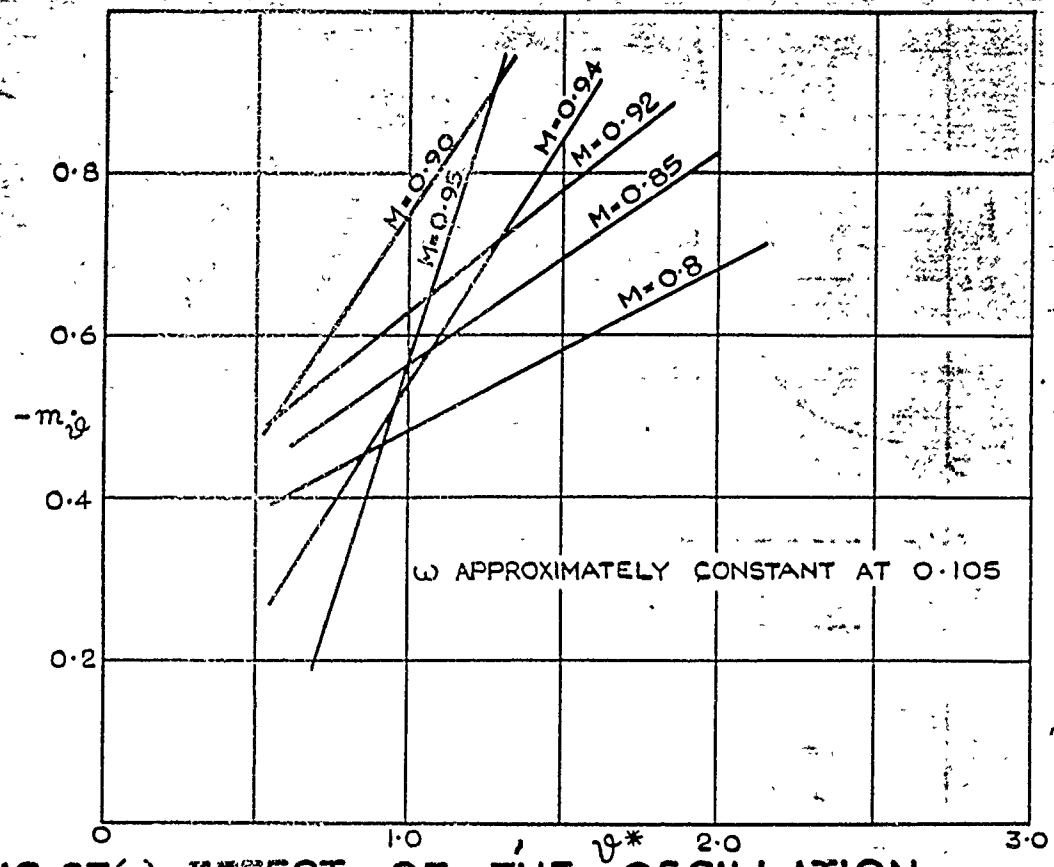

FIG. 37(a) EFFECT OF THE OSCILLATION AMPLITUDE AT ZERO INCIDENCE $\frac{\kappa_0}{c_r} = 0 \cdot 567$; $R = 1 \cdot 25 \times 10^6$; ON DAMPING IN PITCH DERIVATIVES OF A DELTA WING - BODY COMBINATION.

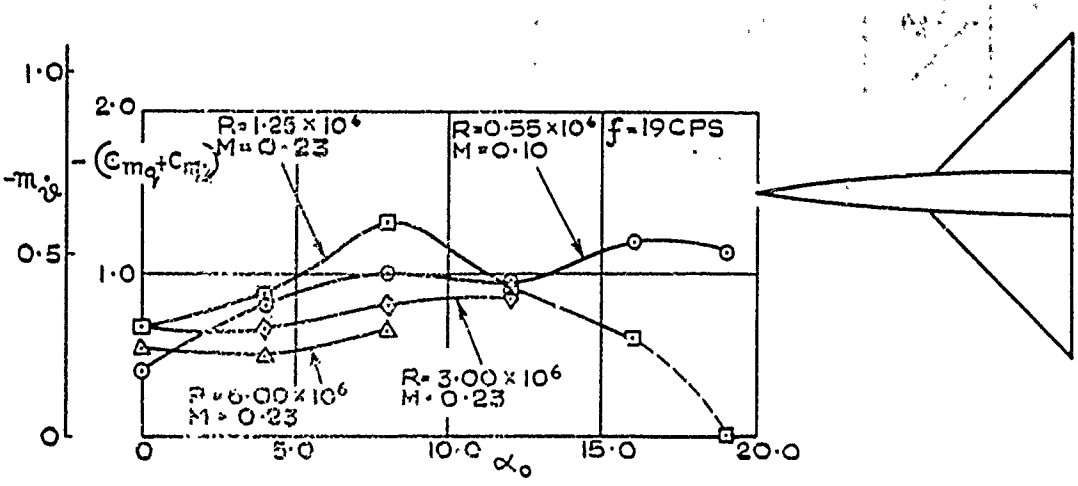

FIG. 37(b) EFFECT OF ANGLE OF INCIDENCE ON DAMPING IN PITCH DERIVATIVES FOR AN OSCILLATION AMPLITUDE OF 2°; $\frac{\kappa_0}{c_r} = 0 \cdot 567$.
(DELTA WING - BODY COMBINATION)

DETACHABLE ABSTRACT CARDS

These abstract cards are inserted in RAE Reports and Technical Notes for the convenience of Librarians and others who need to maintain an Information Index.

Detached cards are subject to the same Security Regulations as the parent document, and a record of their location should be made on the inside of the back cover of the parent document.

CONFIDENTIAL-DISCREET

Royal Aircraft Estab. Report No. Aero 2561 — 533.6.013.412: 533.6.013.423
1955.11
Thomas, H. H. B. M. and Spencer, B. F. R.

THE CALCULATIONS OF THE DERIVATIVES INVOLVED IN THE DAMPING OF THE LONGITUDINAL SHORT PERIOD OSCILLATIONS OF AN AIRCRAFT AND CORRELATION WITH EXPERIMENT — 1.8.1.2.1 1.8.1.2.3

Apart from an attempt to calculate the contribution of a tailplane to the damping in pitch of an aircraft over the speed range this note is a review of the existing information on the subject, from both experimental and theoretical sources.

A comparison of theory and experiment seems to indicate that theory gives a fairly reliable estimate of trends. There are a number of points requiring further investigation, and these are brought out in the discussion and conclusions at the end of the paper.

CONFIDENTIAL-DISCREET — P.T.O.

CONFIDENTIAL-DISCREET

Royal Aircraft Estab. Report No. Aero 2561 — 533.6.013.412: 533.6.013.423
1955.11
Thomas, H. H. B. M. and Spencer, B. F. R.

THE CALCULATIONS OF THE DERIVATIVES INVOLVED IN THE DAMPING OF THE LONGITUDINAL SHORT PERIOD OSCILLATIONS OF AN AIRCRAFT AND CORRELATION WITH EXPERIMENT — 1.8.1.2.1 1.8.1.2.3

Apart from an attempt to calculate the contribution of a tailplane to the damping in pitch of an aircraft over the speed range this note is a review of the existing information on the subject, from both experimental and theoretical sources.

A comparison of theory and experiment seems to indicate that theory gives a fairly reliable estimate of trends. There are a number of points requiring further investigation, and these are brought out in the discussion and conclusions at the end of the paper.

CONFIDENTIAL-DISCREET — P.T.O.

CONFIDENTIAL-DISCREET

Royal Aircraft Estab. Report No. Aero 2561 — 533.6.013.412: 533.6.013.423
1955.11
Thomas, H. H. B. M. and Spencer, B. F. R.

THE CALCULATIONS OF THE DERIVATIVES INVOLVED IN THE DAMPING OF THE LONGITUDINAL SHORT PERIOD OSCILLATIONS OF AN AIRCRAFT AND CORRELATION WITH EXPERIMENT — 1.8.1.2.1 1.8.1.2.3

Apart from an attempt to calculate the contribution of a tailplane to the damping in pitch of an aircraft over the speed range this note is a review of the existing information on the subject, from both experimental and theoretical sources.

A comparison of theory and experiment seems to indicate that theory gives a fairly reliable estimate of trends. There are a number of points requiring further investigation, and these are brought out in the discussion and conclusions at the end of the paper.

CONFIDENTIAL-DISCREET — P.T.O.

CONFIDENTIAL-DISCREET

Royal Aircraft Estab. Report No. Aero 2561 — 533.6.013.412: 533.6.013.423
1955.11
Thomas, H. H. B. M. and Spencer, B. F. R.

THE CALCULATIONS OF THE DERIVATIVES INVOLVED IN THE DAMPING OF THE LONGITUDINAL SHORT PERIOD OSCILLATIONS OF AN AIRCRAFT AND CORRELATION WITH EXPERIMENT — 1.8.1.2.1 1.8.1.2.3

Apart from an attempt to calculate the contribution of a tailplane to the damping in pitch of an aircraft over the speed range this note is a review of the existing information on the subject, from both experimental and theoretical sources.

A comparison of theory and experiment seems to indicate that theory gives a fairly reliable estimate of trends. There are a number of points requiring further investigation, and these are brought out in the discussion and conclusions at the end of the paper.

CONFIDENTIAL-DISCREET — P.T.O.

CONFIDENTIAL-DISCREET

The main conclusion to be drawn from the available information is that tailless aircraft, having leading edge sweep of less than 55° or thereabouts, and of moderate or large aspect ratio, are almost certain to suffer some loss of damping in the transonic speed range, the severity of this loss depending on the sweep, the aspect ratio, the moment of inertia in pitch, and the relative density μ.

It seems likely that the addition of a tailplane in a suitable position would remove most, if not all, of this loss, but this requires further investigation particularly as regards incidence effects.

CONFIDENTIAL-DISCREET

The main conclusion to be drawn from the available information is that tailless aircraft, having leading edge sweep of less than 55° or thereabouts, and of moderate or large aspect ratio, are almost certain to suffer some loss of damping in the transonic speed range, the severity of this loss depending on the sweep, the aspect ratio, the moment of inertia in pitch, and the relative density μ.

It seems likely that the addition of a tailplane in a suitable position would remove most, if not all, of this loss, but this requires further investigation particularly as regards incidence effects.

CONFIDENTIAL-DISCREET

CONFIDENTIAL-DISCREET

The main conclusion to be drawn from the available information is that tailless aircraft, having leading edge sweep of less than 55° or thereabouts, and of moderate or large aspect ratio, are almost certain to suffer some loss of damping in the transonic speed range, the severity of this loss depending on the sweep, the aspect ratio, the moment of inertia in pitch, and the relative density μ.

It seems likely that the addition of a tailplane in a suitable position would remove most, if not all, of this loss, but this requires further investigation particularly as regards incidence effects.

CONFIDENTIAL-DISCREET

END

Information Centre
Knowledge Services
[dstl] Porton Down
Salisbury
Wilts
SP4 0JQ
22060-6218
Tel: 01980-613753
Fax 01980-613970

Defense Technical Information Center (DTIC)
8725 John J. Kingman Road, Suit 0944
Fort Belvoir, VA 22060-6218
U.S.A.

AD#: AD091769

Date of Search: 10 December 2008

Record Summary: AVIA 6/18020
Title: Calculations of the derivatives involved in the damping of the longitudinal short period of oscillations on an aircraft and correlation with experiment
Availability Open Document, Open Description, Normal Closure before FOI Act: 30 years
Former reference (Department) REPORTS AERO 2561
Held by The National Archives, Kew

This document is now available at the National Archives, Kew, Surrey, United Kingdom.

DTIC has checked the National Archives Catalogue website (http://www.nationalarchives.gov.uk) and found the document is available and releasable to the public.

Access to UK public records is governed by statute, namely the Public Records Act, 1958, and the Public Records Act, 1967.
The document has been released under the 30 year rule.
(The vast majority of records selected for permanent preservation are made available to the public when they are 30 years old. This is commonly referred to as the 30 year rule and was established by the Public Records Act of 1967).

This document may be treated as UNLIMITED.